Gabion Stability

FINAL REPORT

Master of Science Thesis

Author: R.H.P.A. Beekx Bsc

Delft, December 2006

Graduation committee:
prof. drs. ir. J.K. Vrijling
ir. H.J. Verhagen
drs. R. Booij
ir. K. Dorst

Preface

This thesis is written as the final assignment of my Master of Science study in Hydraulic Engineering at Delft University of Technology. The graduation project consisted of a 2 month fieldtrip to the Saemangeum project in South Korea, model tests in Delft and analysis of all data gathered in this report.

This thesis could never have been established without the support and advice of others. Special gratitude is expressed towards the following persons and companies:

Bouwdienst Rijkswaterstaat

Gé Beaufort, Kees Dorst, Arie Vrijburcht and Marina Rebel who accompanied me to South Korea and supported me in the Netherlands. Also I would like to thank Wilco Meijerink for letting me use his EFD output in this report.

Korea Rural Community & Agriculture Corporation

All of the staff of KRC and RRI (Rural Research Institute) who provided information and showed us around at the Saemangeum project in South Korea.

Delft University of Technology

My supervisors of the sections of hydraulic engineering and fluid mechanics of the faculty of Civil Engineering and Geosciences of Delft University of Technology: Prof. drs. ir. J.K. Vrijling, ir. H.J. Verhagen, drs. R. Booij and of course Maartje van der Sande who accompanied me to South Korea to gather information for our graduation projects.

Picture on cover: Application of gabions at the Saemangeum dike, just before the final closure

Abstract

In 1932 the Dutch 'Afsluitdijk', stretching over 30 kilometers, was completed. This made it possible to reclaim land in the former 'Zuiderzee' by means of constructing the 'Flevopolder' and the ‘Noordoostpolder’. Since then technological developments have made it possible to build even larger dams in more difficult circumstances.

One of the countries that is also reclaiming land by constructing dams and polders is South Korea. Because of the large mountainous areas and the growing population in this country, arable land is becoming rare and land reclamation may offer a solution. The large tidal differences along the Korean coast make building these dams a challenging job.

One of the solutions in South Korea to cope with the high flow velocities in closure projects is to apply sack gabions. These are steel nets with rocks inside them that weigh up to 3 tons. It is not clear how stable these sack gabions are exactly. The **objective** of this report is to make a preliminary study on the stability of sack gabions.

In 2006, after a 20 year preparation, the Saemangeum estuary in South Korea was closed with a dam. During the closure **sack gabions** were used in the bed protection, sill construction and dam heads. In corporation with Delft University of Technology, Rijkswaterstaat and the Korea Rural Community & Agriculture Corporation a field trip to the Saemangeum project was made, in order to collect useful data on the stability of gabions. Also the experimental data of RRI (Korean Rural Research Institute) on model tests on the stability of gabions was obtained. As an addition to the data from the Saemangeum project and the model tests performed by RRI, also model tests in Delft were done.

All data are compared to come up with an advice for calculating the stability of gabions. To calculate the depth averaged critical velocity for 3 t - 5 t rock with 3 t sack gabions mixtures, formula [15] proves to be useful.

$$u_{cM} = 2.513x + 5.4 \qquad [15]$$

Where:

u_{cM} = critical velocity of a mixture of 50 % rocks of 3.0 to 5.0 t and 50 % 3.0 t gabions

x = the proportion of gabions in the mixture

$0.2 < x < 0.5$

For the calculation of the local critical velocity for a bed of sack gabions, it is advised to use Izbash' formula with a gabion stability factor (**γ** in formula [10]) while calculating the nominal diameter of a sack gabion as in formula [1] (a mass based approach):

$$\Delta D_n = \frac{\beta}{\gamma}\frac{u_c^{\,2}}{2g} \qquad [10]$$

$$D_n = \sqrt[3]{\frac{M}{\rho_S}} \qquad [1]$$

Where **γ = 1.26** for sack gabions (while for loose rocks γ = 1)

Also a qualitative analysis of the Delft model tests is made that leads to several considerations for the design of gabion bed protections:

- When applying gabions one has to take into account the difference in behavior between gabions and loose rocks. Gabions tend to start moving more abruptly and with more gabions at a time. If one gabion fails, mostly other gabions fail as well because they stabilize each other. Loose rocks have less overlap and therefore they have a less stabilizing effect on each other.
- Another behavior that needs to be investigated further is the effect of applied pressure on a gabion bed. If a gabion bed is pressed together, the stability of the bed is increased significantly. In practice this means that a lower layer of gabions is pressed together by the weight of the upper layers of gabions. So if the upper layer fails, the more stable lower layer will be able to withstand higher flow loads, thus preventing progressive failure of the gabion bed.

There is still much unknown about the stability of gabions. Things that should be further investigated are:

- The stabilizing effect of top layers on lower layers in a gabion bed.
- The amount of failure of more gabions at once.
- The stability of a gabion bed after incipient motion has occurred.
- The influence of the amount of rocks in a gabion on its stability.
- The influence of turbulence on the stability of gabions.
- The stability of a sill construction when the weir becomes a free flow weir instead of a submerged weir.
- The effect of tying more gabions together.
- The amount of damage to gabions using certain dumping methods.
- The costs - benefit relation of gabions vs. large rocks with comparable stability.

Also it is advised to use sluices in the Netherlands or in South Korea as flumes for extensive prototype tests on the stability of gabions.

Table of contents

1. Introduction

In 1932 the Dutch 'Afsluitdijk' (figure 1.1), stretching over 30 kilometers, was completed. This made it possible to reclaim land in the former 'Zuiderzee' by means of constructing the 'Flevopolder' and the 'Noordoostpolder'. Since then technological developments have made it possible to build even larger dams in more difficult circumstances.

Figure 1.1: Final closure of the 'Afsluitdijk' (http://www.anno.nl)

In order to progress in science and to improve the possibilities of practical applications it is of great importance to learn from experiences of previous projects. This is also valid for the field of hydraulic engineering. Closures and the accompanying difficulties with stability of bed, sill and dam materials exist all over the world. As part of this graduation project experiences from previous closures in difficult circumstances will be implemented into a theoretical study on the stability of gabions.

In this chapter, 2 land reclamation projects in South Korea are described. These projects were executed under difficult circumstances and the knowledge that could be harvested from the experiences of these projects can increase the understanding of gabion stability in general. There are several types of gabions. In chapter 1.2 these types will be described and a shift will be made on which type of gabion this report focuses. In paragraph 1.3 the objective of this report is stated. To achieve the goals several sources of information will be combined to provide a method to determine the stability of sack gabions. The last paragraph of this chapter deals with the structure of the remainder of this report.

1.1 Land reclamation in South Korea

One of the countries that is reclaiming land by constructing dams and polders is South Korea. Because of the large mountainous areas and the growing population in this country, arable land is becoming rare and land reclamation may offer a solution. Because of the large tidal differences (over 6 meters during spring tide) along the Korean coast, building these dams is a challenging job. In the past decades several initial closures in Korea were even delayed because of instability of sill and bed protection materials.

Two Korean land reclamation projects deserve special attention in this study: the 'Sihwa' project near Inchon and the 'Saemangeum' project near Kunsan (figure 1.2). The Sihwa project is interesting because the closure was delayed and the Saemangeum project is interesting because the problems encountered in the Sihwa project were converted into practical solutions for this closure.

In the 1990's the 'Sihwa' dam was built for land reclamation. The first closure attempt in December 1993 was delayed because one of the closure gaps eroded to rock bottom as a result of the high flow velocities caused by large tidal differences. The dam was successfully closed in January 1994.

Figure 1.2: Map of South Korea (http://wikitravel.org) / Sihwa dam / Saemangeum project

After the Sihwa dam was constructed, several problems arose. Pollution of the water in the closed estuary still proves to be a problem. To solve the Sihwa project water quality problem, a tidal power plant is being constructed in the dam at this moment. It is expected that the exchange of sea water and basin water will dilute the pollution significantly.

With the experiences of the Sihwa project in mind, the land reclamation project of 'Saemangeum' started several years later. The Saemangeum dam was designed to close the estuary near Kunsan. The actual construction started in 1991. The storage area of the estuary is approximately 400 km^2 and the total length of the dam is about 33 km. In the dam 2 discharge sluices are situated: The Garyeok sluice and the Sinsi sluice.

The Saemangeum estuary is a wetland with an ecosystem with many birds and fish. When the dam was only partially finished, a lawsuit of environmentalists (figure 1.3) led to a delay in the construction. The last gaps in the dam could not be closed. This caused the sand at the unprotected locations next to the gaps to erode to rock bottom (this can clearly be seen in figure 6.4). This was a risky development, but no severe instability problems occurred. By ruling of the Korean Supreme Court on March 16th 2006 the estuary could be completely closed. The final closure of the estuary took place on April 21st 2006.

Figure 1.3: Environmental protests (http://www.ngotimes.net)

The Saemangeum project is unique in the world in several ways: First of all it is one of the biggest closure works on earth. Besides that, the tidal difference in this area is very large, over 6 meters during spring tide. This caused high flow velocities during the final closure that could endanger the stability of the bed protection, the sill and the dam heads and made the closure a challenging task. To cope with the high flow velocities, a mixture of rocks and gabions, adapted to the expected flow velocities, was applied. This method proved to be successful in earlier Korean closure projects. Therefore it is considered necessary to take a closer look at the stability of gabions in a scientific way. In this study this is done using the information from Korea and new flume investigations at Delft University of Technology.

1.2 Gabions

A gabion is defined as 'a wire container filled with rocks used for structural purposes'. Gabions are used for retaining walls, revetments, slope protection, channel linings and other structures (http://www.ieca.org).

There are many different types of gabions, each with its own use and properties. The most commonly used are **box gabions** (often used as river bank protection, figure 1.4), **gabion mattresses** (often used as bed or bank protection, figure 1.4) and **cylindrical gabions** (Mainly used for emergency and river and stream training works where local conditions require fast installation or the water does not allow easy access to the site, figure 1.5).

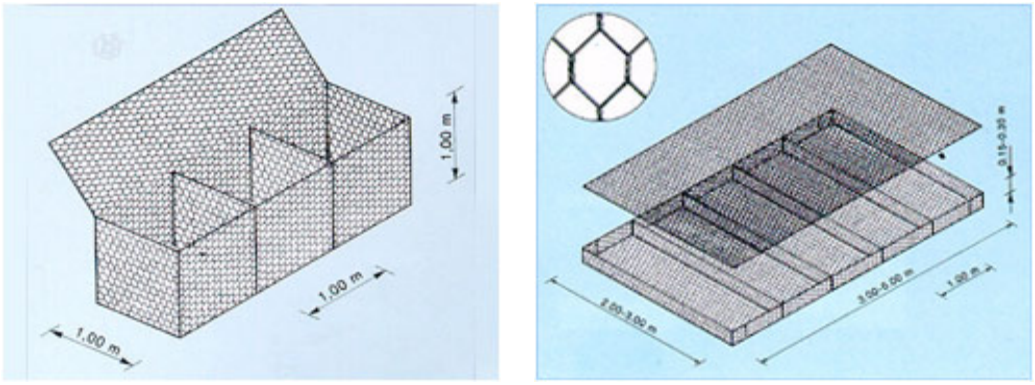

Figure 1.4: Examples of a box gabion and a gabion mattress (http://www.egetra.be)

In the Saemangeum project **sack gabions** (figure 1.5) were used in the sill construction, bed protection and dam head protection during the closure of the Saemangeum dam. This is a type of gabion that consists of a steel wire mesh (figure 1.6) filled with rocks which is tied together like a sack. The focus of this report is on these sack gabions. In the remainder of this report, sack gabions will be referred to as gabions.

Figure 1.5: Cylindrical gabion (http://www.africangabions.co.za) and sack gabion

The reason that in the Saemangeum project sack gabions were used is because the high flow velocities required material that was more stable than a 3 ton rock, and such large rocks are not abundant in a quarry. To reach the proper weight, simply more rocks can be added to a gabion. Depending on the stability needed, different sizes of gabions were applied depending on the expected local flow velocities at certain locations.

Gabions are stable not only because of their large weight, but also because of their flexibility. This causes them to settle on the bed and to deform before actual failure occurs. The wire mesh is vulnerable to corrosion and to damage by the movement of the rocks inside the gabion. Therefore an application like a dam closure is excellent for the use of gabions, because after the dam is finished, no water flows over the gabions anymore. The wire mesh becomes obsolete and the gabion is mere filling of the dam like other rocks.

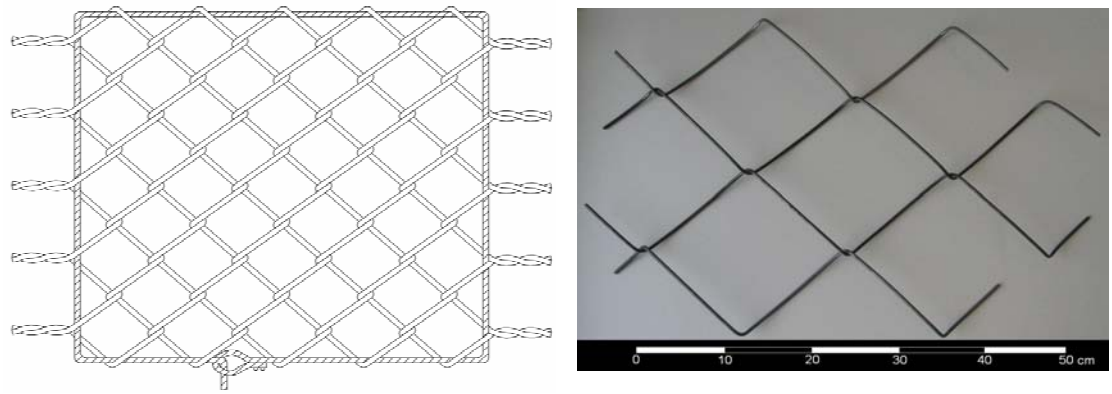

Figure 1.6: Wire mesh for the production of sack gabions

In the Saemangeum project sack gabions of 1, 2 and 3 tons were used in the bed protection, in the sill of the dam and as dam head protection. They were dumped from the water by split barges and pontoons and from the dam heads with dump trucks (figure 1.7). During the dumping not all gabions arrived on the intended location intact.

The Saemangeum project is perfectly fit for the application of gabions. The rocks that were used came from nearby quarries were rocks were harvested using explosives. This method produced large amounts of rocks with different sizes. Rocks heavier than 3 tons were rare while due to the large tidal differences even larger rocks were needed. Because these were not available in large quantities, the solution was sought for in the form of gabions. The gabions would be integrated in the dam design, so the wear of the wire mesh of the gabions was not a problem. Before they would deteriorate too much, the dam would be finished.

In the Netherlands, where rocks are imported from abroad, one can order larger sizes of stones rather than produce gabions. Also the tidal differences in the Netherlands are smaller, which means that very large rocks (> 3 tons) are hardly needed for bed protection or dam projects. This makes the application of sack gabions in the Netherlands redundant.

Figure 1.7: Dumping of gabions and settled gabions

In general the application of sack gabions may be considered if the following conditions are present:

- High flow velocities (e.g. at locations with large tidal differences)
- Shortage of large rocks
- Manufacturing of gabions is less expensive than importing rocks with the same stability
- Gabions will only be exposed to a hydraulic load during a relatively short period (e.g. in a closure). Otherwise the wear of the wire mesh or corrosion may cause failure of the gabions

Because there is no general stability formula for sack gabions available, RRI (Korean Rural Research Institute) performed several scale model tests on gabions. The stability of the gabions needed for the Saemangeum project was determined with these tests, but no general stability formula for gabions was made with these data.

1.3 Objective of this report

Some stability formulas on the stability of different types of gabions exist. One of the problems when applying these formulas is the many different types of gabions that have different properties. For example in Schiereck (2001) (p. 72) it is stated that because of the loss of flow load due to the porosity of a gabion, the critical velocity of a box gabion increases by a factor 1.5 in comparison with the critical velocity of a rock with the same volume as the gabion. This is a rough estimate based on the influence of the porosity of a gabion.

Another problem is the large range of possible outcomes for the calculations of the stability of a gabion. For example Wallingford (2005) (p. 42) states that Izbash and the Discharge Criterion give critical velocities of 7.3 m/s and 9.8 m/s respectively for the sack gabions used at the Saemangeum project. This is a difference of 25 %, which makes a useful estimation of the stability of a gabion very difficult. Other literature provides more methods to estimate the stability of gabions, but there is no explicit method to calculate the stability of sack gabions.

The objective of this thesis is: ***"A preliminary study on the stability of sack gabions"***

Theoretical studies, experimental data and practical data will be compared and combined with known formulas for stone stability to result in a formula for calculating the stability of gabions (figure 1.8).

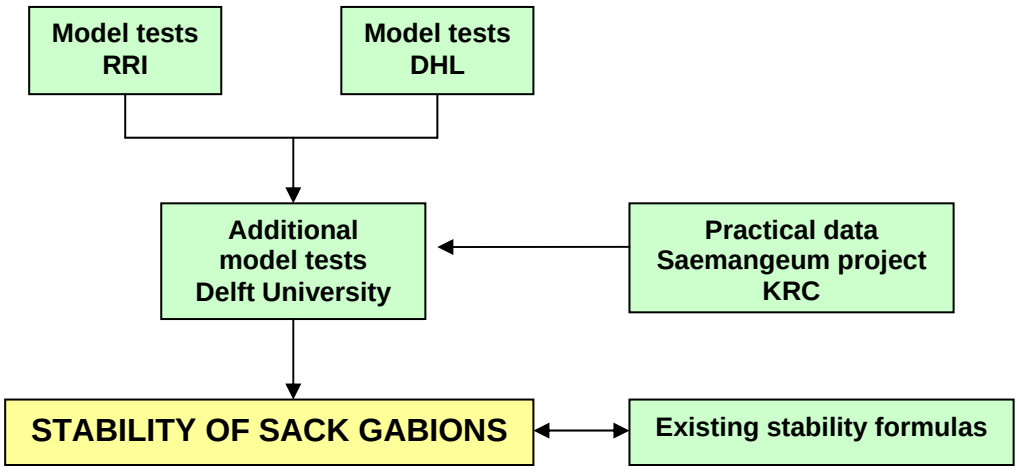

Figure 1.8: Objective of this thesis

Based on model tests done by RRI (Korean Rural Research Institute) for the Saemangeum project (RRI 2004) and DHL (Delft Hydraulics Laboratory) on the stability of stones (DHL (1963 t/m 1985)) some additional model tests at Delft University of Technology have been done in order to find a stability relation for sack gabions. The results of these tests are compared with the RRI model tests, the DHL model tests (annex VIII) and practical data gathered at the Saemangeum project. Based on existing stability formulas, a method to calculate the critical velocity of sack gabions is proposed.

1.4 Structure of this report

In order to find a relation between the weight or volume of a gabion and its critical velocity, several definitions and the applicable theory of stability have to be defined. Therefore in chapter 2 a list of symbols, several definitions, the theory of stability, the difference between a mass and a volume based approach and the most important stability formulas are explained. Chapter 2 is meant as a reference for the rest of the report.

As a base for the Delft model tests, the RRI model tests are used. In chapter 3 an extensive abstract of these model tests on the gabions used at the Saemangeum project is given. Later on in the report the results of the Delft model tests are compared with the results of the RRI model tests.

In chapter 4 the model tests that were done in Delft are described and the results are presented. In the next chapter these results are analyzed and a formula for the stability of gabions is determined.

To evaluate the validity of the results for practical applications, it is important to compare them to practical data. During the field trip to South Korea, a lot of data on the Saemangeum project was gathered. The data that are useful for the evaluation of the stability of gabions is presented in chapter 6.

All data combined leads to several conclusions that are presented in chapter 7. Not all questions on the stability of gabions could be answered and during the process of writing this thesis more questions and ideas came up. These can be found in the recommendations of chapter 8.

A reference list with all literature and web sites used for this report is also added, followed by annexes.

2. Formulas and definitions

In this chapter a general list of symbols used throughout this report is given. Some of these symbols are explained further in paragraph 2.2. The general idea of stability is shortly discussed in paragraph 2.3. Paragraph 2.4 deals with the differences between a volume based approach and a mass based approach in the case of stability of a gabion. The most important formulas on stability are discussed in the last 3 paragraphs of this chapter.

2.1 Symbols

These are the symbols used throughout this report.

Table 2.1: List of symbols

symbol	meaning	value	unit
c	wave celerity	-	m/s
C	Chezy coefficient	-	$\sqrt{}$m/s
d	water depth	-	m
d_*	dimensionless particle diameter	-	-
D_n	nominal diameter	-	m
Fr	Froude number	-	-
g	gravitational acceleration	9.8	m/s^2
h	water depth	-	m
l	length	-	m
L	wave length	-	m
M	mass	-	kg
$_M$	model test conditions	-	-
n	porosity of a gabion	-	-
$_P$	prototype conditions	-	-
Re	Reynolds number	-	-
T	wave period	-	s
u	flow velocity	-	m/s
u_c	critical flow velocity	-	m/s
u_d	depth averaged flow velocity	-	m/s
u_l	local flow velocity	-	m/s
β	flow coefficient	-	-
δ	uncertainty	-	-
Δ	relative density	-	-
v	kinematic viscosity	-	m^2/s
ρ	density	-	kg/m^3
ρ_{fw}	density of fresh water	1000	kg/m^3
ρ_s	density of stone	-	kg/m^3
ρ_{sea}	density of sea water	1030	kg/m^3
ρ_w	density of water	-	kg/m^3
ψ	Shields' parameter	-	-
ψ_c	critical Shields' parameter	-	-

2.2 Definitions

The symbols that need a more clear explanation of their definition are explained in this paragraph. Some explanations use the definition of a mass based approach and a volume based approach. These approaches are explained in paragraph 2.4.

The **nominal diameter** (D_n) is a representative value for the size of a rock or a gabion. According to Schiereck (2001) the side of a cube with the same volume as the considered stone can be taken as the nominal diameter. Because a gabion has a porosity of about 40 % formula [1] does not represent the side of a cube of the total volume of the gabion, however the nominal diameter remains representative as a mass to density ratio, and the stability of single rocks and gabions can be compared based on this relation. According to formula [1] the porosity of a gabion has no influence on its nominal diameter.

$$D_n = \sqrt[3]{\frac{M}{\rho_S}} \qquad [1]$$

Where:

In case of stones:	**In case of gabions, mass based approach:**
M is the mass of the stone	M is the total mass of stones in the gabion
ρ_S is the density of the stone	ρ_S is the density of the stones in the gabion

In the case of **volume based approach** the nominal diameter of a gabion is defined as:

$$D_n = \textit{the height of a gabion} \qquad [2]$$

In the case of sack gabions, the form of the gabion is not clearly defined and a mass based approach will be used. In the case of a cube shaped box gabion a volume based approach is used. If the porosity of a gabion is known (usually about 40 %) these approaches can be compared.

The **relative density** (Δ) of a stone is given by the following relation:

$$\Delta = \frac{\rho_s - \rho_w}{\rho_w} \qquad [3]$$

This formula can also be used for the relative density of a gabion if a **mass based approach** is applied. If a **volume based approach** is used, the formula for the relative density becomes:

$$\Delta = \frac{(1-n)\rho_s - \rho_w}{\rho_w} \qquad [4]$$

The **critical flow velocity** (u_c) of materials regarding their stability is defined as the flow velocity at which the material becomes unstable. This is usually defined as the moment at which incipient motion occurs. This definition is subjective and therefore one should always clearly define the amount of movement for which one speaks about the critical flow velocity.

The **Froude number** (F_r) is the relation between the flow velocity and the wave celerity. If the flow velocity exceeds the wave celerity, the waves can not propagate in the upstream direction. This is called 'supercritical flow'. If the wave celerity exceeds the flow velocity it is called 'subcritical' flow.

$$F_r = \frac{u}{\sqrt{gd}} \qquad [5]$$

If Fr = 1, it is called ***critical flow***. When talking about stability of bed materials, also the term critical flow exists, but with a different meaning. Therefore one should be aware of this difference.

To calculate critical shear stress (ψ_c) a **dimensionless particle diameter** (d_*) can be used;

$$d_* = d\sqrt[3]{\frac{\Delta g}{\nu^2}} \qquad [6]$$

The critical shear stress according to Shields - van Rijn is represented by the graphs in figure 2.1. The line in the graphs depicts the boundary for incipient motion according to Shields (paragraph 2.6). The value for the diameter stated in the upper part of figure 2.1 depends on several variables like the density of the water and the density of the stone. This has to be kept in mind when using figure 2.1.

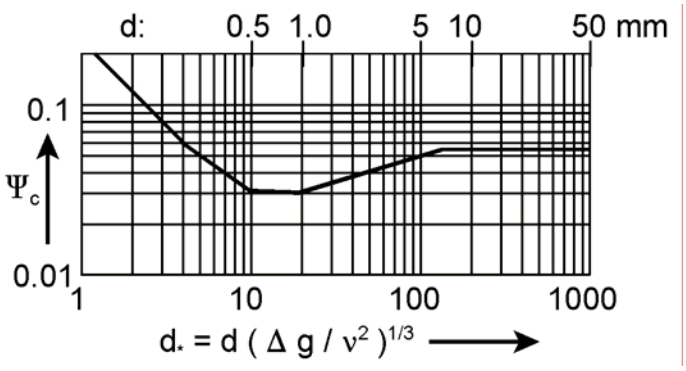

Figure 2.1: Shields van Rijn graph (Schiereck (2001))

2.3 Theory of stability

Regarding the stability of bed materials, an **object** (e.g. grain, stone, rock, gabion) becomes unstable if it moves from one location to another. This is the case if the forces on the object are out of equilibrium. The forces acting on an object are depicted in figure 2.2.

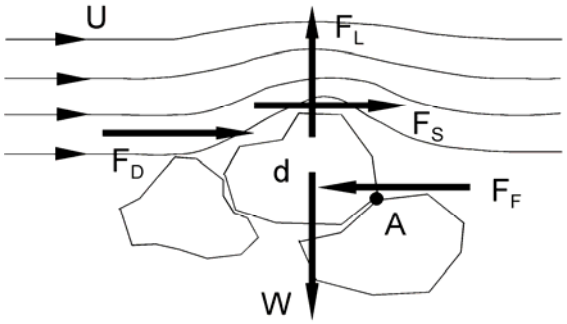

Figure 2.2: Forces acting on an object in a flow (Schiereck (2001))

These forces are a lift force (F_L), the weight of the object (W), a drag force (F_D), a shear force (F_S) and a friction force (F_F).

For a **bed** of stones the definition of instability is more subjective. In Schiereck (2001) 8 stages for different stages of transport are described. This is depicted in figure 2.3.

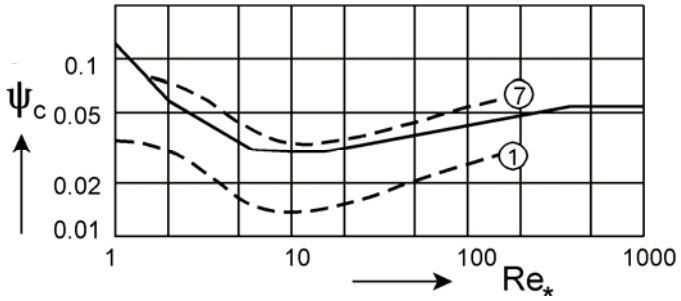

Figure 2.3: Different stages of transport (Schiereck (2001))

The different stages of transport are described as:

0. No movement at all.
1. Occasional movement at some locations.
2. Frequent movement at some locations.
3. Frequent movement at several locations.
4. Frequent movement at many locations.
5. Frequent movement at all locations.
6. Continuous movement at all locations.
7. General transport of the grains.

The Shields criterion for incipient motion (figure 2.1) fits stage 6 rather well.

2.4 Volume based vs. mass based approach

Traditionally a volume based approach is applied to calculate the stability of box gabions or gabion mattresses, where the nominal diameter is defined as the height of the gabion (formula [2]). In the case of a cube shaped box gabion, the stability of the gabion is comparable with the stability of a cube shaped rock with a lower relative density than a solid rock, because of the porosity of the gabion (figure 2.4). This is calculated with formula [4]. Since a gabion is more stable than a rock with the same volume and the gabion relative density, a factor should be added to calculate the stability of the gabion.

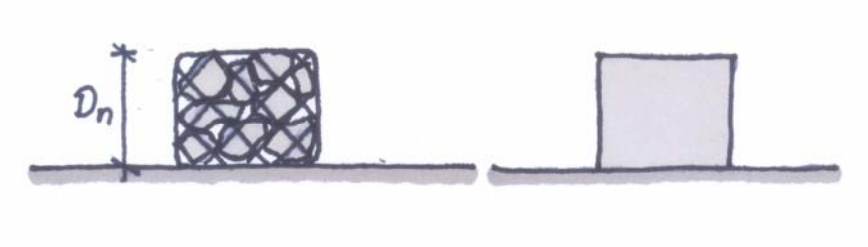

Figure 2.4: Cube shaped box gabion and same size cube shaped rock with lower Δ

The form of sack gabions is irregular and therefore a simple gabion height is hard to define for sack gabions. Instead of using the height, the nominal diameter of a sack gabion is defined by using the mass to density ratio in the same way as with stones (formula [1]). This value does not represent the height of a gabion, since the porosity of the gabion is not taken into account. The stability of a sack gabion is comparable with the stability of a cube shaped rock with a smaller volume than the volume of the gabion and with the same density as the stones in the gabion (figure 2.5). Here also a factor should be added because sack gabions are more stable than solid rocks.

Figure 2.5: Sack gabion and smaller cube shaped rock with same Δ

The physical meaning of the nominal diameter (D_n) and the relative density (Δ) differ in a volume based and a mass based approach, but if the correct method for the calculation of stability is applied, the same result should be found, independent of the applied approach. An example of this can be found on the next page and in annex VIII.

To compare the volume based and the mass based approach, the following values are used:

porosity (n)	= 40 %
rock density (ρ_s)	= 2650 kg/m^3
water density (ρ_w)	= 1030 kg/m^3

These values are comparable with the practical circumstances of the Saemangeum project.

The nominal diameter of a volume based approach ($D_{nVOLUME}$) can now be expressed as the nominal diameter of a mass based approach (D_{nMASS}) times a factor;

$$\Delta_{MASS} D_{nMASS} = \Delta_{VOLUME} D_{nVOLUME}$$

$$\frac{\rho_s - \rho_w}{\rho_w} \times D_{nMASS} = \frac{(1-n)\rho_s - \rho_w}{\rho_w} \times D_{nVOLUME}$$

$$D_{nVOLUME} = 2.9 \times D_{nMASS}$$

This 'representative height' of a sack gabion can not be measured in practice since the form of a sack gabion is irregular. Therefore a mass based approach is recommended when using sack gabions, while a volume based approach is recommended using a box gabion or a gabion mattress. For a 3 ton gabion, both approaches are now compared using Izbash' formula (formula [8]) with β = 0.7;

Mass based;

$$D_n = \sqrt[3]{\frac{M}{\rho_s}} = \sqrt[3]{\frac{3000}{2650}} = 1.04m$$

$$\Delta = \frac{\rho_s - \rho_w}{\rho_w} = \frac{2650 - 1030}{1030} = 1.57$$

$$u_c = x\sqrt{\frac{\Delta D_n 2g}{\beta}} = x\sqrt{\frac{1.57 \times 1.04 \times 2 \times 9.8}{0.7}}$$

$$u_c = 6.76x\frac{m}{s}$$

Volume based;

$$D_n = 2.9 \times \sqrt[3]{\frac{M}{\rho_s}} = 2.9 \times \sqrt[3]{\frac{3000}{2650}} = 3.02m$$

$$\Delta = \frac{(1-n)\rho_s - \rho_w}{\rho_w} = \frac{0.6 \times 2650 - 1030}{1030} = 0.54$$

$$u_c = x\sqrt{\frac{\Delta D_n 2g}{\beta}} = x\sqrt{\frac{0.54 \times 3.02 \times 2 \times 9.8}{0.7}}$$

$$u_c = 6.76x\frac{m}{s}$$

Clearly the same result is obtained using both approaches. x is a factor that is different for different types of bed protection material (like sack gabions or box gabions).

2.5 Izbash' formula for critical velocities

Izbash' formula uses a local velocity and there is no influence of water depth in this equation. The tests were done in 1930 using shallow water conditions and a stone diameter that was relatively large in comparison with the water depth. Izbash focuses on the force action on a single grain. The formulation presented in Schiereck (2001) is:

$$u_c = 1.2\ \sqrt{2\,\Delta\, g\, d} \quad or \quad \frac{u_c}{\sqrt{\Delta\, g\, d}} = 1.7 \quad or \quad \Delta\, d = 0.7\ \frac{u_c^2}{2\, g} \qquad [7]$$

Where in this case d means the diameter of a stone. In Rijkswaterstaat (1995) the formula is slightly adapted to:

$$\Delta D_n = \beta \frac{u_c^{\,2}}{2g} \qquad [8]$$

Where β is a flow coefficient varying from 0.7 for relatively low turbulence (this coincides with the definition used by Schiereck (2001)) and 1.4 for relatively high turbulence.

2.6 Shields' formula for critical velocities

Shields focuses on the average shear stress on the bed. The formula is intended for uniform flow and gives good results in relatively deep water conditions. Shields uses a flow velocity averaged over the entire flow depth in his equation. The water depth is taken into account using the Chezy coefficient. Rijkswaterstaat (1995) gives the following form of the formula:

$$\Delta D_n = \frac{u_d^{\,2}}{C^2 \psi} \qquad [9]$$

The **Chezy coefficient** is a measure for the hydraulic roughness of the stream profile. According to Schiereck (2001) the Chezy coefficient can be determined by various methods like White-Colebrook [10] or Manning-Strickler [11];

$$C = 18 \log\left(\frac{12h}{2D_n}\right) \qquad [10]$$

$$C = 25\left(\frac{h}{D_n}\right)^{\frac{1}{6}} \qquad [11]$$

2.7 Pilarczyks formula for critical velocities

According to CUR (1994) Pilarczyk has added some special factors and coefficients to the formulas of Izbash and Shields to arrive to the following formula for making a preliminary assessment of the size of rock and rock related units, designed to resist current attack in various civil engineering applications. The formula is presented as follows;

$$\frac{U^2/2g}{\Delta' D'} = \frac{\psi_{cr}'}{0.035}\Lambda_h' k_{sl} k_t^{-2} \frac{1}{\varphi_{sc}} \qquad [12]$$

Where:

- 0.035 = “reference” critical Shields value (-)
- k_t = turbulence factor (-)
- k_{sl} = slope factor (-)
- Λ_h’ = special depth factor (-)
- Ψ_{cr}’ = system-dependent Shields-type stability number (-)
- D’ = Characteristic size of the protection element (m)
- Δ’ = relative density of the protection element (-)
- Φ_{sc} = geometry-determined stability factor for current (-)

The further use of this formula and these variables is explained in CUR (1994), sub-section 5.2.4.1. This formula is mentioned because it was used by RRI for stability calculations (table 3.3 & 3.4). It is not known to me which values were used by RRI for the variables in formula [12].

3. Rural Research Institute model tests

In order to successfully close the Saemangeum estuary in South Korea, RRI (Korean Rural Research Institute) performed scale model tests on the stability of rocks and gabions in their hydraulic laboratories in Ansan (figure 3.1). In this chapter a summary of these tests follows. The information from table 3.1 to 3.6 and figures 3.2 to 3.10 is derived from RRI (2004) and the information of table 3.7 and figure 3.11 is taken from Wallingford (2005).

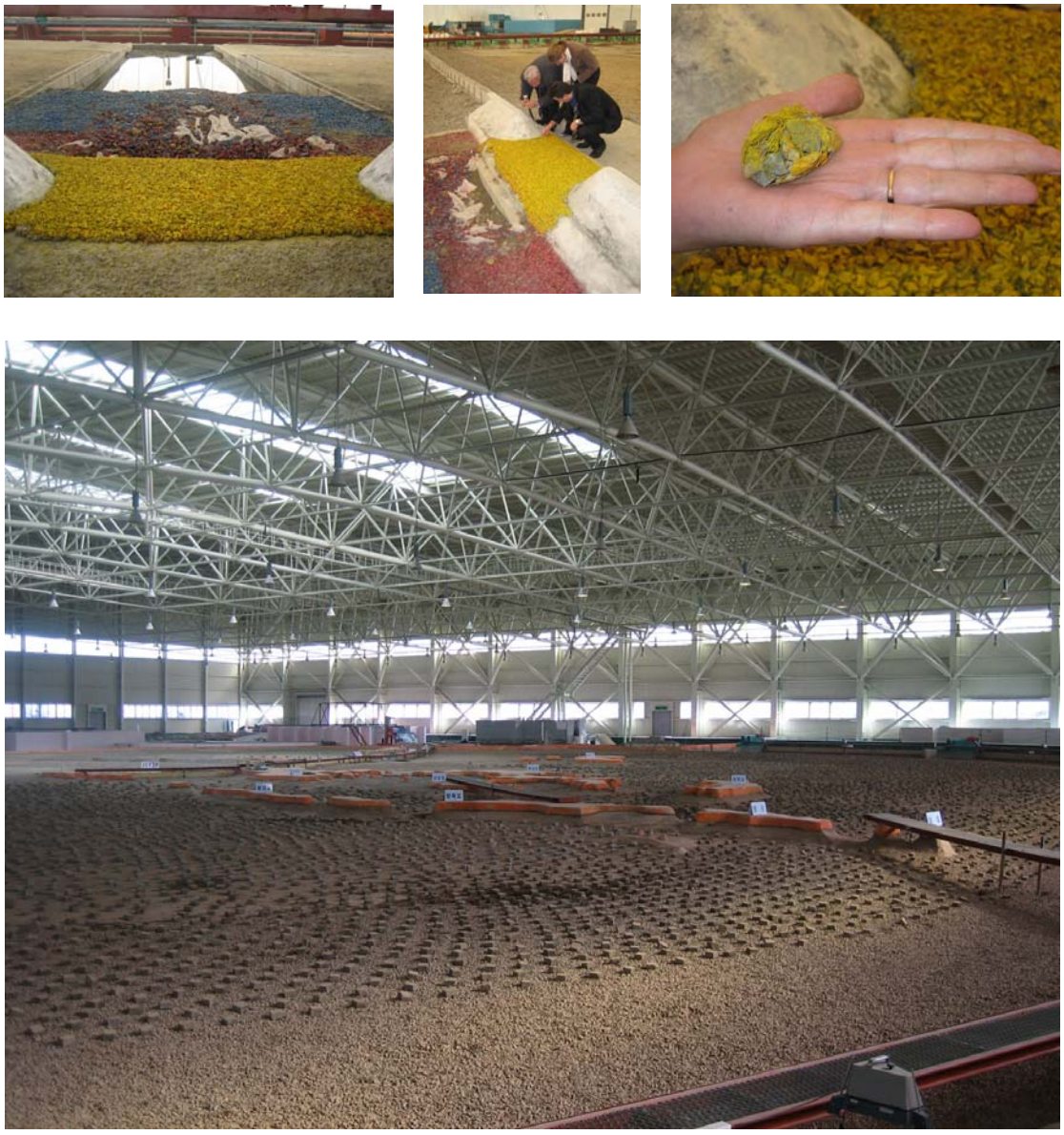

Figure 3.1: RRI hydraulic laboratory in Ansan

3.1 Test properties

The **scales** of the tests are stated in table 3.1. As can be seen from this table, the geometrical scale is 1:50 and the scales are based on a Froude scale. A summary of the **sample properties** is given in table 3.2.

Table 3.1: Scales of the tests

	Symbol	scale ratio
Length	Lr = Lp/Lm	50
Velocity	$Lr^{0.5}$	7.07
Discharge	$Lr^{2.5}$	17,678
Area	Lr^{2}	2,500
Froude number	1	1

Table 3.2: Sample properties

Weight Prototype (Ton)	Weight Model (g)	Diameter Nominal (mm)	Diameter Average (mm)
0.3	2.07	9.2	11.4
1.0	6.9	13.7	17.0
2.0	13.79	17.2	21.4
3.0	20.69	19.7	24.5

As **stability criteria** were taken:

For bed/sill: If 1 to 3 stones or gabions move, the bed/sill is unstable. (Incipient motion)

For dumping process: If 20 % or more of the material does not reach the intended location, the dumping process is unstable.

A general idea of the **measures** used in the model tests in Ansan can be seen in figure 3.2. The distances given are in prototype conditions, so the actual measures in test conditions are 50 times smaller.

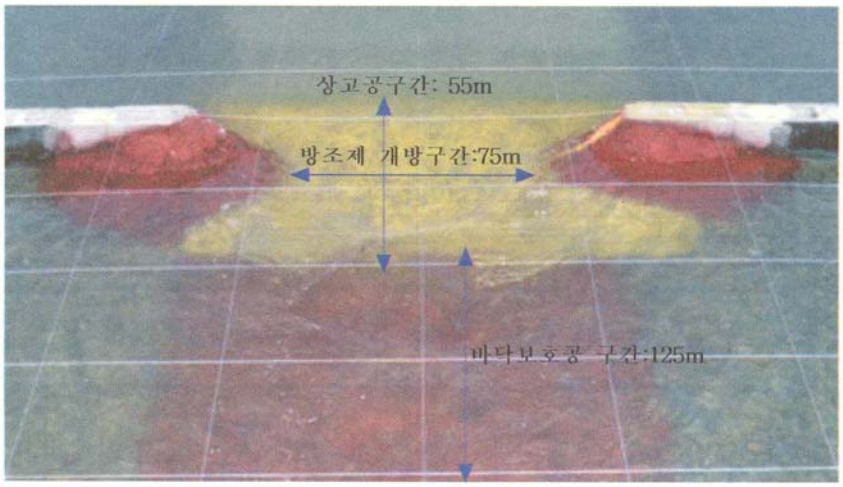

Figure 3.2: Measures used in the model tests

3.2 Sill tests

Tests on the stability of rocks (figure 3.3) and gabions (figure 3.1) in the sill of the Saemangeum dam have been done. A comparison between the results of these tests and the stability formulas of Izbash [8] and Pilarczyk [12] is given in table 3.3 and figure 3.4.

Figure 3.3: Sill test setup

Table 3.3: Results of sill tests

Sample weight (ton)	critical velocity (m/s)	Izbash β=0.7 (m/s)	Pilarczyk (m/s)
0.3 (rock)	4.40	4.6	4.0
1.0 (rock)	5.09	5.7	4.9
2.0 (rock)	6.01	6.4	5.5
3.0 (rock)	6.72	6.8	5.9
3.0 (gabion)	8.49	-	-

Figure 3.4: Graph of the sill test results

3.3 Bed protection tests

Tests on the stability of rocks and gabions (figure 3.5) in the bed protection of the Saemangeum dam have been done by RRI. A comparison between the results of these tests and the stability formula of Pilarczyk [12] is given in table 3.4 and figure 3.6.

Figure 3.5: Bed protection test setup

Table 3.4: Results of bed protection tests

Sample weight (ton)	Critical velocity (m/s)	Pilarczyk (m/s)
0.3 (rock)	3.89	4.2
1.0 (rock)	4.70	5.1
2.0 (rock)	5.52	5.7
3.0 (rock)	6.22	6.1
3.0 (gabion)	8.49	-

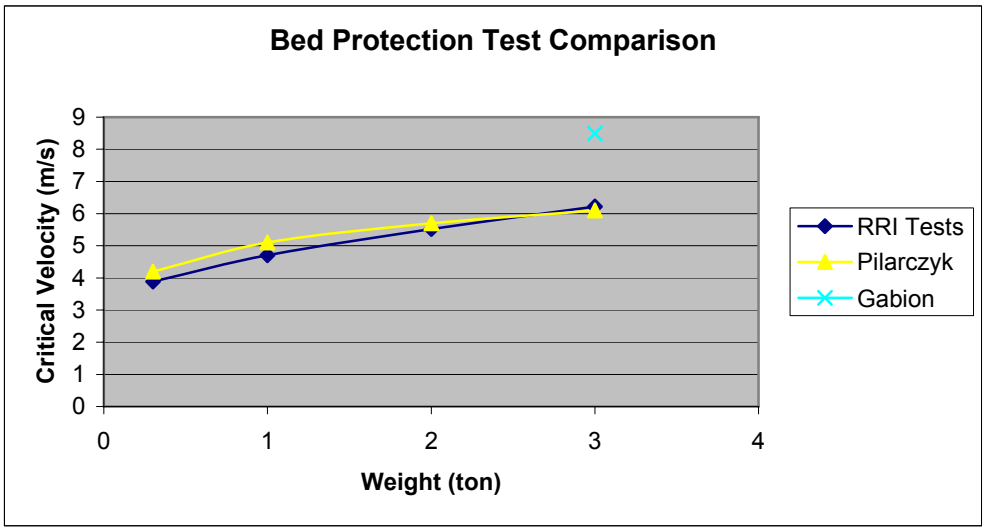

Figure 3.6: Graph of the bed protection test results

3.4 Dam head tests

Tests on the stability of rocks (figure 3.7) and gabions in the dam heads of the Saemangeum dam during the closure have been done by RRI. A comparison between the results of these tests and the stability formulas of Izbash [8] and a formula that RRI calls 'Netherlands' is given in table 3.5 and figure 3.8. It is not clear which formula is meant by 'Netherlands'.

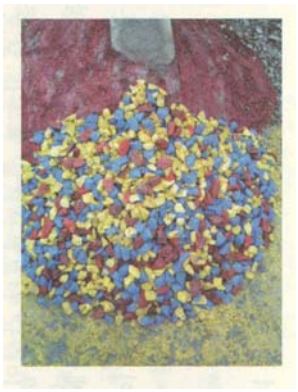

Figure 3.7: Dam head test setup

Table 3.5: Results of Dam head tests

Sample weight (ton)	critical velocity (m/s)	Izbash β=0.7 (m/s)	Netherlands (m/s)
0.3 (rock)	4.00	3.5	3.6
1.0 (rock)	4.85	4.3	4.4
2.0 (rock)	5.38	4.8	4.9
3.0 (rock)	5.76	5.2	5.2
3.0 (gabion)	7.02	-	-
5.0 (gabion)	7.78	-	-

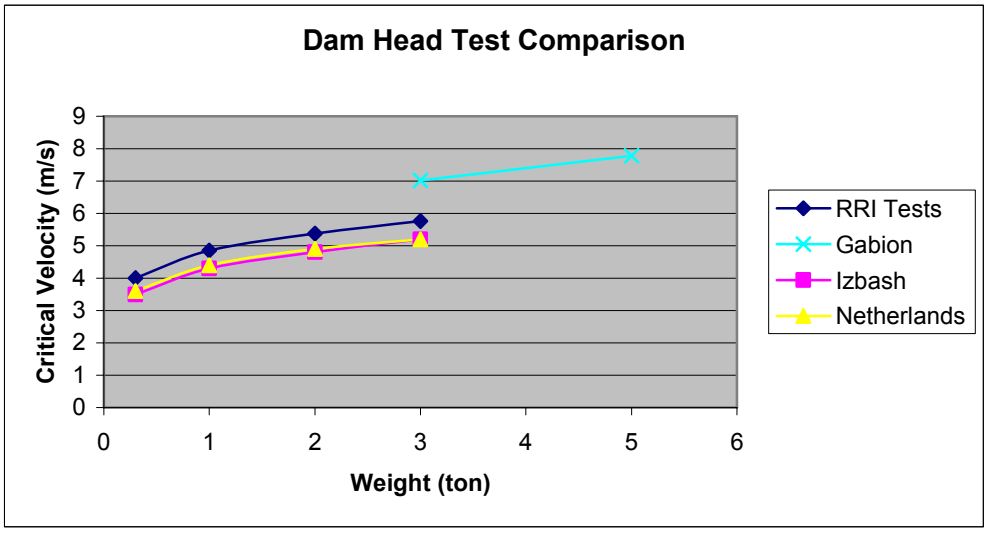

Figure 3.8: Graph of the dam head test results

3.5 Dumping process tests

Tests on the stability of rocks and gabions during the dumping process (figure 3.9) of the Saemangeum dam during the closure have been done by RRI. The results of these tests are given in table 3.6.

Table 3.6: Results of dumping process tests

Sample weight (ton)	critical velocity (m/s)
1.0, 2.0, 3.0 (rock)	6.36
1.0, 2.0, 3.0 (rock) 80 % + 3.0 (gabion) 20 %	7.07
1.0, 2.0, 3.0 (rock) 70 % + 3.0 (gabion) 30 %	7.20

Figure 3.9: Dumping of rocks

3.6 Rock-gabion mixtures

In Wallingford (2005) there is a summary of the RRI test results on the stability of rock-gabion mixtures (table 3.7) and a derivation of the stability relations of these mixtures (figure 3.10).

Table 3.7: Stability of rock gabion mixtures

Place	Gap	Phase	Weight (rock)	Amount (rock)	Weight (gabions)	Amount (gabions)	u_c settled	u_c dumping
			(ton)	(%)	(ton)	(%)	(m/s)	(m/s)
Bed			0.5-1.0	90	2.0	10	4.7	5.06
Sill	1		2.5-3.0	50-90	3.0	10-50	6.7	5.89
Sill	2		4.0-5.0	50-90	3.0	10-50	-	-
Dike	1	1	1.5-3.0	70	3.0	30	7.2	6.15
Dike	2	1	1.5-3.0	60	3.0	40	7.2	-
Dike	1	2	3.0-5.0	80	3.0	20	-	5.89
Dike	2	2	3.0-6.0	80	3.0	20	-	6.31
Dike	1	3	3.0-5.0	70	3.0	30	-	6.15
Dike	2	3	3.0-6.0	50	3.0	30	-	7.18

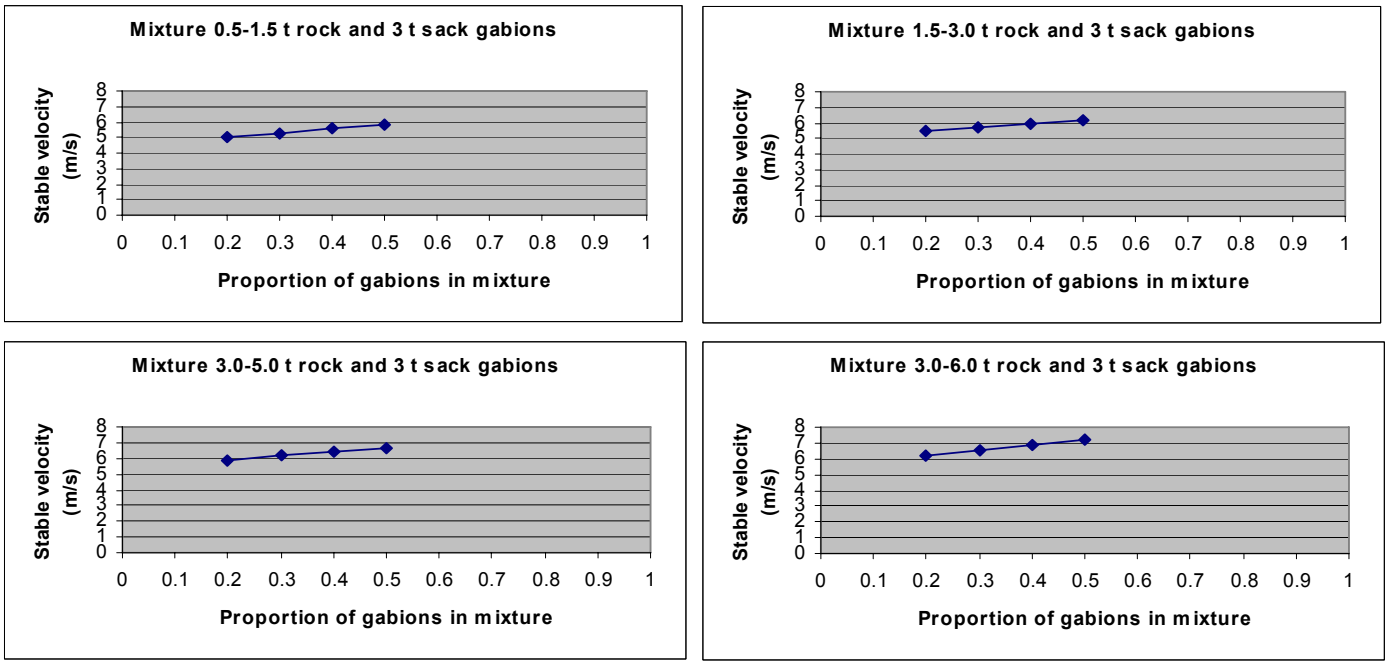

Figure 3.10: Graphs of the stability of rock gabion mixtures

The stable velocities of the gabion rock mixtures, with a proportion of gabions from 0.2 to 0.5 and β = 0.7, can be calculated using these formulas:

0.5 t - 1.5 t rock with 3 t sack gabions: $u_c = 2.6074x + 4.5$ [13]

1.5 t - 3 t rock with 3 t sack gabions: $u_c = 2.3481x + 5$ [14]

3 t - 5 t rock with 3 t sack gabions: $u_c = 2.513x + 5.4$ [15]

3 t - 6 t rock with 3 t sack gabions: $u_c = 3.2296x + 5.6$ [16]

Where x is the proportion of gabions in the mixture.

3.7 Analysis of RRI model tests

Of all tests done by RRI, the ones on the bed protection and the sill construction are the most interesting for this report, because these are the most comparable with the situation of settled sack gabions, on which additional model tests in Delft were done (chapter 4). A factor for a rock gabion mixture depending on the weights of the rocks and gabions, and the percentage of gabions used, may be deducted from the Wallingford data. These data can be compared with the data collected at the Saemangeum project (chapter 6).

In general it can be concluded that the stability of a mixture increases with an increasing percentage of gabions. Gabions alone are more stable than when applied in mixtures.

4. Delft model tests

From the 24th of July 2006 until the 4th of August 2006, several tests were done in the Fluid Mechanics Laboratory of Delft University of Technology in order to get more insight in the behavior of gabions. These tests are described in this chapter and the results are presented.

4.1 Objectives of the tests

The objectives of the stability tests on gabions at Delft University of Technology are:

- To determine the mode of failure of gabions.
- To determine the relation between mass and critical velocity of model gabions.

4.2 Sample properties

To determine the critical velocity of prototype gabions using model tests, the outcomes of the tests will have to be scaled. Using scale rules for every model weight the scaled critical velocity of several prototype weights will be determined.

The samples are chosen in a way that the maximum flow velocity in the flume will be used at the heaviest model gabion. From the RRI test results and test runs in the flume it is determined that a 300 g gabion is the upper limit for the gabion model mass to fail in the flume.

To get reliable results with the tests several different weights are tested. The lightest model gabion uses a different stone with a different density, because there were no stones available with the same density that would give enough stones in the 50 g model gabion. If a model gabion smaller than 50 g would be used, the holes in the net would be too large and the stones would simply fall out of the net. This determines the lower model mass boundary.

The tests are done on beds of model gabions with 4 sample masses. Their properties are stated in table 4.1. As a reference for existing formulas on stone stability, also 2 tests were done on beds with different stone masses in similar circumstances.

Table 4.1: Sample properties

Type	Mass (g)	Accuracy (g)	Density (kg/m^3)	Amount of stones
Gabion	50	+/- 1	2460	7 - 12
Gabion	100	+/- 2	2280	10 - 14
Gabion	200	+/- 2	2280	12 - 16
Gabion	300	+/- 2	2280	10 - 14
Stone	100	+/- 5	2280	-
Stone	200	+/- 10	2280	-

The model gabions are made with nets that have a mesh with diagonals of 6 mm. The amount of stones per net is limited by the mesh size, the available stones, and the desired gabion mass. Therefore not all model gabions have the same amount of stones. The range of stone amounts however is considered realistic to represent the behavior of real size gabions.

Figure 4.1: Samples of 50 g, 100 g, 200 g and 300 g

The model gabions are intended to represent the behavior of the real gabions that were applied in the Saemangeum project in South Korea. The porosity of the model gabions is about 40 %, which is similar to prototype conditions.

Since not all samples are made with the same type of stone (figure 4.1), the densities of the samples differ. The model gabions were weighed during the manufacturing process. The weight had to be within the accuracy range in order for the gabion/stone to be used in the tests. In practice this means that the weight of the model stones/gabions is representative for the individual weight of a failing stone/gabion.

The gabion nets are made of plastic and are flexible. This corresponds to the tests done by RRI.

4.3 Equipment

The most important equipment that is used in the tests is described in this paragraph.

A **flume** (figure 4.2) in the Fluid Mechanics Laboratory of Delft University of Technology was used for the tests. The flume has the following properties:

Length of the flume:	15 meters
Width of the flume (inside):	40 cm
Maximum Discharge:	Approximately 0.4 m^3/s

The discharge of the flume can be controlled by a valve at the upstream side of the flume. The flow velocity can be decreased or increased by turning a weir at the downstream side of the flume up or down respectively.

Figure 4.2: Flume at Delft University of Technology

The **local flow velocities** are measured by a **Vectrino** (figure 4.3). This is a 3 dimensional echo sounding device. In order to get accurate measurements, the water should not be to clear. Therefore a **hydrogen generator** is placed upstream of the Vectrino so there are small hydrogen bubbles in the water that the Vectrino can detect.

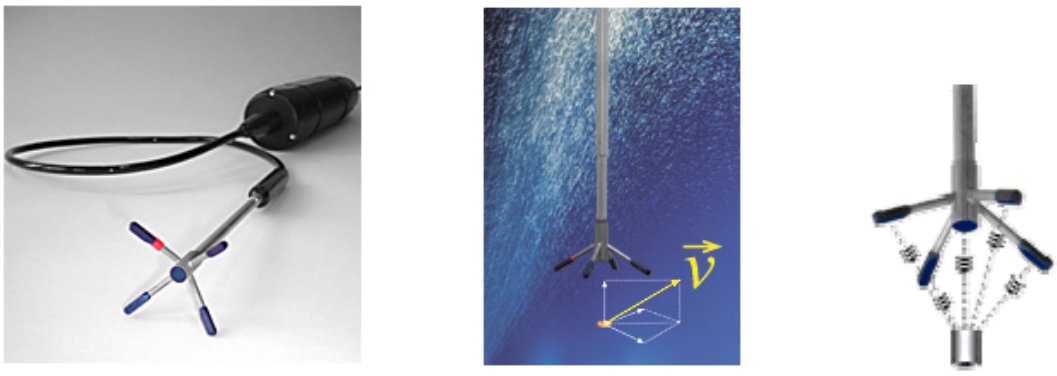

Figure 4.3: Vectrino (http://www.nortek-as.com)

This device measures the flow velocity in 3 directions. This gives an insight in the flow velocity in the direction of the flow as well as in the turbulence. The probe area is a cylindrical volume at a distance of 5 mm from the probe, with a diameter of 6 mm and a height that can be chosen by the user, in this case 7 mm.

4.4 Tests

The way in which the tests were done is described in this paragraph.

The **test setup** is meant to create circumstances comparable with reality. Because the flume has a smooth bottom, a bed of stones and gabions is placed as a layer for the actual samples to be placed on (figure 4.4).

Figure 4.4: Side and top view of the test bed

At the upstream side a stone bed (average mass of 150 g) with a length of 60 cm is placed to create some turbulence. Next, a 300 g gabion bed with a length of 30 cm is placed, to make a bed for the samples with properties similar to reality. At the downstream side another stone bed (average mass of 150 g) with a length of 60 cm is placed to prevent the gabion bed from washing away because of instability at the rear end of the gabion bed. Because the tests are done in high flow velocities, the bed is covered with a net to prevent the bottom layer of stones to wash out. The average height of the test bed is 7 cm and 2 layers of samples are placed on top of this.

Over the samples, the vectrino is placed on a distance of 12 to 20 mm, in a way that a clear reading is obtained as close to the samples as possible. The hydrogen generator is placed at the upstream side of the Vectrino to create detectable hydrogen bubbles in the flow. The test setup is shown in figure 4.5.

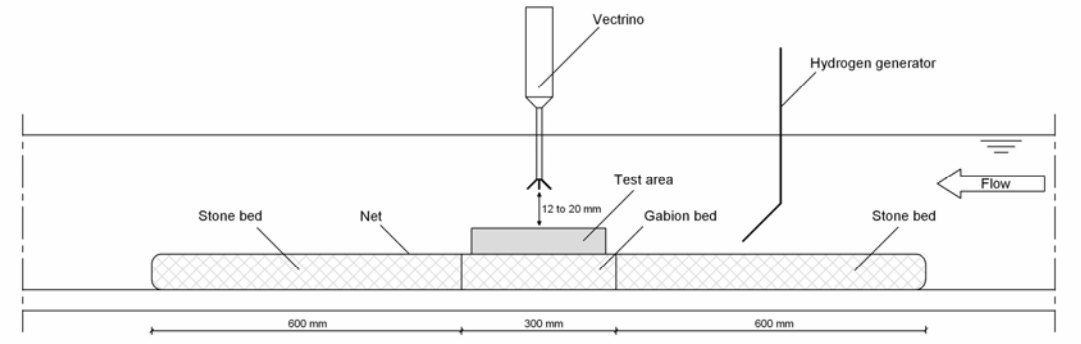

Figure 4.5: Test setup

The **test procedure** is as follows: A bed of samples is placed on the test bed for each test. This is done by dropping the samples from the water surface to create a bed comparable with reality, where the gabions are dumped from split barges or dump trucks. Samples that settle outside the bed are taken out of the water and are dropped again.

The flow velocity is increased step by step by lowering the weir at the downstream side of the flume. One step is equal to a turn of 2 teeth of the sprocket that turns the weir up or down, which corresponds to about 0.05 m/s flow velocity difference.

When one or more gabions move out of the bed into the downstream area of the sample bed (figure 4.6), the local velocity is measured. We then speak of 'incipient motion' and 'critical velocity'. Each test is done at least 3 times to decrease the influence of chance.

Figure 4.6: Test setup just after occurrence of incipient motion

In total, 20 tests are done:

- 3 tests per gabion mass
- 3 tests per stone mass
- 2 tests on 100 g gabions that are manipulated by compressing the test setup

The Vectrino measures the local velocity in the probe area 25 times per second and displays the average velocity per second. The velocity that occurs when one or more of the samples fail is called the 'critical velocity'. The output of the tests can be found in annex I. The Vectrino gives the velocities in 3 directions, u(x) is the flow velocity in the direction of the flow, u(y) is the horizontal flow velocity perpendicular to the flow direction and u(z) is the vertical flow velocity perpendicular to the flow direction. At t = 0 s incipient motion occurred.

4.5 Test results

The measurement data can be found in annex I. These tables give the local flow velocities just above the sample bed from 5 seconds before until 5 seconds after incipient motion has occurred. The results presented in this paragraph are based on observations and readings during the tests.

Failure mode

During the tests a qualitative analysis of the failure mode of gabions was made. A brief description of the way gabions move and eventually fail is presented in a 5 stage development:

1) At first some stones inside the gabions and some gabions itself move a little and settle in a more stable manner than before. This is not seen as incipient motion, but as stabilizing.

2) Then for a range of flow velocities, the bed remains relatively stable.

3) The smaller outer stones inside the gabions start to vibrate, but the gabions remain stable.

4) If the critical velocity is reached, 1 or more gabions will start to move significantly. Mostly if 1 gabion fails, one or more neighboring gabions will also fail, because the first gabion stabilized them.

5) After incipient motion occurs the rest of the bed often remains stable for a considerable increase of the flow velocities. (Because the flow velocity in the flume is restricted to 1.4 m/s, these values could not be measured).

When failing some movement will occur within the gabion, but separate stones will not actually change places, the general positions are maintained. The gabion will roll as a whole when failing, changing form slightly by relative movement of the stones inside.

A large difference between the failure mode of a bed of gabions and a bed of stones is that in a bed of stones the amount of failing stones gradually increases, while the bed of gabions gives a sudden failure of several gabions at the same time and then remains relatively stable again. This behavior should be considered when designing a bed protection of gabions.

Critical velocities

The critical velocities of the samples that were determined during the Delft model tests on sack gabions are presented in table 4.2. (Also see annex I).

Table 4.2: Delft model test results

Test	Type	Mass (g)	Stone density (kg/m^3)	u critical (m/s)	Average (m/s)	+/- (m/s)
1a	Gabion	50	2460	0.98	**0.95**	0.03
1b	Gabion	50	2460	0.93		
1c	Gabion	50	2460	0.95		
2a	Gabion	100	2280	1.14	**1.11**	0.03
2b	Gabion	100	2280	1.08		
2c	Gabion	100	2280	1.10		
3a	Gabion	200	2280	1.23	**1.25**	0.02
3b	Gabion	200	2280	1.27		
3c	Gabion	200	2280	1.25		
4a	Gabion	300	2280	1.36	**1.36**	0.01
4b	Gabion	300	2280	1.35		
4c	Gabion	300	2280	1.36		
5a	Stone	100	2280	1.03	**0.99**	0.04
5b	Stone	100	2280	0.96		
5c	Stone	100	2280	0.99		
6a	Stone	200	2280	1.05	**1.11**	0.06
6b	Stone	200	2280	1.16		
6c	Stone	200	2280	1.11		
7a	Gabion	100	2280	>1.29	Samples did not fail	
7b	Gabion	100	2280	>1.34	Samples did not fail	

From tests 7a and 7b follows that compressing the test setup increases the stability of a gabion bed significantly. A bed of 100 g model gabions was tested to the maximum possible flow velocity in the flume twice. Failure did not occur, while for the non-compressed tests the 100 g gabions failed at 1.11 m/s.

The tests were intended to determine a lower boundary value for the threshold of motion for gabions. Therefore these values should be seen as conservative.

It has to be taken into account that only 3 tests were performed per model. The more tests the more reliable the results.

+/- gives the value of the maximum deviation from the average. The deviation from the average is determined by the largest difference from a measured value with the averaged value. It should be noted that the real accuracy will be slightly less because only 3 tests were done. If the deviations from the averaged values of the gabion sample measurements are compared it can be seen that the greater the gabion mass, the higher the accuracy. This coincides with expectations since the relative difference in the measurements should decrease with increasing mass.

The error of the measurements is analyzed in annex II by means of a quadratic summation of the partial derivatives of each variable that is used to calculate the prototype critical velocity of formula [17].

5. Analysis of Delft test results

In the previous chapter the data that were collected during the model tests in Delft are presented. These data will be further analyzed in this chapter. First, a representative value for the critical velocities of different sizes of gabions will be determined. With this information a gabion factor to be used in existing stability formulas is calculated.

5.1 Scales

The scales are based on the stability number. Using these scaling rules, the Froude number in model and prototype conditions is similar. The Reynolds numbers are very high because of the large stone diameters in the model and prototype gabions, which give a constant critical shear stress (ψ) in both model and prototype conditions (figure 2.1).

Using formula [1] for the nominal diameter of a gabion (applying a mass based approach) these scales are calculated as follows:

$$D_n = \sqrt[3]{\frac{M}{\rho_S}} \qquad [1]$$

Scaling based on the stability number:

$$\left(\frac{u^2}{\Delta D_n}\right)_P = \left(\frac{u^2}{\Delta D_n}\right)_M$$

$$\frac{u_P^2}{u_M^2} = \frac{\Delta_P D_{nP}}{\Delta_M D_{nM}}$$

$$\frac{u_P^2}{u_M^2} = \left(\frac{\Delta_P}{\Delta_M}\right)\left(\frac{M_P}{\rho_{sP}}\right)^{\frac{1}{3}}\left(\frac{\rho_{sM}}{M_M}\right)^{\frac{1}{3}}$$

$$\frac{u_P^2}{u_M^2} = \left(\frac{\Delta_P}{\Delta_M}\right)\left(\frac{M_P}{M_M}\right)^{\frac{1}{3}}\left(\frac{\rho_{sM}}{\rho_{sP}}\right)^{\frac{1}{3}}$$

This leads to the following equation:

$$u_P = u_M \bullet \sqrt{\left(\frac{\Delta_P}{\Delta_M}\right)\left(\frac{M_P}{M_M}\right)^{\frac{1}{3}}\left(\frac{\rho_{sM}}{\rho_{sP}}\right)^{\frac{1}{3}}} \qquad [17]$$

Using equation [17], for every model gabion mass, the corresponding critical velocity for prototype masses of gabions is calculated. The result can be seen in table 5.1 and figures 5.1 and 5.2. The material density used for prototype conditions (ρ_P) is 2650 kg/m^3 which gives a relative density (Δ_P) of 1.64 (as used by RRI (2004) and Wallingford (2005) for the gabions of the Saemangeum project). Other values are calculated using the formulas of chapter 2.

Table 5.1: Scaled critical velocities for prototype gabions (ρ_P = 2650 kg/m^3)

Model gabions				Prototype gabions: critical velocities (m/s)			
M	ρ	Δ	$u_{critical}$				
(kg)	(kg/m3)	-	(m/s)	Mass (kg) →	1000	2000	3000
0.050	2460	1.46	0.95	→	5.18	5.82	6.22
0.100	2280	1.28	1.11	→	5.68	6.38	6.83
0.200	2280	1.28	1.25	→	5.70	6.40	6.85
0.300	2280	1.28	1.35	→	5.76	6.47	6.90
				Representative value	5.7	6.4	6.8

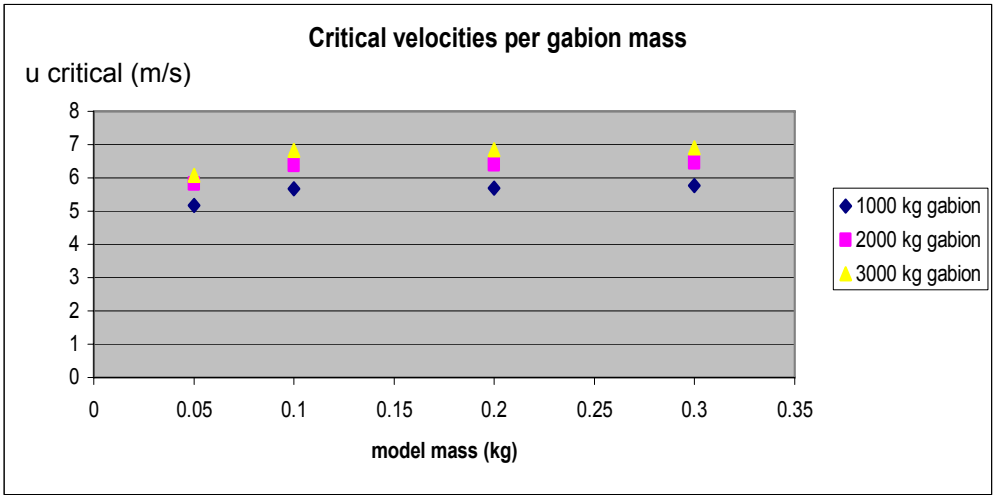

Figure 5.1: Scaled critical velocities per prototype gabion

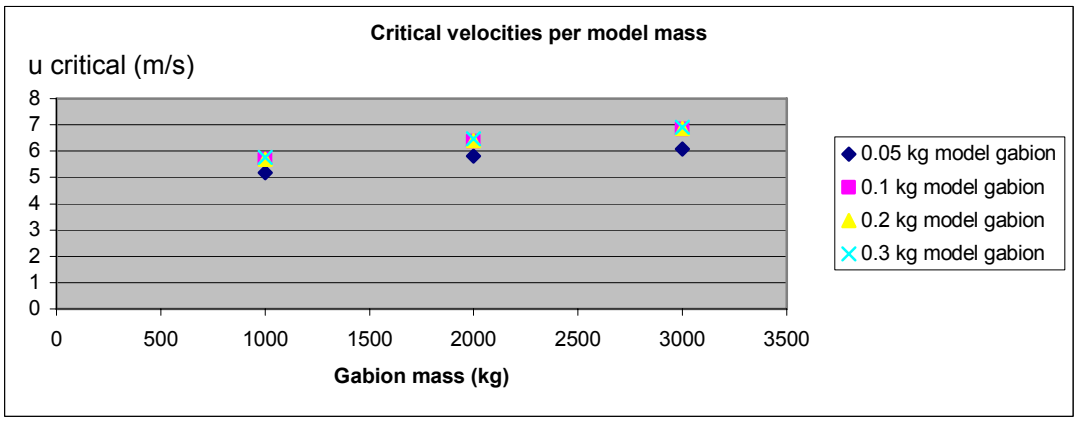

Figure 5.2: Scaled critical velocities per model gabion

The representative value for the critical velocities of the prototype gabions is taken as the lowest value from the scaled model tests. Since this is done with only one decimal and the values only differ little, this is almost equal to the averaged value of the three scaled critical velocities.

The values coming from the 0.05 kg model gabion give significantly lower values than the other model gabions. This is caused by the higher model density that has a relatively big effect in the applied formula [17]. A higher density decreases the lift force and the drag force (smaller area for the hydraulic load in comparison with the weight of a gabion) which should lead to a higher critical velocity than the critical velocity that is shown in table 5.1. This low value for the critical velocity might be caused by turbulence effects that have a relatively large effect on the relatively small gabions.

To use the model test results in a formula, the formula should be calibrated using loose stones as a reference. Since the reference tests are done on loose stones with a density similar to the ones used in the model gabions of 0.1, 0.2 and 0.3 kg, the dustbin factor that will be determined from these tests only holds for model gabions of the same density. Since no reference tests have been done on loose stones with a density of 2460 kg/m^3 the formula can not be calibrated for the 0.05 kg model gabion, and therefore these values will not be considered in determining a gabion coefficient.

To get an idea of the error in the calculated values due to uncertainties in the measurements, annex II calculates the error based on a quadratic summation of the partial derivatives for each of the variables in formula [17].

5.2 Formula for critical velocities of gabions

In chapter 2, 3 formulas to calculate the stability of stones in a flow were presented: Izbash [8], Shields [9] and Pilarczyk [12]. Each of these formulas has its advantages and disadvantages. In this paragraph these formulas will be compared in order to determine the most favorable formula for calculating the stability of a gabion using the results of the Delft model tests.

In the model tests, the local flow velocities were measured with a Vectrino. Since Izbash' formula uses the local flow velocities, while Pilarczyk and Shields use the depth averaged flow velocity, the results of these measurements will be most comparable with Izbash.

The water depth in the flume was relatively small and the water surface was strongly curved over the sample bed. The sample bed itself was not entirely flat, and if a sample failed, the height of the bed changed at that location. This means that an accurate reading of the water depth at the exact location of the bed failure could not be obtained within a reasonable accuracy. Since Pilarczyk and Shields both use the water depth in their formula to calculate the critical velocity, Izbash is the preferred method to use in this case.

The sample configuration was a bed of gabions, instead of a single gabion. This is more comparable with Shields than with Izbash.

All three methods do not clearly define the term 'incipient motion'. This remains a subjective matter.

According to Schiereck (2001) Shields gives better results in deep water than Izbash. In the model tests the relative depth (h/d, with d = the diameter of a stone) remained below the value of 10 (5 > h/d > 10). In this range for ψ ~ 0.04 (figure 2.3, high Reynolds number, stage 4), according to figure 5.3 Izbash is conservative in comparison with Shields.

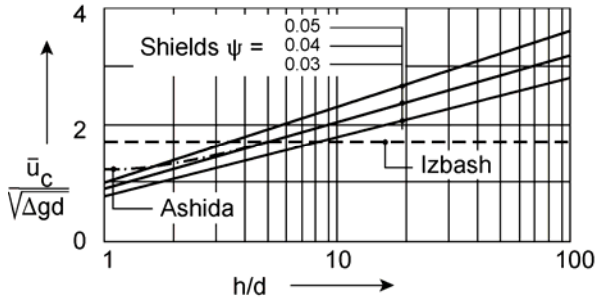

Figure 5.3: Comparison between Izbash and Shields (Schiereck (2001))

In general **Izbash'** formula [8] seems to be the most suited formula to calculate the stability for a gabion based on the Delft model tests.

5.3 Gabion coefficient

The reference tests on loose stones will be used to calibrate Izbash' formula for the stability of stones in hydraulic loads. Izbash' formula uses a local velocity and there is no influence of water depth in this equation. In Rijkswaterstaat (1995) the form of Izbash' formula is given as:

$$\Delta D_n = \beta \frac{u_c^{\ 2}}{2g} \qquad [8]$$

Where β is a flow coefficient varying from 0.7 for relatively low turbulence and 1.4 for relatively high turbulence.

Using this equation, the factor β is determined to get the best fitting results for the model tests done on loose stones in Delft. The results can be seen in table 5.3. β is determined to be 0.9. In this case other factors might influence the value of β, and β should be seen as a dustbin factor instead of merely a flow coefficient.

Table 5.3: Stability calculations using Izbash' formula with β = 0.9

	Izbash	Delft tests
Stone mass	u critical	u critical
(g)	(m/s)	(m/s)
100	0.99	0.99
200	1.11	1.11

It should be noted that the accuracy of the tests on loose stones was less than the accuracy of the tests on gabions, because the form of each stone is very different from each other stone, while the form of gabions is much more similar to one another.

To get a useful formula to calculate the critical velocity of a gabion, a stability factor for gabions (**γ**) is introduced to Izbash' formula. This method is comparable with the method that is proposed in Wallingford (2005) to use a representative stone diameter for gabions. In order to keep the formula transparent, the gabion factor is added on the right side of the equation. Izbash' formula then becomes:

$$\Delta D_n = \frac{\beta}{\gamma} \frac{u_c^{\ 2}}{2g} \qquad [18]$$

Where **γ = Gabion stability factor.**

Using the results of the Delft model tests γ can be determined for the model gabions. The test results are compared and a best fit for a calculation is looked for. This is done in figure 5.4. The purple line depicts the best fit for the test results. Using this figure γ is determined to be 1.26. The results of the calculations with this gabion stability factor are shown in table 5.4 and figure 5.4.

Table 5.4: Calculation of gabion stability (β = 0.9, γ = 1.26)

Gabion mass (kg)	Test result & scaled $u_{critical}$ (m/s) ρ_P = 2650 kg/m^3	Gabion Izbash $u_{critical}$ (m/s) ρ_P = 2650 kg/m^3
0.100	1.11	1.11
0.200	1.25	1.25
0.300	1.35	1.34
1000	5.7	5.7
2000	6.4	6.4
3000	6.8	6.8

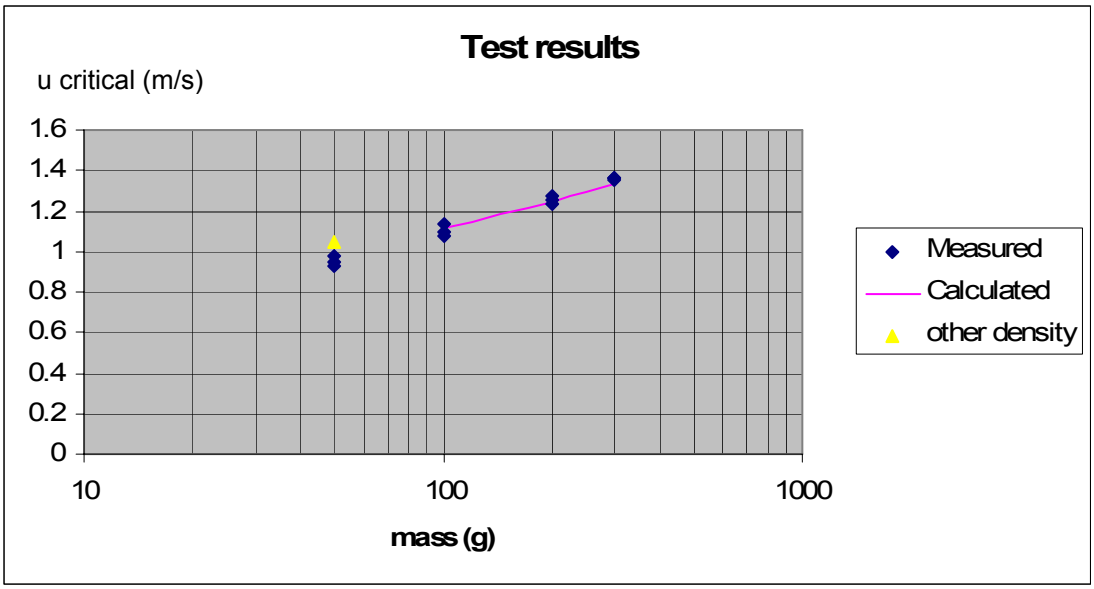

Figure 5.4: Measured vs. calculated values (semi-logarithmic scale)

The results of the calculations using the adapted Izbash' formula and γ = 1.26 are almost exactly the same as the results from the Delft model tests and the scale calculations. In prototype conditions the formula is correct within one decimal.

5.4 Conclusions on the analysis

It is proposed to use Izbash' formula with a gabion stability factor (γ) to calculate the stability of a gabion bed. When **γ = 1.26** is used in a mass based approach, a conservative lower boundary for incipient motion of a gabion bed is calculated. Izbash' formula then takes the form of equation [18] (using a local flow velocity). The variables used in formula [18] are explained in chapter 2 of this report.

$$\Delta D_n = \frac{\beta}{\gamma}\frac{u_c^{\,2}}{2g} \qquad [18]$$

Where γ = 1.26 for sack gabions (γ = 1 for loose rocks)

If a value for β of 0.7 is used, and the local velocity is converted to a depth averaged velocity, the results of the Delft model tests can be compared with the results of the RRI model tests. In prototype conditions, using equation [18], for a 3 ton gabion the critical velocity would be:

$$u_c = \sqrt{\frac{\Delta\gamma D_n 2g}{\beta}} = \sqrt{\frac{1.64\times1.26\times1.04\times2\times9.8}{0.7}} = 7.77\,\frac{m}{s}$$

Compared with the velocity profile of the ADCP measurement (figure 6.15), the local near bed velocity is about 8.85 % lower than the depth averaged velocity which gives a depth averaged velocity of 8.46 m/s for the scaled results of the Delft model tests. This result is comparable with the result of RRI. Table 3.3 gives a value for the depth averaged critical velocity of a 3 ton gabion of 8.49 m/s.

It is advised to use formula [18] to determine a conservative lower boundary value for the critical velocity of sack gabions.

6. Saemangeum practical data

The data that was collected at the Saemangeum project is used to analyze the stability of the sack gabions and rock-gabion mixtures that were applied during the closure. In order to get useful results it is necessary to compare the damage that occurred during the closure with the flow velocities that were present. Also the exact materials that were applied on the locations where damage occurred must be known.

In paragraph 6.1 the materials used in the sill construction of the last remaining gaps in the dam that were submitted to heavy flow loads are shown. In paragraph 6.2 to 6.8 the occurred maximum flow velocity is estimated. In paragraph 6.9 the occurred damage is described. Finally an estimation can be made of the critical velocity for the sill materials in paragraph 6.10.

6.1 Sill and bed protection design

In annex III and figures 6.2 and 6.3, the geometry of gap 1 and 2 of the Saemangeum project can be seen in plan view. A model of the cross section of the design of the Saemangeum dam is shown in figure 6.1.

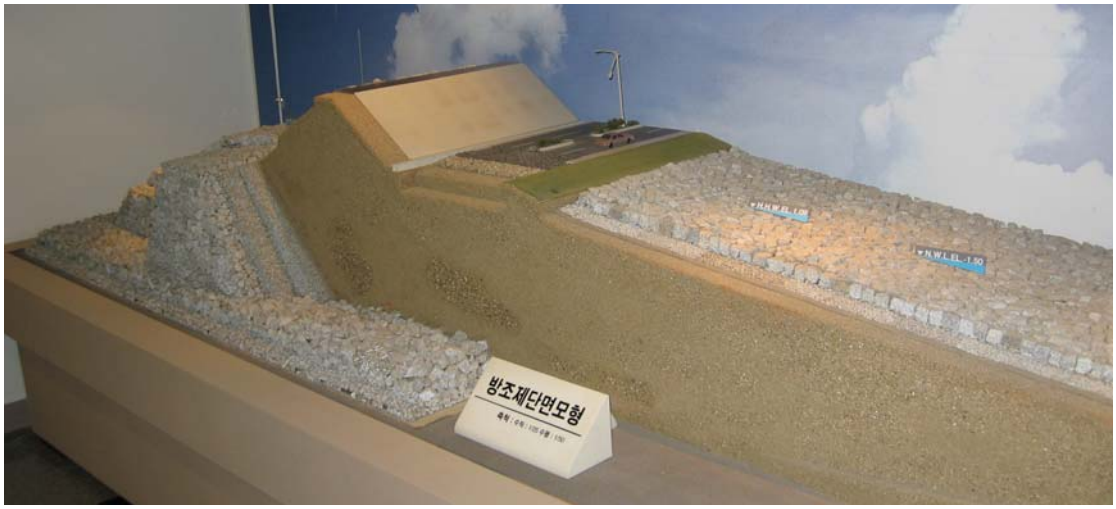

Figure 6.1: Model of the cross section of the Saemangeum dam

From figure 6.2 and 6.3 it can be seen that on the locations where the highest flow velocities are expected the most stable mixtures are applied (At the downstream end of the highest part of the sill, in the middle of the gap. The orange part is the last part of the gap that will be closed). In this case for gap 1 a mixture of 50 % rocks weighing 3.0 to 5 tons and 50 % 3.0 ton gabions and for gap 2 a mixture of 50 % rocks weighing 1.0 to 5.0 tons and 50 % 3.0 ton gabions are applied.

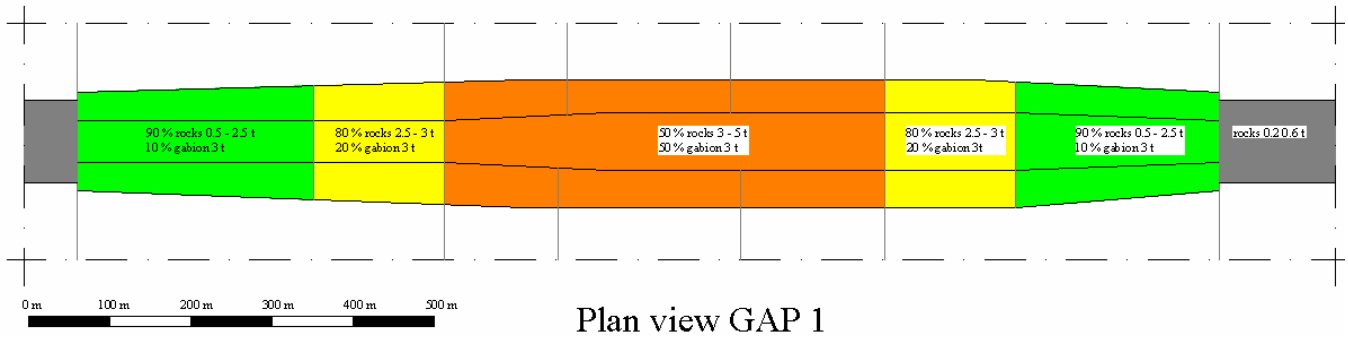

Figure 6.2: Plan view of the Saemangeum sill, gap 1

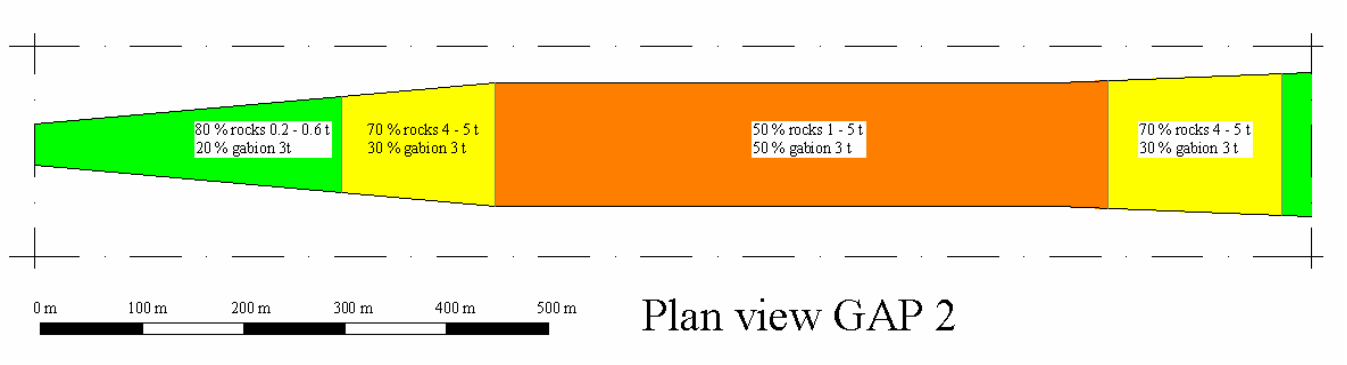

Figure 6.3: Plan view of the Saemangeum sill, gap 2

The total width of gap 1 is 1350 m, and the depth is 10 m. The total width of gap 2 is 2850 m, and the depth is 16 m.

According to the results of the RRI model tests of chapter 3 these mixtures have a critical velocity of about **6.7 m/s** (figure 3.10 and formula [15]).

Using a storage area approach and data gathered at the Saemangeum project, the flow velocities that actually occurred during the closure will be estimated and compared with this value.

6.2 Storage area approach

To get an insight in the flow velocities that occurred during the closure of the Saemangeum estuary, a basic Storage area approach was used (made in close corporation with Maartje van der Sande, van der Sande (2006)). The basics of this approach and the results of the calculations are presented in this paragraph and in annex V of this report.

According to Battjes (2002) the Storage area approach may be applied if the dimensions of a reservoir are small in respect to the wave length. A value for the boundary is given by the following formula:

$$L_{reservoir} < \frac{L_{wave}}{20} \qquad [19]$$

Where:

$L_{reservoir}$ = A representative length of the reservoir

L_{wave} = The wave length of an incoming wave

The wave celerity of a low translation wave can be calculated as follows:

$$c = \sqrt{gd} \qquad [20]$$

The average depth of the Saemangeum reservoir is estimated to be 10 m with an average water level of MSL (figure 6.4). In that case the wave celerity is about 10 m/s. According to Battjes (2001), the following relation is valid:

$$c = \frac{L}{T} \qquad [21]$$

For a tidal wave with a wave period T of 44700 seconds and a celerity of 10 m/s, this leads to a wave length of 447 kilometers, which is much more than 20 times the reservoir length (which is about 20 x 15 km = 300 km, figure 6.4). In this case, the Storage Area Approach can be used.

The **river discharge** data of the Saemangeum estuary can be found in table 6.1.

Table 6.1 Average River Discharge (m^3/s)

Season	Spring	Summer	Autumn	Winter
Northern River	23	90	17	8
Southern River	20	74	17	8

In comparison with the average tidal discharges through the gaps in the order of tens of thousands m^3/s (annex V), the river discharges can be neglected completely.

The tidal levels outside the reservoir are calculated every 10 minutes by constructing a sinusoidal function between the spring and neap tide at the location of Gunsan Outer Port, which is near the project site (original tidal predictions can be found in annex IV). This data is provided by KRC.

From the water level difference, using a weir equation, the specific discharge over the sill of the sluice can be calculated. The weir equation according to Rijkswaterstaat (1995) for a submerged weir is as follows:

$$q = \mu(h_{downstream} - H_{sill})\sqrt{2g(h_{upstream} - h_{downstream})} \qquad [22]$$

Where:

q	= specific discharge	(m^2/s)
μ	= coefficient	(-)
$h_{downstream}$	= water level downstream of the sluice	(m, Mean Sea Level)
$h_{upstream}$	= water level upstream of the sluice	(m, Mean Sea Level)
H_{sill}	= height of the sill	(m)
g	= gravitational acceleration	(m/s^2)

μ is taken 0.9 (CUR (1994)) but according to Wallingford (2005) this value might increase to about 1.1 during the closure due to less loss of flow energy with a smaller gap width.

With this discharge formula, the volume of water that flows into the reservoir is calculated for each time step of 10 minutes. This volume is assumed to spread equally and instantly over the reservoir storage area, which depends on the water level in the basin as can be seen in figure 6.4 and table 6.2 (the steep part in the graph at 390 km^2 is due to dikes surrounding the reservoir area). From these data, the new water level in the reservoir is calculated, and the procedure starts over again.

Table 6.2: Bathymetry of the reservoir area

Water Level m (MSL)	Storage Area (km2)
-4	121.274.915
-3	160.472.758
-2	208.638.874
-1	254.921.250
0	301.661.598
1	347.002.023
2	374.678.676
3	390.866.630
4	394.042.402

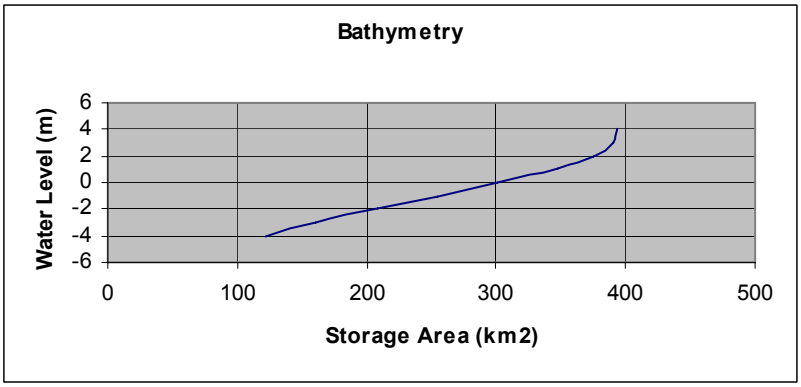

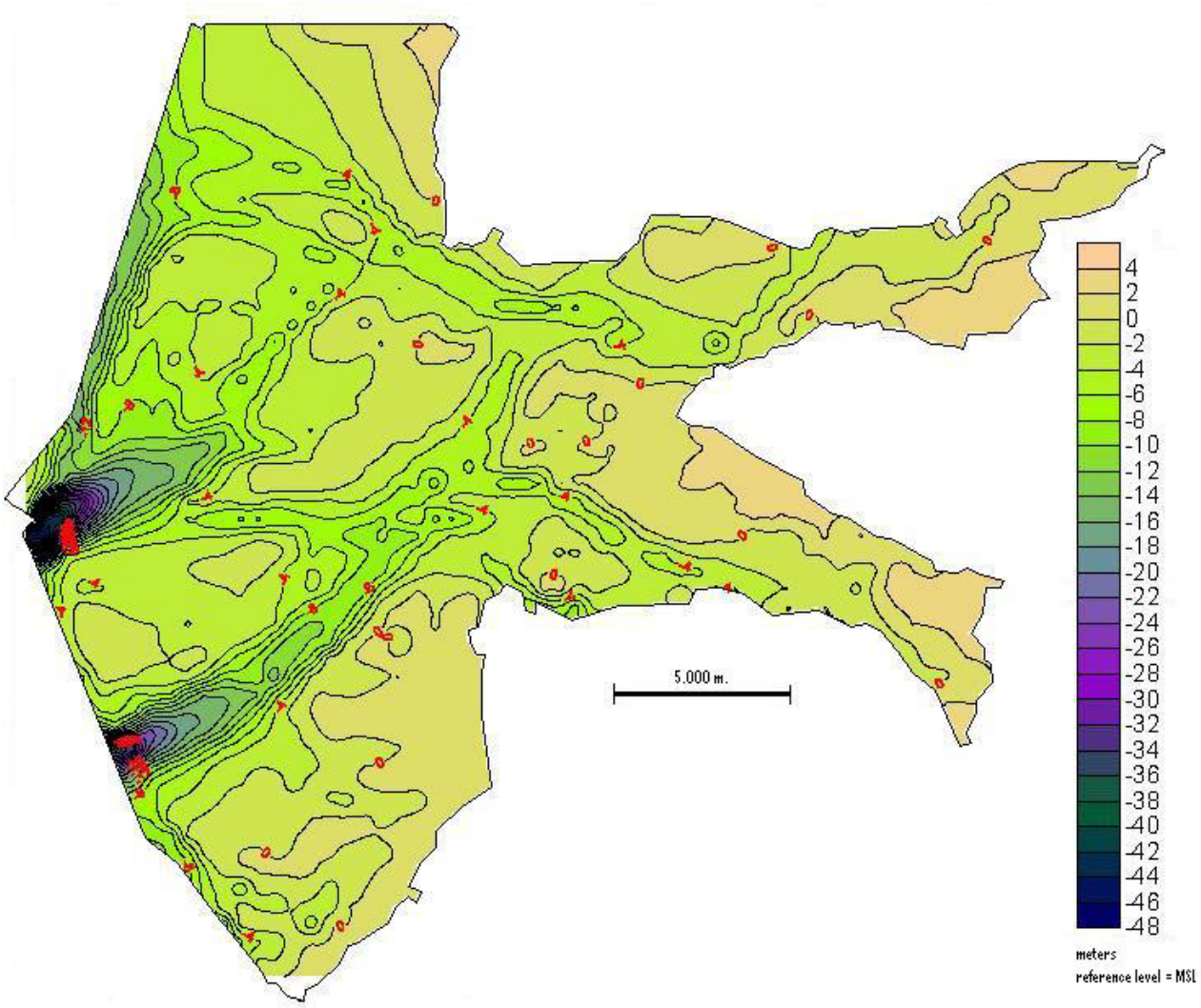

Figure 6.4: Bathymetry of the reservoir area

The depth averaged flow velocity is assumed to be maximal at the downstream side of the sill (see figure 6.5) because the water depth is the smallest there. The specific discharge divided by the difference of the downstream water level and the sill level is taken as the depth averaged flow velocity.

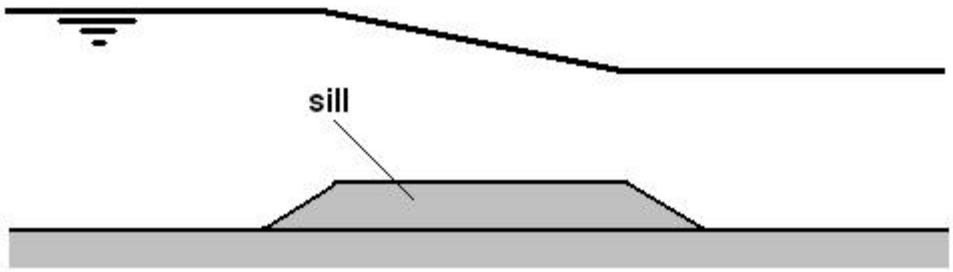

Figure 6.5: Simplified water level difference over sill

The closure of the estuary is also taken into account in the storage area approach. In table 6.3 the input data for the widths of the closure gaps and sluices as well as their depths are given. It must be kept in mind that this approach is very basic, and that the outcome will be an estimation of the vertically averaged flow velocities.

Table 6.3: Input data for the storage area approach

Geometry	wgap1	=	1600	m
	dgap1	=	-10	m MSL
	wgap2	=	1100	m
	dgap2	=	-16	m MSL
	wsluices	=	540	m
	dsluices	=	-6.5	m MSL
	μ	=	0.9	-

		Width Gap 1	Width Gap 2
		m	m
Start	24/03/2006	1600	1100
Waiting period 1	30/03/2006 - 02/04/2006	1300	660
Waiting period 2	14/04/2006 - 16/04/2006	530	310
Final closure	21/04/2006	0	0

The results of the storage area approach are given in annex V. Only the data of April 15th and 18th are given because these were the days with the maximum flow velocities. A graph of the complete result from March 15th to April 21st 2006 can be seen in figure 6.6. During the closure, the amount of water flowing in and out of the basin decreases. This causes the level differences between the sea water level and the basin water level to increase. As can be seen in annex IV, spring tide occurs at April 16th. Around this period also the maximum flow velocities occur.

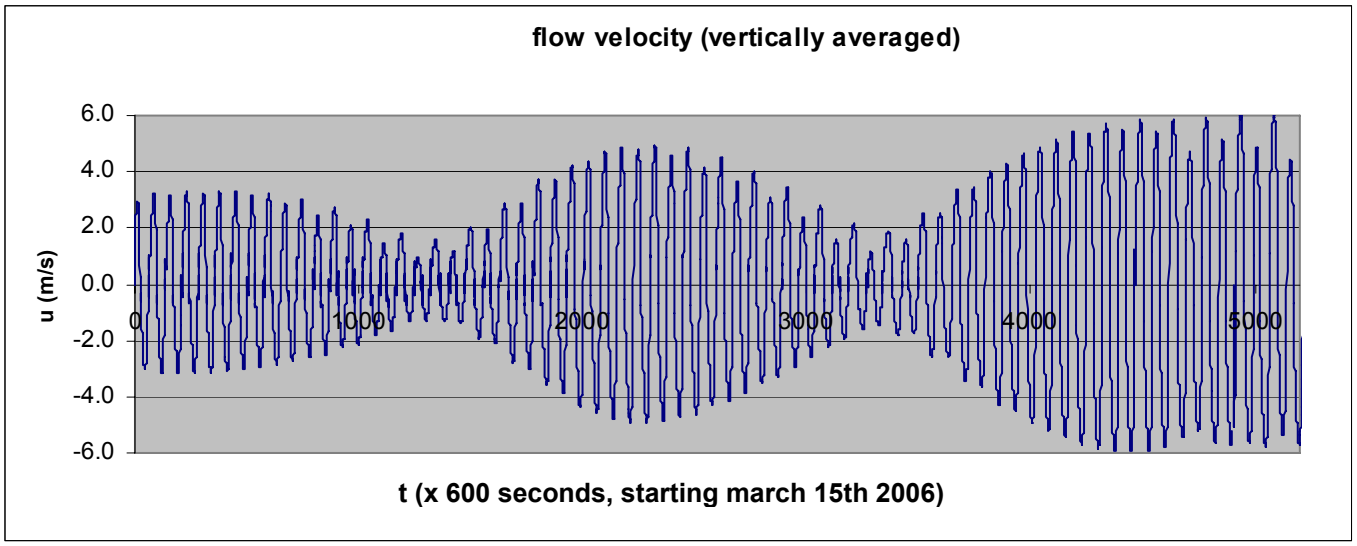

Figure 6.6: Flow velocities during the final closure of the Saemangeum estuary

The weir equation of formula [22] is only valid with a submerged weir. In the Lissajous figure of figure 6.7, the ratio of water depth (relative to the top of the sill) on the sea side and on the basin side is depicted (blue lines).

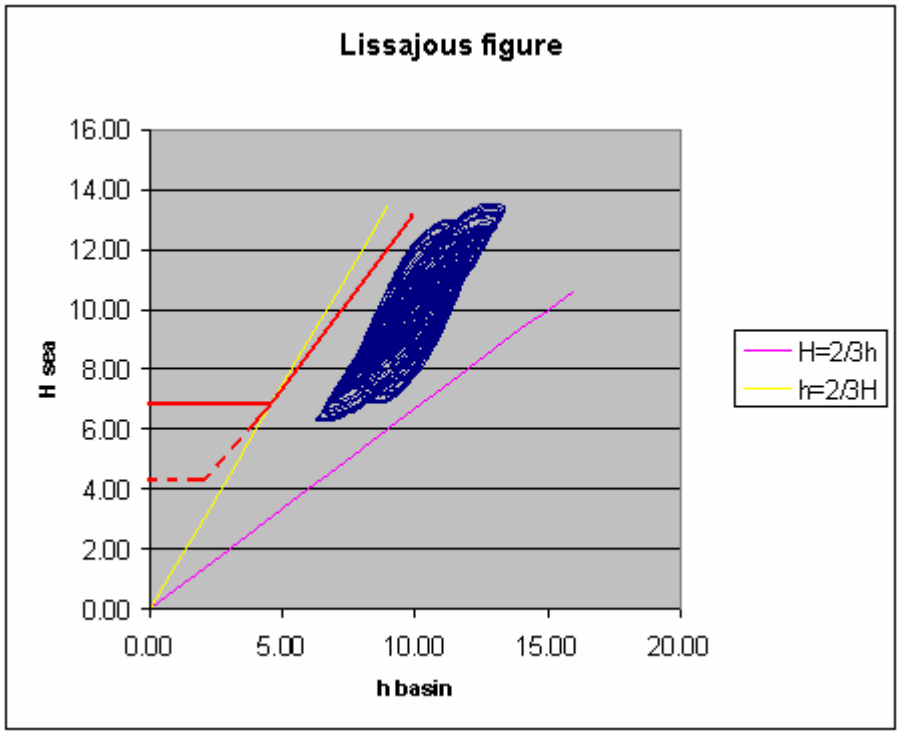

Figure 6.7: Lissajous figure of the Saemangeum closure (March 15 to April 21 2006)

Several remarks need to be made regarding the stability of objects in a hydraulic load. As long as the water level differences are within the borders of H > 2/3 h (purple line in figure 6.7) and h > 2/3 H (yellow line in figure 6.7) the weir is submerged (figure 6.8). This is the case for the Saemangeum project. In this case the flow velocity and the stability of objects in a hydraulic load can be directly related to the water level difference (formula [22]).

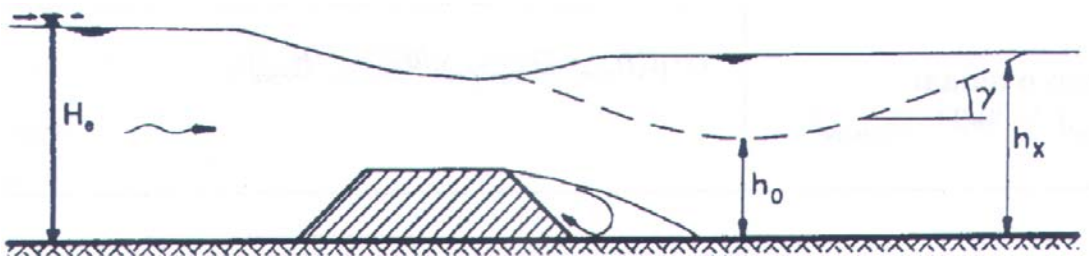

Figure 6.8: Submerged weir (Rijkswaterstaat (1995))

If the boundaries for a submerged weir are exceeded, the weir becomes a free flow weir (figure 6.9). In this case, the flow velocity upstream of the weir does not change with changing downstream waterlevels and this suggests that the stability of an object remains constant (red line in figure 6.7, constant flow velocity). The turbulence effects and the very shallow water on the downstream side of the weir have a significant influence on the stability of the weir material, and in practice the stability will still decrease (dotted red line in figure 6.7), despite the constant flow velocity upstream of the weir. One should always consider the water level difference instead of just the flow velocity to determine the stability of objects in current attack.

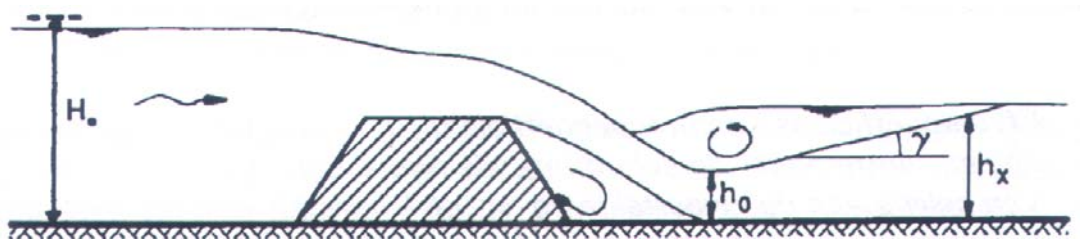

Figure 6.9: Free flow weir (Rijkswaterstaat (1995))

At the Saemangeum project a horizontal closure was applied. This caused the sills to remain submerged at all times during the closure, as can be seen in figure 6.7. In a horizontal closure the sill can also become a free flow weir. If a vertical closure is applied the sill becomes a free flow weir eventually.

The results of the storage area approach show that the minimum and maximum flow velocities that occurred during the closure of the Saemangeum estuary were -6.0 m/s (flow from basin to sea) and 6.0 m/s (flow from sea to basin).

Since Wallingford (2005) suggests that the value of μ might increase from 0.9 to 1.1 during the closure, table 6.4 gives the outcomes of flow velocities with varying μ. 1.0 is considered the best value for μ during the spring tide of April 16th, based on CUR (1994) and Wallingford (2005). A higher value for μ influences the flow velocities, discharges and water level differences, so the maximum flow velocities can not just be multiplied by μ. The new velocities must be calculated using the entire storage area approach.

Table 6.4: Maximum flow velocities with varying μ

μ	u_{max}
0.9	6.0 m/s
1.0	**6.5 m/s**
1.1	7.1 m/s

The storage area approach calculates that the maximum (depth averaged) flow velocities during the closure are in the order of **6.5 m/s**.

6.3 EFD output

To get an impression of the local flow velocities and turbulence, the computer program EFD (Engineering Fluid Dynamics) is used. This program originates from the oil and gas industry and is meant to calculate flow velocities and pressures in pipelines, but when the program is adapted to input a frictionless virtual roof over the free water surface, it can be used for calculations with free water surfaces as well. EFD takes into account the level of turbulence, but it is not yet clear if this is done in a correct manner. At the moment this report is written, the model is still in the process of being calibrated (van der Sande (2006)). Using an uncalibrated model makes the reliability of the results questionable; therefore the results should be analyzed carefully.

Wilco Meijerink of Rijkswaterstaat made several preliminary calculations using a simple model of the Saemangeum dam. The geometry of the sill, dam heads and gaps can be seen in figure 6.8. The input for the sea level is taken MSL +3.00 m and the reservoir level is taken MSL +0.5 m, in order to reproduce circumstances of expected maximum water level differences.

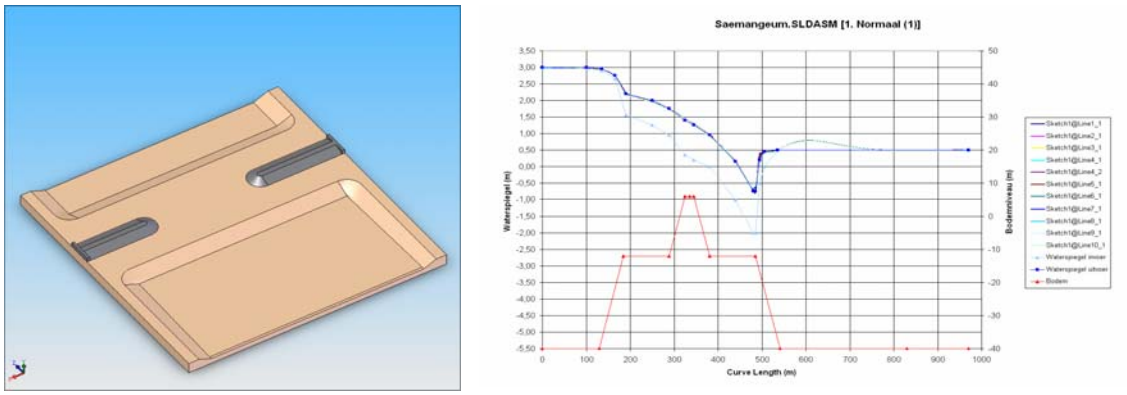

Figure 6.8: Input of the EFD model. Left: geometry, right: Water surface

The results of these computer calculations are shown in figure 6.9.

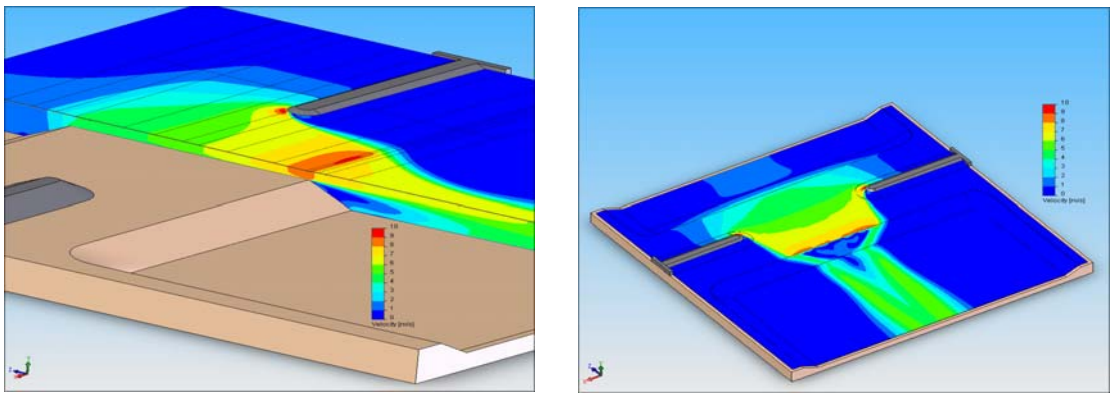

Figure 6.9: Flow velocities. Left: vertical section and surface. Right: near bottom

The areas where the highest flow velocities occur are at the dam heads and at the end of the sill. The calculated maximum local flow velocity using the EFD model is **10.54 m/s**. This value seems very high in comparison with the outcomes of the storage area approach. The major differences between the storage area approach and the EFD model are:

- The EFD model calculates a local flow velocity while the storage area approach calculates a depth averaged flow velocity.

- The water level difference used to determine the maximal flow velocity in the EFD model it is 2.5 m while for the storage area approach this is 2.29 m. Using a water level difference of 2.5 m in the storage area approach would give a maximum flow velocity of 7.0 m/s, which still is much less than the 10.54 m/s for the EFD model.

- The EFD model estimates the turbulence level and takes this into account calculating the flow velocities.

A big disadvantage of using the results of the EFD model is that for me it is a 'black box model'. From an input an output is generated, but the exact method is not known to me. The results of the EFD model seem very high and will be compared with other data from the Saemangeum project to determine the reliability of its outcomes.

6.4 Delft 3D output

KRC made some calculations of the flow velocities for the Saemangeum project using the computer program Delft 3D. The output of this calculation can be seen in annex VI. Only data of March 25th and March 26th 2006 are available. On these dates, the tidal difference was not maximal and the flow velocities were not as high as during spring tide. The flow velocities that were calculated using Delft 3D are between 3 m/s and 3,5 m/s around 16.00 h on March 26th. In the storage area approach this value is 3.2 m/s maximum (using $\mu = 1$). This means that the Delft 3D output gives outcomes that are comparable with the storage area approach.

Like the EFD model, the Delft 3D model is a 'black box' model to me. It is not known which parameters were used as input and the method for calculating the output is not clear to me.

A big disadvantage of the Delft 3D output is that only data of March 25th and March 26th 2006 are available. To determine a maximum occurred flow velocity, at least the output of a date on which spring tide occurred should be known. This makes the Delft 3D output less useful for the purposes of this report. The conclusion that can be made from the Delft 3D output is that the storage area approach has outcomes in the same order as Delft 3D.

6.5 KRC proceedings reports

KRC made daily reports of the proceedings of the closure. In these reports also maximum flow velocities are mentioned. The draft unofficial proceeding reports of April 15th, 16th, 19th and 20th are added in this report as figures 6.10 to 6.13. The last spring tide before the final closure of the Saemangeum dam occurred on April 16th, therefore this date is important. April 15th has the highest flow velocity according tot the storage area approach. April 19th and 20th are the last 2 days before the final closure. On these days the gaps were very small.

Ⅰ. 공사사항

☐ 현장 기상 및 조위 상황

velocity.

기 상		조 위				유 속		
		구분	시 각	조위 (EL.m)	조위차 (m)	구 분	시 각	최대유속 (m/s)
날씨	구름 조금	고조	04:10	+2.68	5.40	GAP1	03:00(창조)	6.43
기온	5~17℃	저조	10:30	-2.72	4.99		21:20(낙조)	6.60
풍향	북동-남동(7~11m/s)	고조	16:20	+2.27	5.40	GAP2	05:50(창조)	6.59
파고	1.0~1.5m	고조	22:20	-3.13	-		21:00(낙조)	6.68
특보	없음							

Figure 6.10: KRC draft unofficial proceedings report of April 15th 2006

새만금방조제 끝막이공사 추진상황

2006. 4. 16(일), 06:00

Ⅰ. 공사사항

☐ 현장 기상 및 조위 상황

HW-LW

velocity

기 상		조 위				유 속		
		구분	시 각	조위 (EL.m)	조위차 (m)	구 분	시 각	최대유속 (m/s)
날씨	맑음	고조	4:40	+2.76	5.36	GAP1	03:00(창조)	6.39
기온	2~13℃	저조	11:00	-2.60	4.73		21:50(낙조)	6.43
풍향	서-북서(9~13m/s)	고조	16:50	+2.13	5.25	GAP2	03:10(창조)	6.70
파고	1.5~2.5m	고조	22:30	-3.12	-		21:30(낙조)	6.67
특보	없음							

Figure 6.11: KRC draft unofficial proceedings report of April 16th 2006

새만금방조제 끝막이공사 추진상황

2006. 4. 19(수), 12:00

Ⅰ. 공사사항

☐ 현장 기상 및 조위 상황

velocity

기 상		조 위				유 속		
		구분	시 각	조위 (EL.m)	조위차 (m)	구 분	시 각	최대유속 (m/s)
날씨	흐리고 가끔 비	고조	6:30	+2.43	4.27	GAP1	04:50(창조)	6.21
기온	13~15℃	저조	12:30	-1.84	3.22		23:10(낙조)	6.19
풍향	남서서(14~18m/s)	고조	18:40	+1.38	4.01	GAP2	05:20(창조)	6.24
파고	2.0~4.0m	저조	23:40	-2.63	-		22:50(낙조)	6.02
특보	풍랑주위보							

Figure 6.12: KRC draft unofficial proceedings report of April 19th 2006

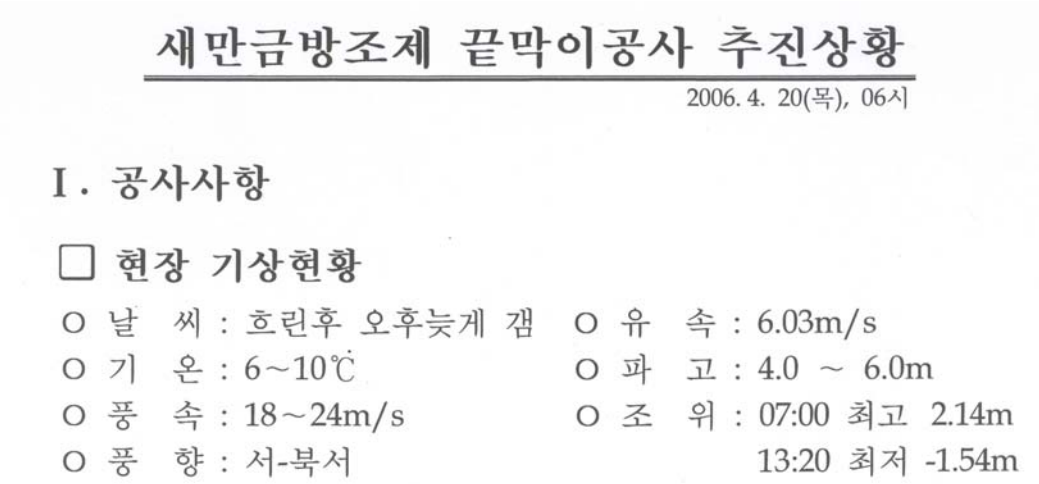

새만금방조제 끝막이공사 추진상황

2006. 4. 20(목), 06시

Ⅰ. 공사사항

☐ 현장 기상현황

○ 날 씨 : 흐린후 오후늦게 갬
○ 기 온 : 6~10℃
○ 풍 속 : 18~24m/s
○ 풍 향 : 서-북서
○ 유 속 : 6.03m/s
○ 파 고 : 4.0 ~ 6.0m
○ 조 위 : 07:00 최고 2.14m
13:20 최저 -1.54m

Figure 6.13: KRC draft unofficial proceedings report of April 20th 2006

As can be seen from the proceedings reports, the maximum flow velocities occurred on April 15th and 16th, and were about **6.7 m/s**. This corresponds very well with the results of the storage area approach using a value for μ of 1.0, and having a maximum flow velocity of 6.5 m/s on April 15th.

From figures 6.12 and 6.13 it follows that no increase in flow velocities occurred later on in the closure. The gap widths decreased but also did the tidal differences.

6.6 Flow velocities according to Wallingford

In Wallingford (2005) the design of the Saemangeum dam is reviewed. As a part of this, a detailed estimation of the maximum mid-gap flow velocities per day is also made (table 6.5).

Table 6.5: Interpolated and estimated velocities, Wallingford (2005)

Gap	Month	Day	Phase	Gap width (m)	u (m/s)	u_{peak} (m/s)
1	March	30	WP 1	1300	5.70	6.08
		31		1300	5.90	6.29
	April	1		1300	5.86	6.25
		2		1300	5.52	5.88
		3	FC 2	1230	5.02	5.37
		4		1160	4.36	4.68
		5		1090	3.63	3.91
		6		1020	3.14	3.39
		7		950	3.06	3.32
		8		880	3.53	3.84
		9		810	4.09	4.47
		10		740	4.55	4.99
		11		670	4.89	5.38
		12		600	5.15	5.68
		13		530	5.37	5.94
		14	WP 2	530	5.64	6.24
		15		530	5.73	6.34
		16		530	5.85	6.48
		17	FC 3	464	6.21	6.90
		18		398	6.40	7.13
		19		331	6.42	7.18
		20		265	5.86	6.57
		21		199	6.12	6.88
		22		132	6.11	6.89
		23		66	6.54	7.41
		24		0	7.33	8.32
2	March	30	WP 1	660	5.62	6.18
		31		660	5.72	6.29
	April	1		660	5.72	6.29
		2		660	5.36	5.89
		3	FC 2	628	4.92	5.42
		4		596	4.33	4.78
		5		565	3.90	4.31
		6		533	3.74	4.14
		7		501	3.67	4.06
		8		469	4.07	4.52
		9		437	4.58	5.10
		10		405	5.04	5.61
		11		374	5.40	6.03
		12		342	5.70	6.37
		13		310	5.97	6.68
		14	WP 2	310	6.21	6.95
		15		310	6.30	7.05
		16		310	6.33	7.08
		17	FC 3	271	6.32	7.09
		18		233	6.25	7.02
		19		194	6.01	6.76
		20		155	5.92	6.67
		21		116	5.26	5.94
		22		78	5.24	5.93
		23		39	5.52	6.25
		24		0	5.95	6.76

The method that is used is that flow velocities that are calculated using Delft 3D are interpolated or extrapolated in order to find mid-range values. In table 6.5, WP means 'waiting period' and FC means 'final closure'. Besides the depth averaged mid-gap flow velocity, also the estimated occurring peak velocities are given.

The maximum value of 7.33 m/s that occurs on April 24th (tidal level 602 - 362 = 240 cm) is considered not valid, because the actual closure took place on April 21st (tidal level 547 - 362 = 185 cm) when the tide was much lower. For the same reason, none of the values past April 21st is considered. The earlier closure might increase all other values for the flow velocities slightly.

From table 6.5, the representative value of the occurred depth averaged maximum flow velocity for the calculations made by Wallingford is **6.4 m/s.**

6.7 GPS floater measurements

On April 16th 2006, during the last spring tide, just before the final closure of the Saemangeum estuary, GPS floater measurements (figure 6.14, the GPS floater is pointed out with an arrow) were done by KRC to determine the flow velocities through gap 2. A disadvantage of floater measurements is that only a superficial flow velocity can be measured, and no information is gained on deeper flow velocities, or the near bed flow velocity.

The results of these measurements can be seen in annex VI. From these data it can be concluded that the maximum superficial flow velocity measured on April 16th 2006 was **5.48 m/s.**

Figure 6.14: GPS floater measurement

6.8 ADCP measurements

On March 30th 2006 an ***Acoustic Doppler Current Profiler*** (ADCP) was used to measure the velocity profile through gap 2. This date was chosen because it was expected to have very high flow velocities due to the spring tide conditions. The results of this measurement are shown in figure 6.15.

□ GAP2 (3월30일)

1. 구간별 유속분포도

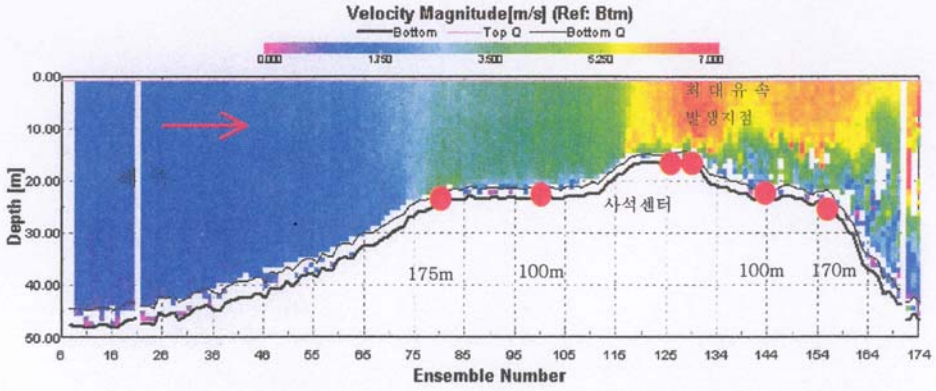

<gap2 수심별 유속분포>

위 치 / 수 심(m)	175m(해측)	100m(해측)	사석센터	최고유속발생 12m(내측)	100m(내측)	170m(내측)
1.16	3.32	3.61	6.57	6.40	5.92	6.16
2.16	3.23	3.62	6.56	6.39	5.83	6.25
3.16	3.21	3.62	6.55	6.50	5.90	6.23
4.16	3.18	3.49	6.48	6.46	5.95	6.15
5.16	3.16	3.49	6.46	6.46	6.12	6.19
6.16	3.27	3.70	6.42	6.49	5.98	6.05
7.16	3.23	3.52	6.58	6.66	6.06	5.95
8.16	3.20	3.50	6.50	6.59	5.88	6.09
9.16	3.14	3.66	6.29	6.60	5.85	5.93
10.16	3.44	3.61	6.19	6.64	5.84	5.93
11.16	3.22	3.66	5.79	6.39	5.59	6.08
12.16	3.53	3.55	5.05	5.96	5.66	6.02
13.16	3.44	3.66	4.70	5.97	5.38	5.56
14.16	3.44	3.63	4.70		4.28	4.54
15.16	3.38	3.67			4.03	4.77
16.16	3.53	3.61			4.74	4.77
17.16	3.45	3.52			4.68	3.97
18.16	3.37	3.59			3.94	4.14
19.16	3.60	3.44			4.42	4.35
20.16	3.57	3.05			4.57	4.70
21.16	3.88	2.32				4.24
최대유속(m/s)	3.88	3.70	6.58	6.66	6.12	6.25
수심평균유속(m/s)	3.38	3.58	6.34	6.55	5.50	5.31

Figure 6.15: ADCP measurements

As expected, the flow velocity is maximal at the end of the sill. About halfway of the depth, the flow velocity is 6.66 m/s. The maximum near bed flow velocity is lower, 5.97 m/s. This means that the gabions that were used had to cope with a maximum flow load of **5.97 m/s**. The depth averaged flow velocity measured by the ADCP is **6.55 m/s**. Taken into account a slight increase of the depth averaged flow velocity during the spring tide of April 16th due to the smaller gap widths, this value is very comparable with the value for the storage area approach and the KRC draft unofficial proceedings reports.

6.9 Damage

KRC used single beam echo soundings to determine if the sill and/or bed protection were damaged during the Saemangeum project. On several locations, some damage did occur. There are no exact data on this. According to the engineers of KRC, only small damages occurred. During the project visits, split barges were observed dumping gabions over the edge of the sill, which might have been for repair purposes.

The amount of gabions that would be lost during the dumping process and the final closure of the dam was estimated to be about 20%. The purpose of the gabions was for extra stability during the closure only, because after the closure, loose rocks could be used that would be less expensive than using gabions. After the final closure, many gabions were still left in the storage area. This indicates that the losses of gabions were smaller than expected (of course, a certain amount of reserve must be taken into account). Engineers of KRC confirmed this.

It can be concluded that the flow velocity for incipient motion at some locations was exceeded; otherwise no damage to the sill and bed protection would have occurred. The small amount of damage indicates that the critical velocity was not exceeded much; otherwise more damage would have occurred.

6.10 Conclusions on the practical data

All estimations and measurements on flow velocities are presented in table 6.6.

Table 6.6: Maximum flow velocities

Method	u_{max} (m/s)	Remarks
Storage Area Approach μ = 0.9	6.0	depth averaged flow velocity
Storage Area Approach μ = 1.0	6.5	depth averaged flow velocity
Storage Area Approach μ = 1.1	7.1	depth averaged flow velocity
EFD	10.54	local peak flow velocity, with turbulence
Delft 3D	3.5	not maximal, comparable with S.A.A.
Proceedings Reports	6.7	depth averaged flow velocity (April 16th)
Wallingford	6.42	depth averaged flow velocity, not including peak velocities
GPS	5.48	superficial flow velocity
ADCP	6.55	depth averaged flow velocity (March 30th)

When analyzing these results, the best value to look at is the measurement of the ADCP. This measurement is from March 30th 2006, during spring tide conditions. During the spring tide of April 16th the gaps were closed further and therefore somewhat higher flow velocities are expected to have occurred. This suits the proceedings report findings of April 16th exactly.

The Storage Area Approach gives an outcome in the same order when μ = 1 is applied. This value for μ seems reasonable according to Wallingford (2005).

The GPS floater measurements give a superficial flow of 5.48 m/s on April 16th. Assuming the same flow profile as with the ADCP measurement of March 30th, this gives a depth averaged flow velocity of 5.48 / (6.40 / 6.55) = 5.6 m/s. This value seems very low.

The non calibrated EFD model gives a very high value for the local flow velocity of 10.54 m/s. Since it is not known in which way the EFD model accounts for the turbulence in its calculations, this value is not taken into account.

It seems reasonable to assume that a depth averaged flow velocity of **6.7 m/s** has occurred during the closure of the Saemangeum estuary. Combined with the slight amount of damage that has occurred, one could estimate that **in prototype conditions incipient motion has occurred for a mixture of 50 % rocks weighing 3 to 5 tons and 50 % 3 ton gabions at a depth averaged flow velocity of about 6.7 m/s.**

This corresponds with Wallingfords calculations (figure 3.10 and formula [15]) that instability for this mixture might occur at a depth averaged flow velocity of 6.7 m/s.

7. Conclusions

In this chapter a method to calculate gabion stability will be derived from the information of the previous chapters. Some considerations that follow from the mode of failure of gabions are stated.

7.1 Calculation method for gabion stability

The depth averaged critical velocity for a mixture of 50 % rocks weighing 3.0 to 5.0 tons and 50 % 3.0 ton gabions was determined to be in the order of 6.7 m/s (paragraph 6.10). This follows from the practical data of the Saemangeum project (chapter 6) and from the calculations in Wallingford (2005). Wallingford uses a representative stone diameter (Dn) of 0.8 m for this mixture applied in a bed protection. This representative diameter follows from the RRI test results. Formula [15] is assumed to be a good estimation of the depth averaged critical velocity for this gabion/rock mixture.

$$u_{cM} = 2.513x + 5.4 \qquad [15]$$

Where:

u_{cM} = critical velocity of a mixture of 50 % rocks of 3.0 to 5.0 t and 50 % 3.0 t gabions

x = the proportion of gabions in the mixture

0.2 < x < 0.5

From the model tests done in Delft, a formula for the stability of gabions using a local velocity follows that suits the findings of RRI;

$$\Delta D_n = \frac{\beta}{\gamma}\frac{u_c^{\,2}}{2g} \qquad [18]$$

Where:

$$D_n = \sqrt[3]{\frac{M}{\rho_S}} \qquad [1]$$

$$\Delta = \frac{\rho_s - \rho_w}{\rho_w} \qquad [3]$$

and γ = 1.26 for sack gabions

(γ = 1 for loose rocks)

7.2 Considerations using sack gabions

During the model tests in Delft, research is done on the mode of failure of gabions. It turns out that the behavior of a bed of gabions is different from the behavior of a bed of loose stones. The results of this research can not be quantified but lead to several important considerations on the application of sack gabions.

When applying gabions one has to take into account the difference in behavior between gabions and loose rocks. Gabions tend to start moving more abruptly and with more gabions at a time. If one gabion fails, mostly other gabions fail as well because they stabilize each other. Loose rocks differ in shape and therefore they have a less stabilizing effect on each other. This effect is illustrated by figure 7.2. Loose stones (right picture of figure 7.2) are inflexible and have relatively small dimensions (less overlap) in comparison with gabions.

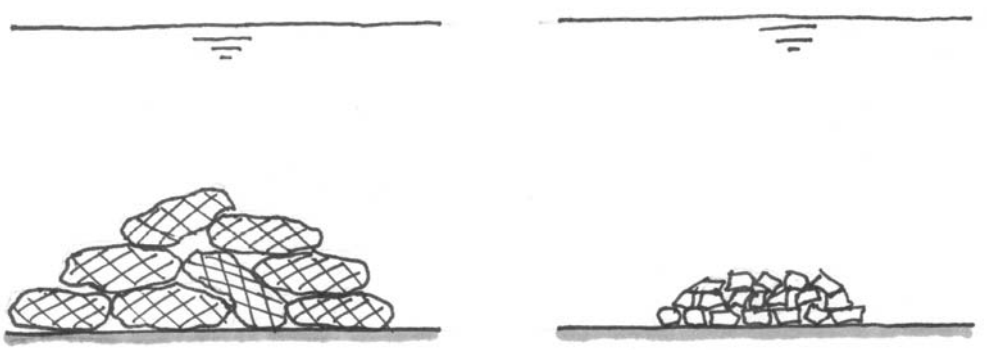

Figure 7.2: Stabilizing effect of sack gabions vs. loose stones

Another behavior that needs to be examined in more detail is the effect of applied pressure on a gabion bed. If a gabion bed is pressed together, the stability of the bed is increased significantly. In practice this means that a lower layer of gabions is pressed together by the weight of the upper layer of gabions. So if the upper layer fails, the more stable lower layer will be able to withstand higher flow loads, thus preventing progressive failure of the gabion bed (figure 7.3).

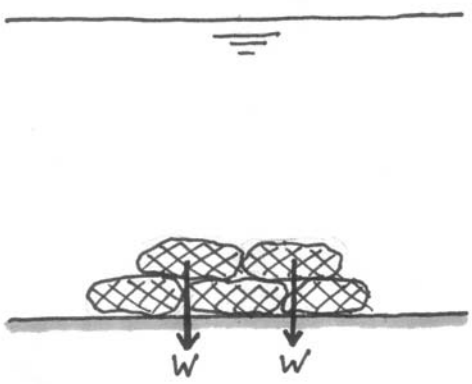

Figure 7.3: Compressing effect of top layer

8. Recommendations

During the model tests in Delft and the analyses of the data gathered in this report, several issues emerged that could not be dealt with in this report. Therefore several recommendations are made.

- Some phenomena that have influence on the stability of gabions or the application of gabions in general might be further investigated. These phenomena are:

  - The stabilizing effect of top layers on lower layers in a gabion bed.
  - The amount of gabions failing at the same moment.
  - The stability of a gabion bed after incipient motion has occurred.
  - The influence of the amount of rocks in a gabion on its stability.
  - The influence of turbulence on the stability of gabions.
  - The stability of a sill construction when the weir becomes a free flow weir instead of a submerged weir.
  - The effect of tying more gabions together.
  - The amount of damage to gabions using certain dumping methods.
  - The costs - benefit relation of gabions vs. large rocks with comparable stability.

- To calibrate the formulas that were derived from the available data for practical applications it is necessary to do some additional tests in prototype conditions, for example in the Netherlands or in South Korea. At the Saemangeum project, the Sinsi sluice provides one of the biggest prototype sized flumes in the world, which would be fit for prototype tests on the stability of gabions. Perhaps these tests (figure 8.1) will be possible in the future.

Figure 8.1: Proposal for prototype tests (ir. K. Dorst, RWS)

References

BATTJES, J.A. (2001) Korte golven. *Delft*

BATTJES, J.A. (2002) Stroming in waterlopen. *Delft*

CUR (1994) Report 169 manual on the use of rock in hydraulic engineering. *Gouda*

DELFT HYDRAULICS LABORATORY (1963) M 711 deel II Stroombestendigheid sluitgatdrempel (Dutch)

DELFT HYDRAULICS LABORATORY (1964) M 711 deel III Stroombestendigheid sluitgatdrempel (Dutch)

DELFT HYDRAULICS LABORATORY (1981) M 1741 deel I Compartimenteringswerken Oesterdam (Dutch)

DELFT HYDRAULICS LABORATORY (1982) M 1741 deel II Compartimenteringswerken Oesterdam (Dutch)

DELFT HYDRAULICS LABORATORY (1983) M 1741 deel III Compartimenteringswerken Oesterdam (Dutch)

DELFT HYDRAULICS LABORATORY (1985) M 1741 part IV Hydraulic design criteria for rockfill closure of tidal gaps

DELFT HYDRAULICS LABORATORY (1982 II) Stroombestendigheid van gabions (Dutch)

HR WALLINGFORD (2005) Report EX 5192 Engineering review on the final closure of Saemangeum dike

KUIJPER (editor) (2006) Probability in civil engineering, CT 4130 *Delft*

NORTEK AS (2004) User guide Vectrino velocitymeter *Norway*

RURAL RESEARCH INSTITUTE (2004) Annual report 2004 (Korean)

RIJKSWATERSTAAT (1995) Handleiding voor het ontwerpen van granulaire bodemverdedigingen achter tweedimensionale uitstromingsconstructies *Bouwdienst Rijkswaterstaat, Utrecht* (Dutch)

VAN DER SANDE, M. (2006), Computational modeling on the final closure gaps in the Saemangeum dam, South Korea. *Delft*

SCHIERECK, G.J. (2001) Introduction to bed bank and shore protection. *Delft University Press, Delft*

Internet

http://www.anno.nl

http://wikitravel.org

http://www.ngotimes.net

http://www.egetra.be

http://www.ieca.org

http://www.africangabions.co.za

http://www.nortek-as.com

ANNEX I: Delft model test results

The data of the Delft model tests on the critical velocity of model gabions are presented in this annex. At t = 0 seconds incipient motion occurred. u(x) is the flow velocity parallel to the direction of the flow. u(y) and u(z) are the flow velocities perpendicular to the direction of the flow.

Test	1a
Type	Gabions
Mass	50g

Time	u(x)	u(y)	u(z)
(s)	(m/s)	(m/s)	(m/s)
-5	0.85	-0.18	0.10
-4	0.86	-0.04	0.04
-3	0.96	0.05	-0.01
-2	0.96	0.02	0.01
-1	0.96	0.41	-0.11
0	0.98	-0.04	0.02
1	0.91	-0.02	0.03
2	0.99	-0.02	-0.01
3	1.08	0.03	0.06
4	0.96	0.01	0.02
5	0.91	0.12	-0.03

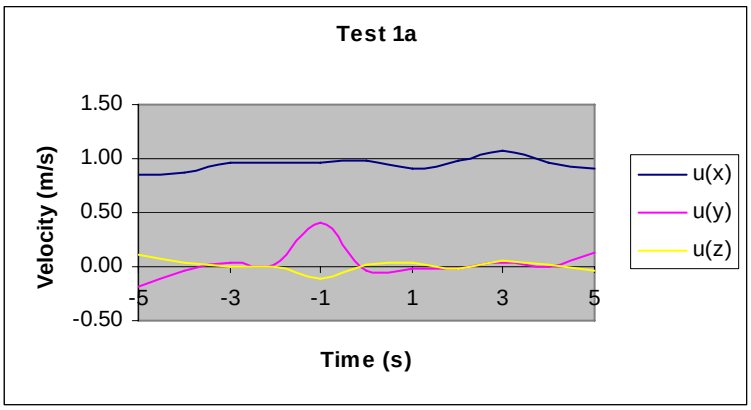

Test	1b
Type	Gabions
Mass	50g

Time	u(x)	u(y)	u(z)
(s)	(m/s)	(m/s)	(m/s)
-5	0.83	0.10	0.06
-4	0.91	0.00	0.04
-3	0.91	-0.01	0.04
-2	0.91	-0.02	0.03
-1	0.93	-0.01	0.02
0	0.93	0.02	0.01
1	0.85	-0.02	-0.01
2	0.92	0.02	0.01
3	0.80	0.13	0.05
4	0.92	0.01	0.04
5	0.94	0.02	0.03

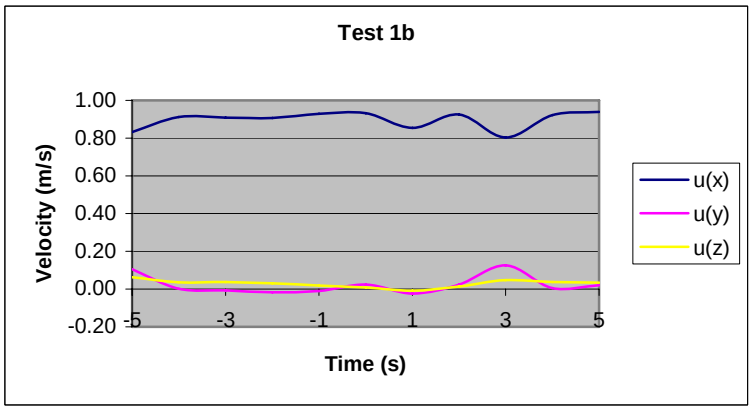

Test	1c
Type	Gabions
Mass	50g

Time	u(x)	u(y)	u(z)
(s)	(m/s)	(m/s)	(m/s)
-5	0.77	-0.02	0.09
-4	0.89	-0.08	0.06
-3	0.85	0.14	-0.01
-2	0.86	-0.09	0.04
-1	0.94	0.00	0.01
0	0.95	-0.10	-0.01
1	0.98	-0.02	0.01
2	1.16	0.47	-0.02
3	0.89	0.16	0.05
4	0.80	0.05	0.09
5	0.81	0.05	0.06

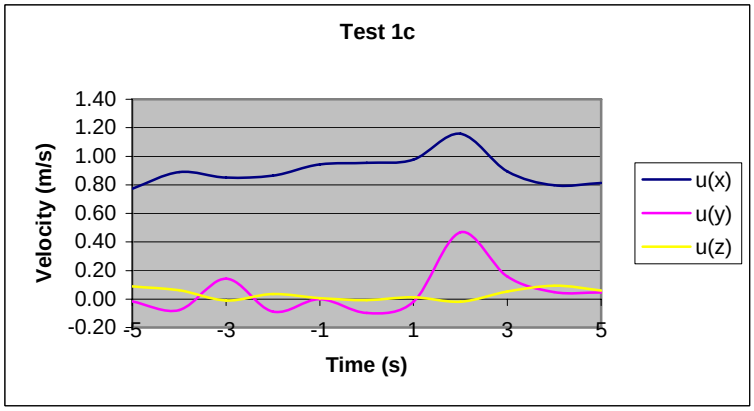

Test	2a
Type	Gabions
Mass	100g

Time (s)	u(x) (m/s)	u(y) (m/s)	u(z) (m/s)
-5	1.08	0.04	0.00
-4	1.04	0.07	0.01
-3	1.03	0.02	0.00
-2	1.00	0.06	0.04
-1	1.11	0.06	-0.01
0	1.14	-0.01	0.02
1	1.01	0.01	-0.01
2	1.04	0.02	0.00
3	1.00	0.08	0.00
4	0.94	-0.02	0.01
5	0.90	-0.01	0.01

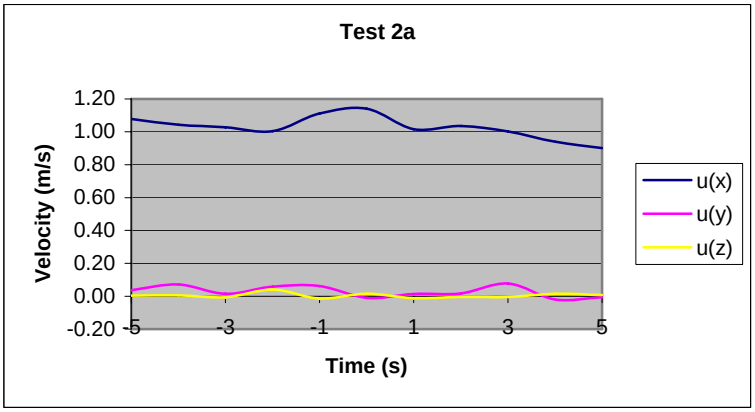

Test	2b
Type	Gabions
Mass	100g

Time (s)	u(x) (m/s)	u(y) (m/s)	u(z) (m/s)
-5	1.00	-0.03	-0.01
-4	0.91	-0.03	0.01
-3	1.02	0.07	0.04
-2	1.00	-0.03	0.07
-1	1.06	-0.05	0.14
0	1.08	-0.07	0.06
1	1.06	0.13	0.10
2	1.11	0.11	-0.04
3	1.00	0.28	-0.09
4	1.07	-0.21	0.04
5	1.06	0.02	0.01

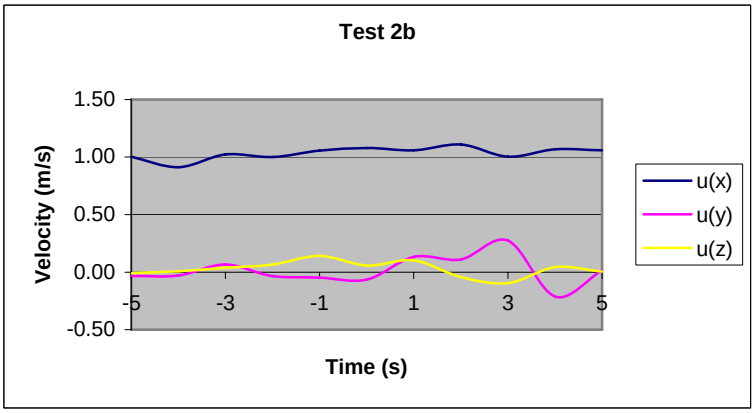

Test	2c
Type	Gabions
Mass	100g

Time (s)	u(x) (m/s)	u(y) (m/s)	u(z) (m/s)
-5	1.05	-0.94	0.08
-4	1.05	-0.03	0.07
-3	1.06	-0.06	0.04
-2	1.01	0.07	0.03
-1	1.03	0.97	0.06
0	1.10	-0.07	0.07
1	1.02	-0.02	0.11
2	1.04	-0.92	0.08
3	0.95	0.03	0.07
4	1.01	1.03	0.10
5	1.08	-0.94	0.17

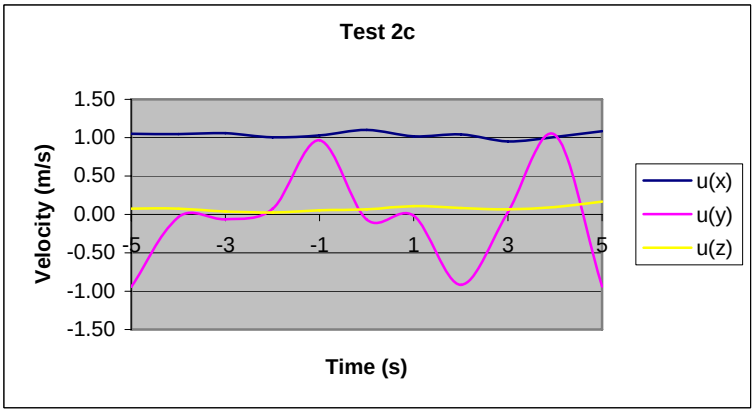

Test	3a
Type	Gabions
Mass	200g

Time (s)	u(x) (m/s)	u(y) (m/s)	u(z) (m/s)
-5	1.22	0.05	-0.02
-4	1.20	-0.03	-0.01
-3	1.16	-0.05	-0.02
-2	1.17	-0.04	0.00
-1	1.19	-0.05	-0.02
0	1.23	-0.08	-0.04
1	1.22	-0.05	0.02
2	1.20	-0.07	-0.02
3	1.21	-0.05	0.01
4	1.17	-0.05	-0.01
5	1.18	-0.06	-0.01

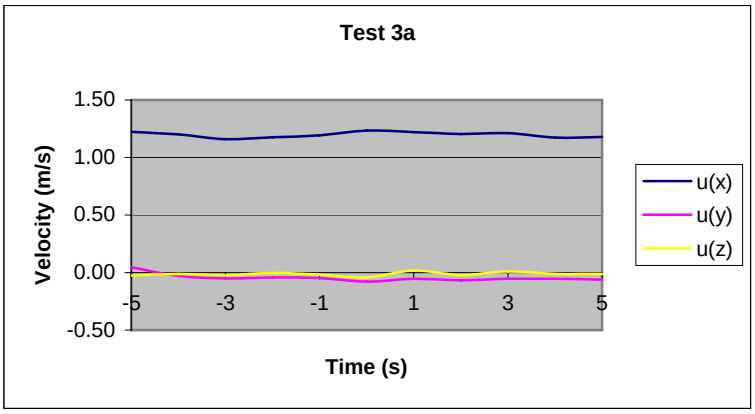

Test	3b
Type	Gabions
Mass	200g

Time (s)	u(x) (m/s)	u(y) (m/s)	u(z) (m/s)
-5	1.23	0.07	0.01
-4	1.24	0.06	0.01
-3	1.25	0.05	0.01
-2	1.25	0.06	0.00
-1	1.25	0.05	-0.01
0	1.27	0.05	-0.02
1	1.25	0.04	-0.03
2	1.25	0.06	-0.01
3	1.25	0.04	-0.01
4	1.24	0.03	0.01
5	1.25	0.03	-0.02

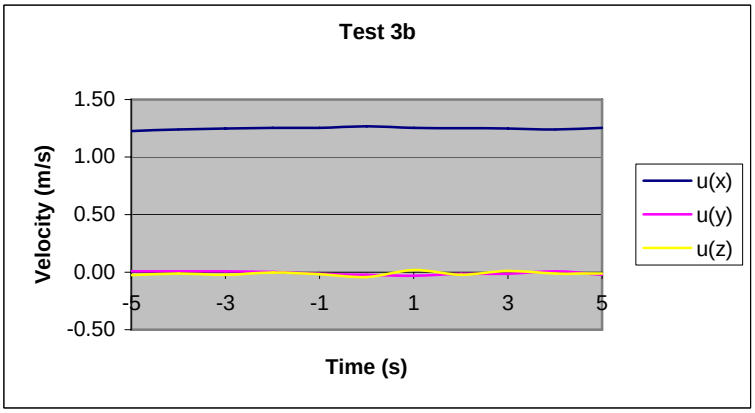

Test	3c
Type	Gabions
Mass	200g

Time (s)	u(x) (m/s)	u(y) (m/s)	u(z) (m/s)
-5	1.16	-0.05	-0.03
-4	1.19	-0.09	-0.03
-3	1.26	-0.06	0.04
-2	1.23	-0.14	-0.02
-1	1.23	-0.12	-0.05
0	1.25	-0.08	-0.04
1	1.22	0.00	-0.04
2	1.22	-0.06	-0.04
3	1.20	-0.08	-0.05
4	1.19	-0.09	-0.04
5	1.22	-0.07	-0.06

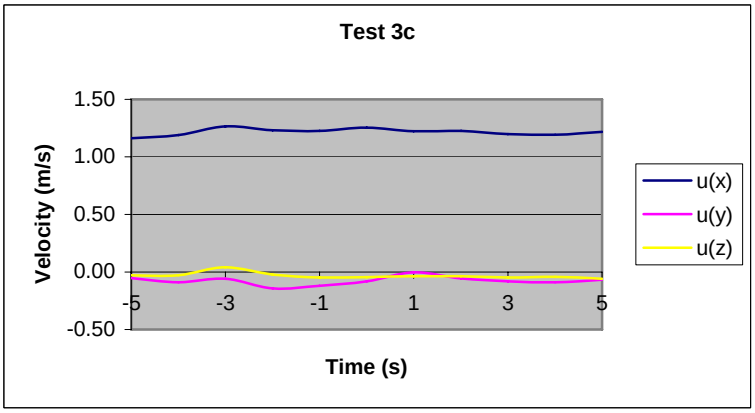

Test	4a
Type	Gabions
Mass	300g

Time	u(x)	u(y)	u(z)
(s)	(m/s)	(m/s)	(m/s)
-5	1.27	-0.04	-0.04
-4	1.29	0.07	0.02
-3	1.24	0.04	-0.01
-2	1.31	0.09	0.02
-1	1.34	0.09	-0.01
0	1.36	0.12	0.04
1	1.32	0.16	-0.03
2	1.29	0.00	0.01
3	1.31	0.04	0.01
4	1.26	0.01	0.00
5	1.28	0.06	0.02

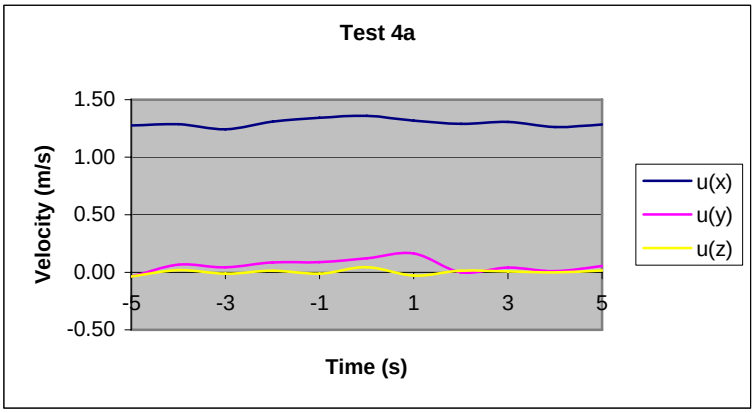

Test	4b
Type	Gabions
Mass	300g

Time	u(x)	u(y)	u(z)
(s)	(m/s)	(m/s)	(m/s)
-5	1.17	0.20	-0.04
-4	1.21	0.13	0.01
-3	1.21	0.12	-0.06
-2	1.23	0.22	-0.02
-1	1.29	0.25	0.07
0	1.35	0.19	0.00
1	1.26	0.21	0.03
2	1.30	0.20	0.01
3	1.35	0.20	-0.01
4	1.33	0.23	0.00
5	1.25	0.05	-0.10

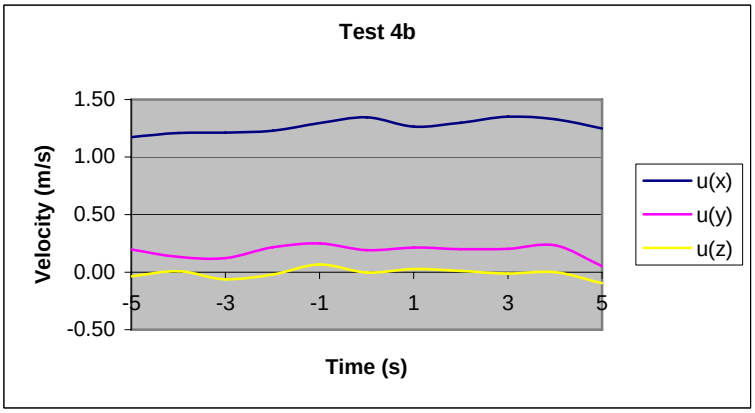

Test	4c
Type	Gabions
Mass	300g

Time	u(x)	u(y)	u(z)
(s)	(m/s)	(m/s)	(m/s)
-5	1.21	0.04	0.01
-4	1.32	-0.07	0.02
-3	1.16	-0.19	0.06
-2	1.23	0.03	-0.02
-1	1.26	-0.10	-0.04
0	1.36	0.00	-0.03
1	1.26	-0.06	-0.06
2	1.26	-0.06	-0.06
3	1.21	0.15	-0.09
4	1.11	0.14	0.07
5	1.25	0.05	-0.10

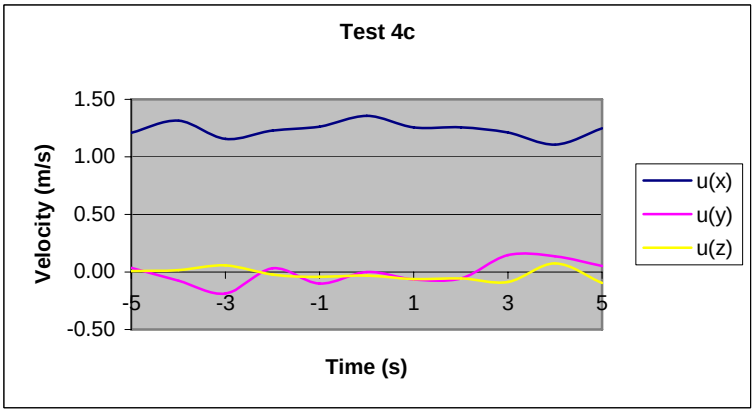

Test	5a
Type	Stones
Mass	100g

Time	u(x)	u(y)	u(z)
(s)	(m/s)	(m/s)	(m/s)
-5	0.96	-0.07	0.04
-4	0.97	0.00	0.03
-3	0.95	0.01	0.04
-2	1.00	0.02	0.01
-1	0.99	0.02	0.00
0	1.03	-0.04	0.05
1	0.96	-0.05	0.03
2	0.99	0.00	0.03
3	1.01	-0.01	0.00
4	1.01	0.03	-0.02
5	1.04	0.06	-0.01

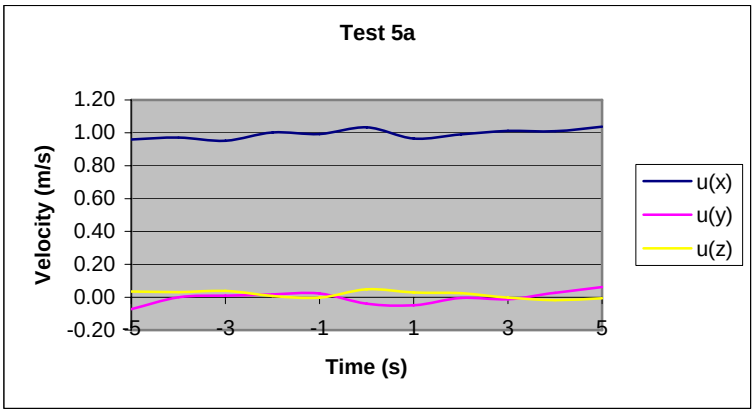

Test	5b
Type	Stones
Mass	100g

Time	u(x)	u(y)	u(z)
(s)	(m/s)	(m/s)	(m/s)
-5	0.94	-0.01	0.07
-4	0.93	0.00	0.08
-3	0.91	0.00	0.06
-2	0.94	0.06	0.06
-1	0.90	0.02	0.06
0	0.96	-0.01	0.07
1	0.95	-0.02	0.09
2	0.97	0.02	0.07
3	0.95	0.03	0.04
4	0.94	0.01	0.04
5	0.97	0.01	0.07

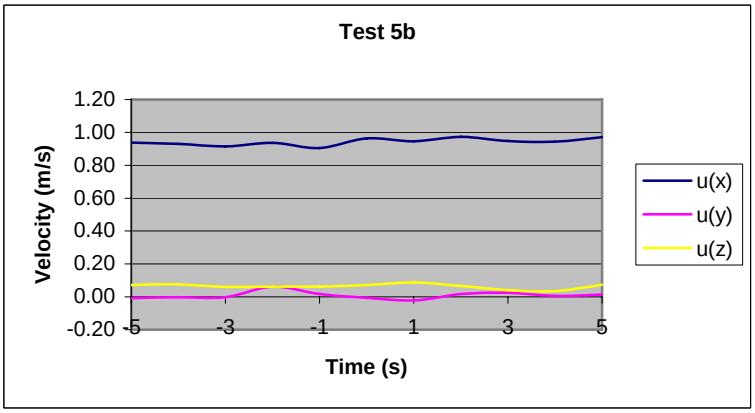

Test	5c
Type	Stones
Mass	100g

Time	u(x)	u(y)	u(z)
(s)	(m/s)	(m/s)	(m/s)
-5	0.96	0.02	0.04
-4	0.95	0.00	0.02
-3	0.94	-0.06	0.05
-2	0.97	0.00	0.04
-1	0.99	-0.01	0.05
0	0.99	0.00	0.05
1	0.99	-0.03	0.03
2	1.00	0.02	0.06
3	1.01	0.00	0.04
4	0.93	0.05	0.06
5	0.98	0.00	0.06

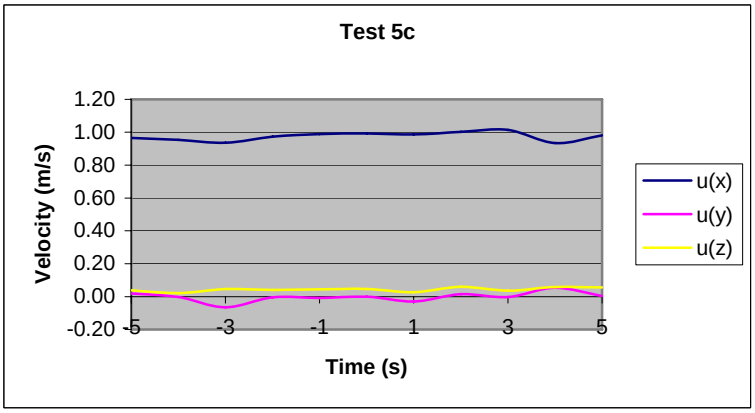

Test	6a
Type	Stones
Mass	200g

Time (s)	u(x) (m/s)	u(y) (m/s)	u(z) (m/s)
-5	0.97	0.07	0.06
-4	0.98	0.08	0.06
-3	1.02	0.14	0.06
-2	0.98	0.07	0.06
-1	1.04	0.14	0.05
0	1.05	0.04	0.03
1	1.02	0.09	0.06
2	1.02	0.11	0.07
3	0.98	0.10	0.11
4	0.98	0.03	0.08
5	0.96	0.08	0.08

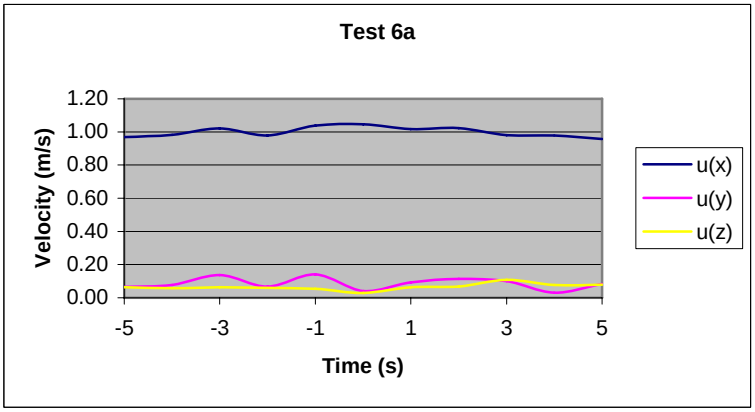

Test	6b
Type	Stones
Mass	200g

Time (s)	u(x) (m/s)	u(y) (m/s)	u(z) (m/s)
-5	1.14	0.04	-0.01
-4	1.08	-0.03	0.00
-3	1.11	0.13	-0.03
-2	1.13	0.00	-0.01
-1	1.14	0.04	-0.05
0	1.16	0.00	-0.03
1	1.16	0.02	-0.03
2	1.13	0.02	-0.03
3	1.10	0.06	-0.02
4	1.10	0.02	-0.03
5	1.10	-0.05	-0.02

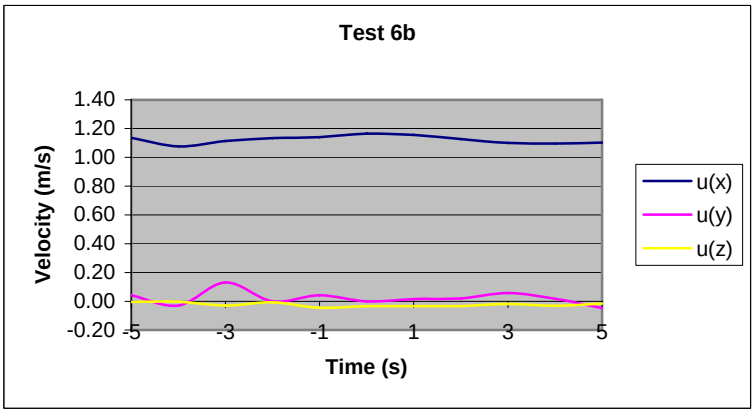

Test	6c
Type	Stones
Mass	200g

Time (s)	u(x) (m/s)	u(y) (m/s)	u(z) (m/s)
-5	1.06	-0.11	-0.04
-4	1.03	-0.06	0.03
-3	0.99	-0.07	-0.04
-2	0.96	-0.02	0.08
-1	1.05	-0.01	-0.05
0	1.11	-0.11	-0.08
1	1.08	-0.09	-0.03
2	1.10	-0.10	-0.03
3	1.09	-0.08	-0.04
4	1.06	-0.05	-0.01
5	1.10	-0.07	-0.06

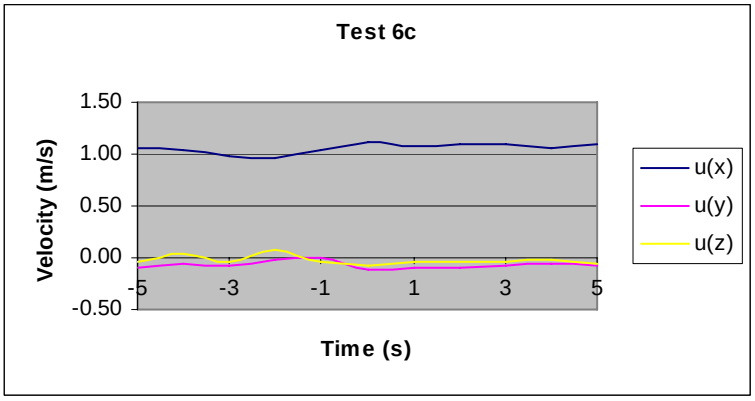

Test	7a
Type	Gabions(compressed)
Mass	100g

Samples did not fail during this test!

Time (s)	u(x) (m/s)	u(y) (m/s)	u(z) (m/s)
-5	1.21	-0.04	0.02
-4	1.26	0.02	-0.02
-3	1.26	0.03	0.00
-2	1.29	0.04	-0.01
-1	1.25	0.02	-0.02
0	1.29	0.02	-0.02
1	1.26	0.02	-0.04
2	1.21	-0.08	0.07
3	1.27	0.02	0.00
4	1.29	0.00	-0.02
5	1.27	0.03	-0.04

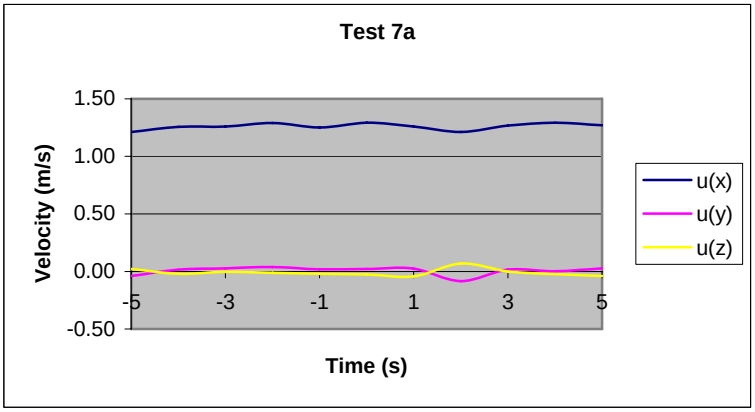

Test	7b
Type	Gabions(compressed)
Mass	100g

Samples did not fail during this test!

Time (s)	u(x) (m/s)	u(y) (m/s)	u(z) (m/s)
-5	1.32	-0.03	0.01
-4	1.22	-0.01	-0.01
-3	1.23	0.02	0.05
-2	1.19	0.03	0.04
-1	1.15	0.06	0.01
0	1.34	0.12	-0.04
1	1.23	0.07	-0.09
2	1.26	0.00	0.00
3	1.21	0.00	0.03
4	1.14	0.01	0.04
5	1.18	-0.04	0.04

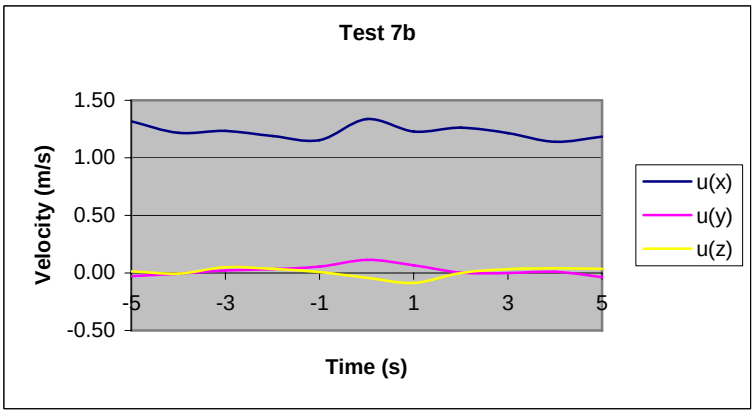

ANNEX II: Propagation of uncertainties

To calculate the possible error in the calculation of the scaled prototype critical velocities using formula [17], a quadratic summation of the partial derivatives of each variable is made.

To determine the error of the calculations of the prototype stability of gabions using equation [17], the combined uncertainty of the variables is calculated using a quadratic summation of the partial derivative for each variable in formula [17].

First each variable is analyzed for its possible error. The results are shown in table II.1.

The **Vectrino** measures 25 values per second and the on screen output is the average of the measured values in one second. This value was read on the moment that one or more model gabions failed, and is considered the representative value for the critical velocity. Since the flow velocities were increased very gently during the model tests, the second in which instability occurred could be defined very well, so this value is considered accurate within two decimals (displayed accuracy of the Vectrino). Therefore the measured values of the tests are considered to have a possible error of +/- 0.005 m/s.

The accuracy of the **Vectrino** is given in the manual Nortek AS (2004) as 0.5 % of the measured value +/- 1 mm/s. These values are added to the error of the Vectrino of +/- 0.005 m/s.

The representative value for the critical velocity of a model gabion is taken as the averaged value of 3 measurements (table 4.2). The possible error of this value is determined by the maximum deviation of a measured value from this averaged value. If the error of the Vectrino is added to the error of the averaged critical velocity, the possible error of the **model critical velocity** is obtained.

In this case, the method of manufacturing determines the accuracy of the **mass of the model gabions**. Each gabion was selected to be within a certain mass range (table 4.1). This range determines the possible error.

The uncertainty of the **mass of the prototype gabions** is not known but is assumed 5%. This means that a 3 ton gabion in reality weighs between 2850 kg and 3150 kg, which seems a reasonable tolerance since the weight of a gabion can simply be adapted by adding more rocks. It is not known how accurate the gabions are produced in reality.

The density of the stones used in the model gabions is determined with the following relation:

$$\rho_s = \frac{M}{V} \qquad [27]$$

For the stones used in the 50 g model gabions, these values were measured to obtain the density:

M = 200.0 g +/- 0.05 g

V = 81.3 ml +/- 0.05 ml

For the stones used in the 100 g, 200 g and 300 g model gabions, these values were measured to obtain the density:

M = 400.0 g +/- 0.05 g

V = 175.4 ml +/- 0.05 ml

The error of the digital balance is determined by the last significant value displayed by the balance. The error of the volume is determined by the measuring cup. The possible error of the stone density is calculated by a quadratic summation.

The **density of the prototype gabions** is given by RRI (2004) and Wallingford (2005) as 2650 kg/m^3. This value is often used as a standard value. It is not clear how much the real densities of the rocks used for the gabions deviated. A possible error of 5 % is assumed here.

The **density of the model test water** (lab conditions) is taken 1000 kg/m^3 +/- 0.1%. The **density of the prototype condition water** can deviate because of temperature and salinity. From 1000 kg/m^3 for fresh water to 1030 kg/m^3 for salt water, the water in the Saemangeum estuary is a mixture of fresh and salt water, because 2 rivers flow into the sea at this point. But since the river discharges are very small (table 6.1), a density of 1030 kg/m^3 is taken with a maximum possible error of 0.5 %. (Keep in mind that a higher value for the density of the water is less favorable for the stability of a gabion due to the increase in lift force acting on the gabion).

The error of the **relative densities** in model and prototype conditions can be calculated from the errors of the rock densities. It has to be taken into account that the water density in the numerator and in the denominator are dependent. Each of these errors is calculated separately by subtracting the lowest possible value from the highest possible value.

With the possible errors of all variables that are needed to calculate the prototype flow velocity the possible error of the prototype flow velocity can be calculated with a quadratic summation of the partial derivatives of each variable (a to g) in formula [17] as follows;

$$a = \left(\frac{\Delta_P}{\Delta_M}\right)^{\frac{1}{2}}\left(\frac{M_P}{M_M}\right)^{\frac{1}{6}}\left(\frac{\rho_{sM}}{\rho_{sP}}\right)^{\frac{1}{6}}\delta u_m$$

$$b = u_m\left(\frac{1}{\Delta_M}\right)^{\frac{1}{2}}\left(\frac{M_P}{M_M}\right)^{\frac{1}{6}}\left(\frac{\rho_{sM}}{\rho_{sP}}\right)^{\frac{1}{6}}\frac{1}{2\sqrt{\Delta_P}}\delta\Delta_P$$

$$c = u_m\Delta_P^{\frac{1}{2}}\left(\frac{M_P}{M_M}\right)^{\frac{1}{6}}\left(\frac{\rho_{sM}}{\rho_{sP}}\right)^{\frac{1}{6}}\times -\frac{1}{2}\Delta_M^{-1\frac{1}{2}}\delta\Delta_M$$

$$d = u_m\left(\frac{\Delta_P}{\Delta_M}\right)^{\frac{1}{2}}\left(\frac{1}{M_M}\right)^{\frac{1}{6}}\left(\frac{\rho_{sM}}{\rho_{sP}}\right)^{\frac{1}{6}}\frac{1}{6}M_P^{-\frac{5}{6}}\delta M_P$$

$$e = u_m\left(\frac{\Delta_P}{\Delta_M}\right)^{\frac{1}{2}}\left(M_P\right)^{\frac{1}{6}}\left(\frac{\rho_{sM}}{\rho_{sP}}\right)^{\frac{1}{6}}\times -\frac{1}{6}M_M^{-1\frac{1}{6}}\delta M_M$$

$$f = u_m\left(\frac{\Delta_P}{\Delta_M}\right)^{\frac{1}{2}}\left(\frac{M_P}{M_M}\right)^{\frac{1}{6}}\left(\frac{1}{\rho_{sP}}\right)^{\frac{1}{6}}\frac{1}{6}\rho_{sM}^{-\frac{5}{6}}\delta\rho_{sM}$$

$$g = u_m\left(\frac{\Delta_P}{\Delta_M}\right)^{\frac{1}{2}}\left(\frac{M_P}{M_M}\right)^{\frac{1}{6}}\left(\rho_{sM}\right)^{\frac{1}{6}}\times -\frac{1}{6}\rho_{sP}^{-1\frac{1}{6}}\delta\rho_{sP}$$

$$\delta_{u_P} = \sqrt{a^2 + b^2 + c^2 + d^2 + e^2 + f^2 + g^2}$$

The results of these calculations can be found in the bottom rows of table II.1.

Table II.1: Maximum possible error due to propagation of uncertainties

Accuracy	50 g gabion	100 g gabion	200 g gabion	300 g gabion
δVectrino (m/s)	+/- 0.01075	+/- 0.01155	+/- 0.01225	+/- 0.01275
$\delta u_{average}$ (m/s)	+/- 0.03	+/- 0.03	+/- 0.02	+/- 0.01
δu_{cM} (m/s)	+/- 0.04075	+/- 0.04155	+/- 0.03225	+/- 0.02275
δM_M (kg)	+/- 0.001	+/- 0.002	+/- 0.002	+/- 0.002
δM_P (kg)	+/- 150	+/- 150	+/- 150	+/- 150
$\delta \rho_{sM}$ (kg/m^3)	+/- 2.1	+/- 0.93	+/- 0.93	+/- 0.93
$\delta \rho_{sP}$ (kg/m^3)	+/- 132.5	+/- 132.5	+/- 132.5	+/- 132.5
$\delta \rho_{wM}$ (kg/m^3)	+/- 1	+/- 1	+/- 1	+/- 1
$\delta \rho_{wP}$ (kg/m^3)	+/- 5.15	+/- 5.15	+/- 5.15	+/- 5.15
$\delta \Delta_M$ (-)	+/- 0.004	+/- 0.0016	+/- 0.0016	+/- 0.0016
$\delta \Delta_P$ (-)	+/- 0.11	+/- 0.11	+/- 0.11	+/- 0.11
δu_P (m/s)	**+/- 0.30**	**+/- 0.24**	**+/- 0.27**	**+/- 0.23**
δu_P	**+/- 4.8 %**	**+/- 3.5 %**	**+/- 3.9 %**	**+/- 3.3 %**

ANNEX III: Gap geometry

A plan view of gap 1 and gap 2 of the Saemangeum project are shown in this annex, as well as a typical cross-section of the Saemangeum dike.

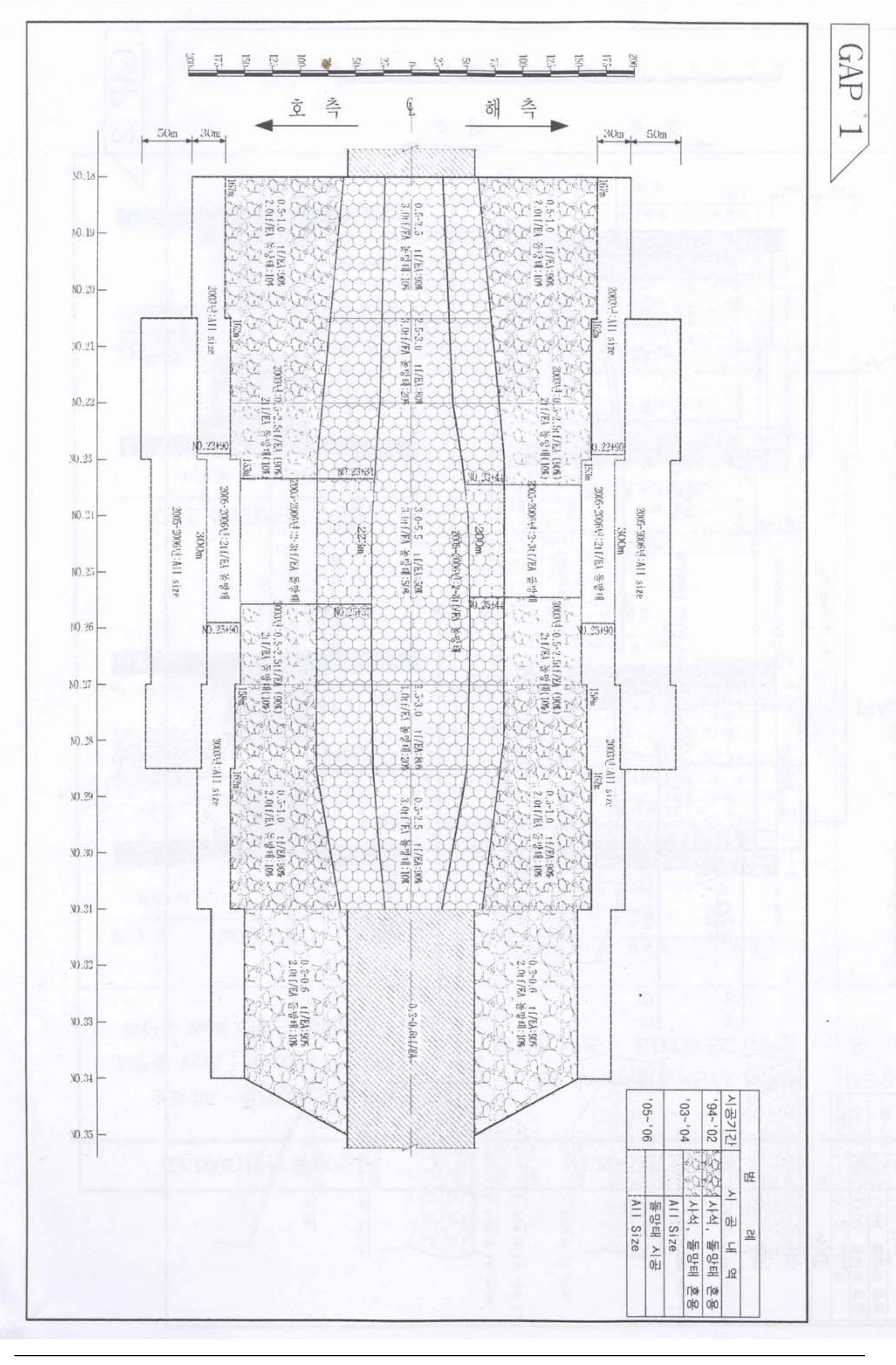
GAP 1
호 측
해 측
50m
30m
300m
All Size
All size
'94~'02
'03~'04
'05~'06

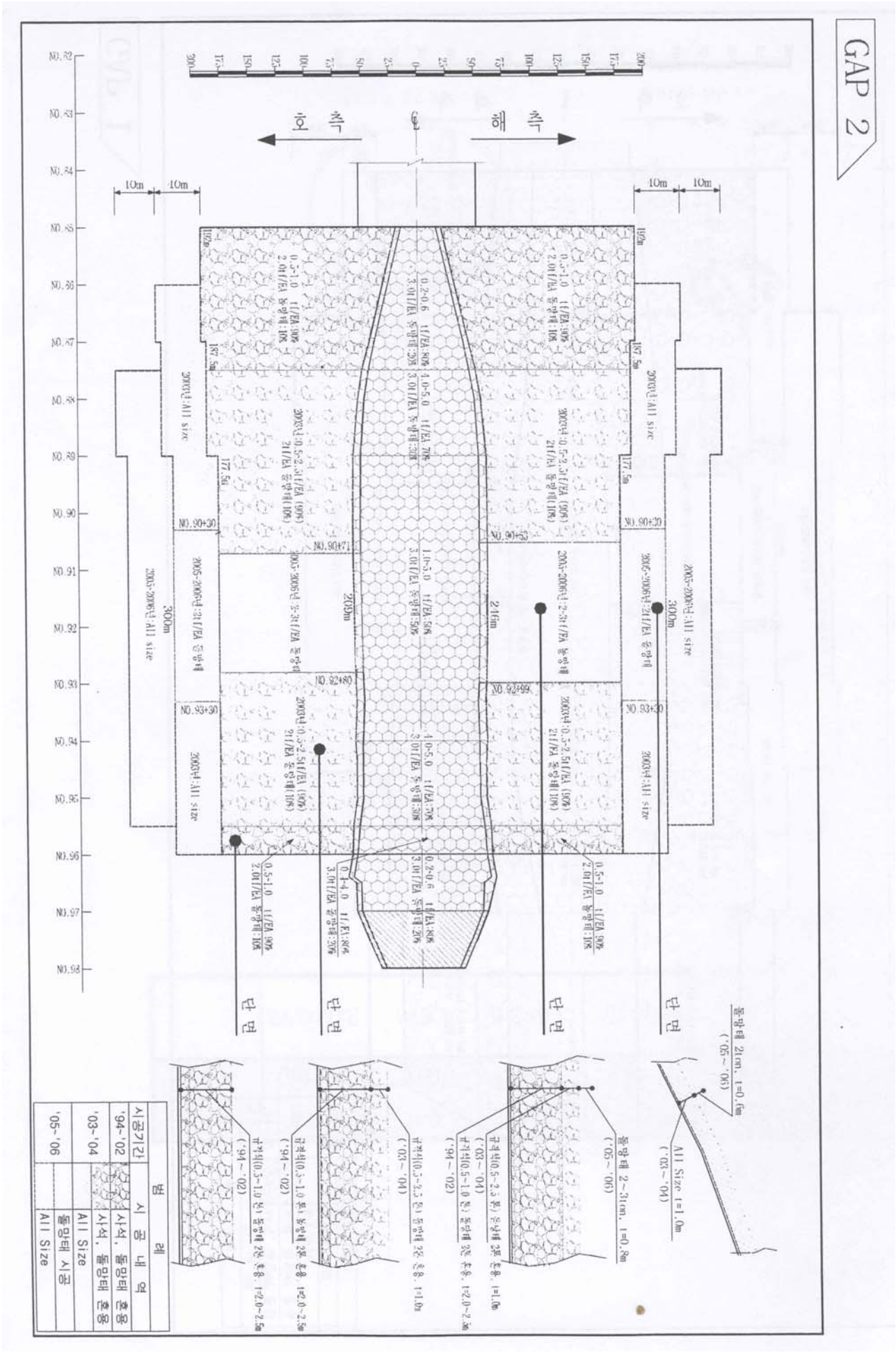
GAP 2
NO.82
NO.83
NO.84
NO.85
NO.86
NO.87
NO.88
NO.89
NO.90
NO.91
NO.92
NO.93
NO.94
NO.95
NO.96
NO.97
NO.98
10m
187.5m
177.5m
NO.90+30
NO.90+53
NO.90+71
NO.92+80
NO.92+99
NO.93+30
210m
216m
300m
단면
범 례
시공기간
시 공 내 역
'94~'02
'03~'04
'05~'06
All Size
All Size t=1.0m
('03~'04)
('05~'06)

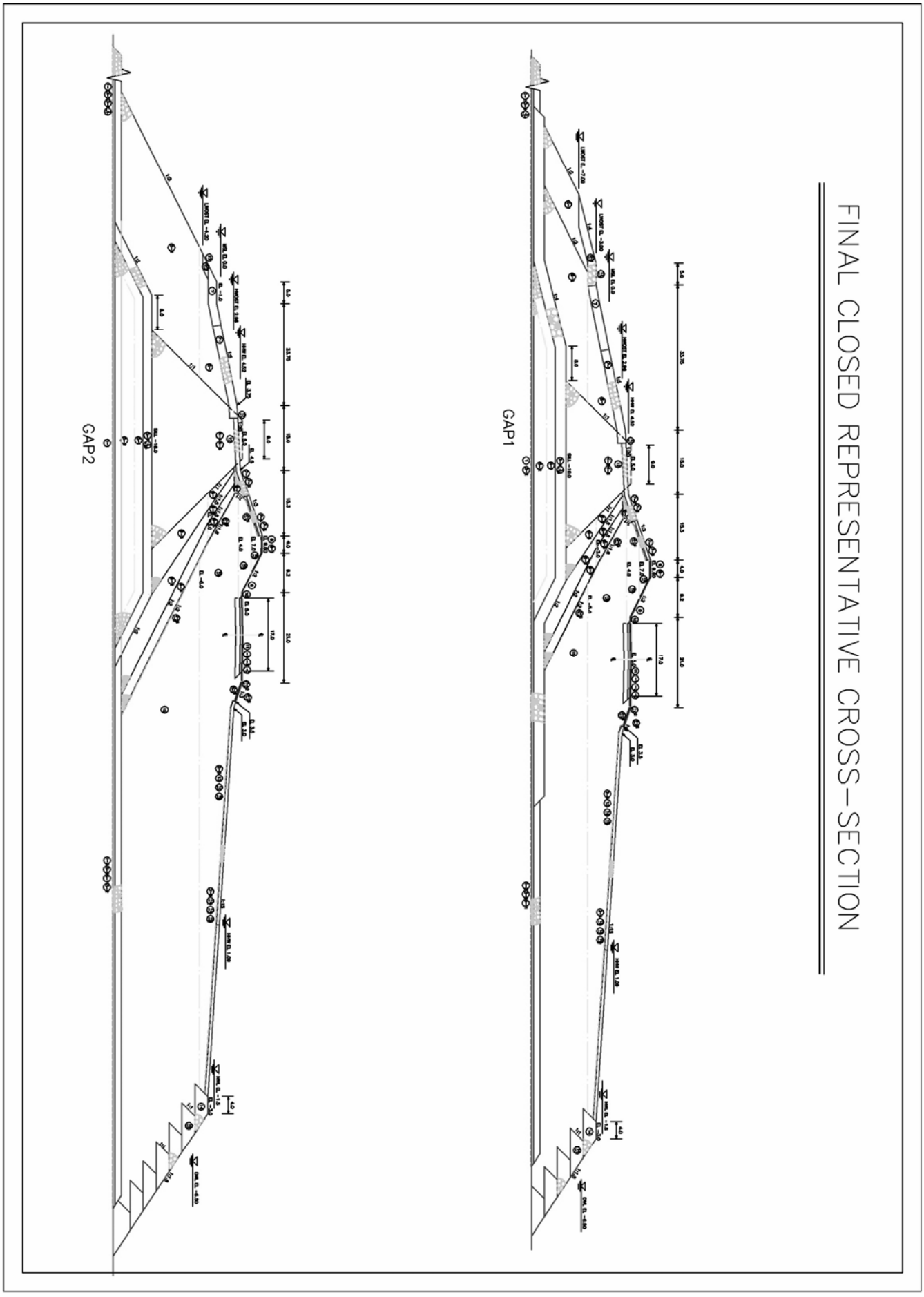
FINAL CLOSED REPRESENTATIVE CROSS-SECTION
GAP1
GAP2

ANNEX IV: Tidal predictions Gunsan Outer Port

The original tidal predictions for Gunsan Outer Port as provided by KRC are given in this annex.

Location: Gunsan Outer Port, South Korea
Months: March (3) and April (4) 2006
Chart datum: 362 cm below Mean Sea Level

3 월

	시각 Time	높이 Ht.		시각 Time	높이 Ht.
	h m	cm		h m	cm
1	04 10	677	16	04 13	626
	10 53	-31		10 46	54
	16 36	724		16 26	638
	23 20	-2		23 02	57
2	04 51	694	17	04 41	635
	11 33	-20		11 16	62
	17 12	705		16 50	628
	23 56	-3		23 29	54
3	05 32	693	18	05 09	637
	12 11	15		11 46	80
	17 47	671		17 14	612
				23 53	60
4	00 30	12	19	05 38	632
	06 13	674		12 16	110
	12 50	67		17 39	589
	18 21	624			
5	01 01	44	20	00 19	74
	06 54	638		06 09	619
	13 26	132		12 47	148
	18 58	567		18 12	559
6	01 33	88	21	00 46	95
	07 41	589		06 47	594
	14 08	201		13 22	193
	19 40	505		18 46	520
7	02 12	140	22	01 18	126
	08 39	533		07 37	560
◐	15 06	265		14 10	242
	20 36	444		19 38	475
8	03 08	193	23	02 10	163
	10 08	491		08 52	524
	17 09	297	◑	15 36	280
	22 16	404		21 03	435
9	04 57	223	24	03 34	194
	12 02	493		10 38	516
	19 05	267		17 46	269
				23 00	438
10	00 15	419	25	05 36	185
	06 51	203		12 14	554
	13 19	527		19 13	211
	20 05	220			
11	01 26	464	26	00 30	491
	07 55	162		07 10	133
	14 07	564		13 19	609
	20 45	177		20 09	143
12	02 11	512	27	01 33	561
	08 41	122		08 15	73
	14 39	595		14 09	657
	21 14	140		20 55	80
13	02 46	554	28	02 23	626
	09 13	91		09 07	25
	15 08	618		14 51	688
	21 45	110		21 36	32
14	03 16	586	29	03 08	676
	09 46	69		09 50	-2
	15 35	633	●	15 30	699
	22 11	86		22 15	1
15	03 45	610	30	03 49	706
	10 17	57		10 34	-5
○	16 01	639		16 07	690
	22 37	68		22 51	-11
			31	04 30	716
				11 13	14
				16 42	666
				23 25	-5

4 월

	시각 Time	높이 Ht.		시각 Time	높이 Ht.
	h m	cm		h m	cm
1	05 08	707	16	04 44	655
	11 50	51		11 29	100
	17 17	631		16 47	584
	23 56	17		23 26	58
2	05 47	681	17	05 18	650
	12 26	100		12 01	127
	17 52	588		17 16	565
				23 54	73
3	00 27	53	18	05 52	635
	06 29	640		12 36	162
	13 01	157		17 51	540
	18 28	539			
4	00 57	99	19	00 25	95
	07 13	588		06 34	610
	13 42	216		13 16	200
	19 11	486		18 36	508
5	01 33	152	20	01 05	126
	08 08	533		07 27	578
◐	14 38	269		14 13	237
	20 05	436		19 37	474
6	02 26	206	21	02 02	163
	09 30	489		08 44	547
	16 29	296	◑	15 38	257
	21 44	404		21 05	453
7	04 09	242	22	03 32	190
	11 20	482		10 17	542
	18 28	271		17 20	235
	23 43	419		22 45	471
8	06 15	228	23	05 20	181
	12 39	507		11 41	566
	19 25	226		18 36	183
9	00 54	466	24	00 07	525
	07 22	189		06 48	140
	13 27	540		12 44	602
	20 03	181		19 33	123
10	01 40	516	25	01 08	590
	08 08	149		07 51	95
	14 01	570		13 35	632
	20 35	141		20 20	71
11	02 15	561	26	02 00	648
	08 44	117		08 43	62
	14 32	593		14 19	648
	21 04	107		21 03	33
12	02 47	598	27	02 44	689
	09 18	93		09 31	46
	15 00	607		14 59	649
	21 32	79		21 43	12
13	03 16	625	28	03 27	709
	09 50	79		10 13	50
	15 26	612	●	15 37	636
	22 01	60		22 19	9
14	03 46	643	29	04 07	710
	10 23	75		10 53	69
○	15 53	609		16 14	614
	22 29	51		22 54	21
15	04 14	653	30	04 47	696
	10 55	83		11 31	99
	16 19	600		16 52	586
	22 58	50		23 27	45

ANNEX V: Storage area approach results

This annex gives the results of the storage area approach for April 15th and 18th 2006. On these dates the maximum flow velocities occurred, these are highlighted in gray. The value of μ for this particular calculation was 0.9.

Output of the storage area approach (positive values mean flow from sea side to basin side)

Time					Level sea	Level basin	Width gap 1	Width gap 2	Q total	q gap 1	q gap 2	q sluices	u max	A basin
year	month	day	hour	minute	m	m	m	m	m3/s				m/s	m2
2006	April	15	0	6	-1.98	-2.23	530	310	21565	15.67	27.78	8.61	2.0	197410996.7
			0	16	-1.76	-2.17	530	310	27479	19.97	35.26	11.04	2.5	200567941.6
			0	26	-1.53	-2.09	530	310	32449	23.58	41.45	13.15	3.0	204527337.9
			0	36	-1.28	-1.99	530	310	36936	26.84	46.94	15.11	3.4	209093855.9
			0	46	-1.03	-1.88	530	310	41130	29.88	51.98	17.00	3.7	213999326.8
			0	56	-0.77	-1.77	530	310	45119	32.78	56.68	18.84	4.0	219336514.7
			1	6	-0.50	-1.65	530	310	48951	35.56	61.11	20.67	4.3	225048902.7
			1	16	-0.24	-1.51	530	310	52648	38.25	65.29	22.47	4.5	231089107.5
			1	26	0.04	-1.38	530	310	56217	40.84	69.26	24.26	4.7	237415642
			1	36	0.30	-1.24	530	310	59656	43.34	73.01	26.03	4.9	243991047
			1	46	0.57	-1.09	530	310	62958	45.73	76.53	27.77	5.1	250780726.9
			1	56	0.83	-0.94	530	310	66108	48.02	79.82	29.47	5.3	257780187.5
			2	6	1.08	-0.78	530	310	69089	50.18	82.86	31.12	5.4	264972136
			2	16	1.33	-0.63	530	310	71880	52.21	85.63	32.71	5.6	272284372.3
			2	26	1.56	-0.47	530	310	74459	54.08	88.13	34.22	5.7	279687741.8
			2	36	1.78	-0.31	530	310	76799	55.78	90.31	35.63	5.8	287153689.7
			2	46	1.98	-0.15	530	310	78872	57.28	92.17	36.93	5.8	294654044.4
			2	56	2.17	0.01	530	310	80649	58.57	93.67	38.09	5.9	302145874.4
			3	6	2.34	0.17	530	310	82099	59.62	94.79	39.10	5.9	309407289.3
			3	16	2.48	0.33	530	310	83186	60.41	95.49	39.94	5.8	316625735.4
			3	26	2.61	0.49	530	310	83875	60.90	95.75	40.58	5.8	323773004.9
			3	36	2.72	0.64	530	310	84127	61.09	95.52	41.00	5.7	330820367.9
			3	46	2.80	0.80	530	310	83902	60.92	94.78	41.17	5.6	337738362.5
			3	56	2.86	0.94	530	310	83155	60.38	93.48	41.07	5.5	344496543.7
			4	6	2.90	1.09	530	310	81837	59.42	91.57	40.67	5.4	349481024
			4	16	2.91	1.23	530	310	79880	58.00	88.98	39.92	5.2	353369597.7
			4	26	2.90	1.37	530	310	77293	56.12	85.74	38.84	4.9	357123403.3
			4	36	2.87	1.50	530	310	74096	53.79	81.87	37.42	4.7	360717482.9
			4	46	2.83	1.62	530	310	70215	50.98	77.30	35.62	4.4	364128569.4
			4	56	2.77	1.73	530	310	65553	47.59	71.92	33.40	4.1	367330700
			5	6	2.69	1.84	530	310	59972	43.54	65.60	30.67	3.7	370294149.1
			5	16	2.60	1.94	530	310	53259	38.66	58.09	27.33	3.2	372983610.2
			5	26	2.49	2.02	530	310	45033	32.69	49.00	23.18	2.7	375074135.5
			5	36	2.37	2.10	530	310	34450	25.01	37.41	17.77	2.1	376240294.3
			5	46	2.23	2.15	530	310	18356	13.33	19.91	9.49	1.1	377129628.7
			5	56	2.08	2.18	530	310	-21513	-15.62	-23.38	-11.09	-1.3	377602384.1
			6	6	1.91	2.15	530	310	-31725	-23.03	-34.63	-16.26	-1.9	377049023.1
			6	16	1.74	2.10	530	310	-38685	-28.08	-42.44	-19.71	-2.4	376231789.4
			6	26	1.55	2.03	530	310	-44148	-32.05	-48.70	-22.34	-2.8	375233098.8
			6	36	1.35	1.96	530	310	-48658	-35.33	-54.00	-24.44	-3.1	373672801.2
			6	46	1.15	1.89	530	310	-52458	-38.09	-58.58	-26.13	-3.4	371510458.7
			6	56	0.94	1.80	530	310	-55681	-40.43	-62.60	-27.50	-3.7	369165657.9
			7	6	0.73	1.71	530	310	-58411	-42.41	-66.14	-28.57	-4.0	366660976.3
			7	16	0.51	1.61	530	310	-60705	-44.08	-69.26	-29.40	-4.2	364015547.7
			7	26	0.28	1.51	530	310	-62606	-45.46	-71.99	-29.99	-4.4	361246243.7
			7	36	0.06	1.41	530	310	-64148	-46.59	-74.37	-30.38	-4.6	358368328.3
			7	46	-0.16	1.30	530	310	-65362	-47.47	-76.42	-30.58	-4.8	355395833.5
			7	56	-0.39	1.19	530	310	-66273	-48.13	-78.17	-30.61	-5.0	352341778.1
			8	6	-0.61	1.08	530	310	-66908	-48.60	-79.63	-30.49	-5.2	349218293.8
			8	16	-0.82	0.97	530	310	-67290	-48.88	-80.82	-30.24	-5.3	345420604.5
			8	26	-1.03	0.85	530	310	-67438	-48.99	-81.76	-29.87	-5.5	340121069
			8	36	-1.23	0.73	530	310	-67368	-48.94	-82.44	-29.40	-5.6	334727066.8
			8	46	-1.43	0.61	530	310	-67102	-48.75	-82.87	-28.84	-5.7	329251842.8
			8	56	-1.62	0.49	530	310	-66661	-48.43	-83.09	-28.21	-5.8	323707571.9
			9	6	-1.79	0.36	530	310	-66066	-48.00	-83.08	-27.54	-5.8	318105398.5
			9	16	-1.96	0.24	530	310	-65334	-47.47	-82.88	-26.82	-5.9	312455493.9
			9	26	-2.11	0.11	530	310	-64482	-46.86	-82.47	-26.08	-5.9	306767138.6
			9	36	-2.25	-0.01	530	310	-63524	-46.16	-81.88	-25.33	-6.0	301029919.7
			9	46	-2.37	-0.14	530	310	-62471	-45.40	-81.10	-24.57	-5.9	295111960.4
			9	56	-2.48	-0.27	530	310	-61328	-44.57	-80.13	-23.83	-5.9	289175429.8
			10	6	-2.57	-0.39	530	310	-60101	-43.68	-78.97	-23.10	-5.9	283227799.4
			10	16	-2.65	-0.52	530	310	-58788	-42.73	-77.61	-22.38	-5.8	277276799.6
			10	26	-2.71	-0.65	530	310	-57383	-41.71	-76.04	-21.68	-5.7	271330894.8
			10	36	-2.75	-0.78	530	310	-55876	-40.61	-74.24	-20.99	-5.6	265399880.7
			10	46	-2.78	-0.90	530	310	-54247	-39.43	-72.20	-20.31	-5.5	259495631
			10	56	-2.79	-1.03	530	310	-52472	-38.14	-69.88	-19.62	-5.3	253645655.8
			11	6	-2.78	-1.15	530	310	-50486	-36.69	-67.18	-18.91	-5.1	247900921.3
			11	16	-2.74	-1.27	530	310	-48195	-35.03	-63.98	-18.14	-4.8	242245613.9
			11	26	-2.68	-1.39	530	310	-45507	-33.07	-60.18	-17.26	-4.5	236720907.2
			11	36	-2.59	-1.51	530	310	-42291	-30.74	-55.63	-16.21	-4.1	231382595.8
			11	46	-2.48	-1.62	530	310	-38355	-27.87	-50.13	-14.89	-3.7	226307069.7
			11	56	-2.35	-1.72	530	310	-33390	-24.26	-43.31	-13.16	-3.2	221600652.9

12	6	-2.20	-1.81	530	310	-26797	-19.47	-34.46	-10.73	-2.5	217416505.4
12	16	-2.03	-1.88	530	310	-16840	-12.24	-21.45	-6.86	-1.5	213993891.4
12	26	-1.84	-1.93	530	310	13021	9.46	16.50	5.36	1.2	211808660.5
12	36	-1.64	-1.89	530	310	22378	16.26	28.30	9.24	2.0	213515827.7
12	46	-1.42	-1.83	530	310	28619	20.79	36.07	11.88	2.5	216426321.7
12	56	-1.19	-1.75	530	310	33792	24.55	42.41	14.13	3.0	220098362.6
13	6	-0.96	-1.66	530	310	38400	27.90	47.97	16.19	3.3	224361845.1
13	16	-0.71	-1.56	530	310	42645	30.98	53.00	18.14	3.7	229114651.1
13	26	-0.46	-1.45	530	310	46623	33.87	57.63	20.01	4.0	234283365
13	36	-0.20	-1.33	530	310	50380	36.60	61.92	21.83	4.2	239809513.3
13	46	0.05	-1.20	530	310	53937	39.18	65.90	23.60	4.5	245643397.2
13	56	0.30	-1.07	530	310	57300	41.62	69.59	25.31	4.7	251740893.6
14	6	0.55	-0.93	530	310	60462	43.92	72.98	26.97	4.8	258092693.4
14	16	0.78	-0.79	530	310	63411	46.06	76.07	28.55	5.0	264662451.7
14	26	1.01	-0.65	530	310	66129	48.03	78.85	30.06	5.1	271381601
14	36	1.23	-0.50	530	310	68592	49.82	81.29	31.46	5.2	278215236.1
14	46	1.43	-0.35	530	310	70777	51.40	83.38	32.75	5.3	285129386.7
14	56	1.62	-0.20	530	310	72652	52.76	85.08	33.91	5.4	292090692.5
15	6	1.79	-0.06	530	310	74186	53.88	86.38	34.91	5.4	299066127.2
15	16	1.94	0.09	530	310	75345	54.72	87.24	35.74	5.4	305892127.8
15	26	2.07	0.24	530	310	76091	55.26	87.63	36.37	5.4	312592894
15	36	2.18	0.39	530	310	76384	55.47	87.51	36.78	5.3	319214946.7
15	46	2.27	0.53	530	310	76178	55.32	86.83	36.93	5.3	325724535.4
15	56	2.33	0.67	530	310	75428	54.77	85.56	36.81	5.1	332086902.1
16	6	2.37	0.81	530	310	74078	53.79	83.65	36.37	5.0	338265889.1
16	16	2.38	0.94	530	310	72065	52.33	81.03	35.58	4.8	344223423.9
16	26	2.37	1.06	530	310	69421	50.40	77.74	34.46	4.6	348782484.4
16	36	2.35	1.18	530	310	66171	48.04	73.82	33.01	4.3	352087705
16	46	2.30	1.30	530	310	62227	45.18	69.18	31.18	4.0	355208620.1
16	56	2.25	1.40	530	310	57478	41.73	63.69	28.92	3.7	358117738.9
17	6	2.17	1.50	530	310	51757	37.58	57.18	26.14	3.3	360783004.2
17	16	2.08	1.58	530	310	44787	32.52	49.36	22.69	2.8	363165266.6
17	26	1.97	1.66	530	310	36011	26.14	39.60	18.29	2.2	365213169.1
17	36	1.85	1.72	530	310	23858	17.32	26.19	12.15	1.5	366850542.8
17	46	1.72	1.76	530	310	-12046	-8.75	-13.22	-6.13	-0.7	367930504.6
17	56	1.57	1.74	530	310	-25567	-18.56	-28.18	-12.95	-1.6	367386820.4
18	6	1.42	1.69	530	310	-33081	-24.02	-36.64	-16.65	-2.1	366231166.9
18	16	1.25	1.64	530	310	-38750	-28.13	-43.14	-19.38	-2.5	364731166.7
18	26	1.07	1.58	530	310	-43370	-31.49	-48.56	-21.53	-2.8	362966915.4
18	36	0.88	1.51	530	310	-47257	-34.31	-53.24	-23.27	-3.2	360982691.5
18	46	0.68	1.43	530	310	-50569	-36.72	-57.34	-24.69	-3.4	358808747.3
18	56	0.48	1.34	530	310	-53397	-38.77	-60.97	-25.82	-3.7	356468370
19	6	0.27	1.25	530	310	-55801	-40.52	-64.19	-26.71	-3.9	353980891.1
19	16	0.06	1.16	530	310	-57822	-41.99	-67.03	-27.38	-4.2	351363169.6
19	26	-0.15	1.06	530	310	-59495	-43.21	-69.54	-27.85	-4.4	348630387.2
19	36	-0.37	0.96	530	310	-60847	-44.19	-71.73	-28.13	-4.6	345027104.1
19	46	-0.59	0.85	530	310	-61897	-44.96	-73.61	-28.24	-4.8	340229510.7
19	56	-0.80	0.74	530	310	-62661	-45.51	-75.20	-28.20	-4.9	335280330.8
20	6	-1.01	0.63	530	310	-63162	-45.88	-76.51	-28.01	-5.1	330196090.2
20	16	-1.22	0.51	530	310	-63423	-46.07	-77.56	-27.71	-5.2	324992251
20	26	-1.42	0.40	530	310	-63465	-46.11	-78.36	-27.29	-5.4	319683256.4
20	36	-1.62	0.28	530	310	-63308	-45.99	-78.92	-26.79	-5.5	314282552.2
20	46	-1.81	0.16	530	310	-62973	-45.75	-79.26	-26.21	-5.6	308802600
20	56	-1.99	0.04	530	310	-62480	-45.40	-79.39	-25.57	-5.7	303254892
21	6	-2.16	-0.09	530	310	-61845	-44.94	-79.32	-24.89	-5.7	297526116.4
21	16	-2.31	-0.21	530	310	-61086	-44.39	-79.05	-24.17	-5.8	291696703.9
21	26	-2.46	-0.34	530	310	-60215	-43.76	-78.59	-23.44	-5.8	285823837.3
21	36	-2.59	-0.47	530	310	-59245	-43.06	-77.95	-22.71	-5.8	279915733.4
21	46	-2.71	-0.59	530	310	-58186	-42.29	-77.12	-21.97	-5.8	273980061.8
21	56	-2.82	-0.72	530	310	-57044	-41.46	-76.11	-21.25	-5.8	268024180.1
22	6	-2.91	-0.85	530	310	-55822	-40.57	-74.92	-20.54	-5.7	262055444
22	16	-2.99	-0.98	530	310	-54516	-39.63	-73.52	-19.85	-5.6	256081612.8
22	26	-3.04	-1.10	530	310	-53122	-38.61	-71.92	-19.19	-5.6	250158495
22	36	-3.09	-1.23	530	310	-51626	-37.53	-70.10	-18.53	-5.4	244261568
22	46	-3.11	-1.36	530	310	-50011	-36.35	-68.02	-17.88	-5.3	238392316.7
22	56	-3.12	-1.48	530	310	-48249	-35.07	-65.66	-17.23	-5.1	232566752.8
23	6	-3.11	-1.61	530	310	-46283	-33.64	-62.94	-16.56	-4.9	226805632.7
23	16	-3.08	-1.73	530	310	-44033	-32.01	-59.74	-15.83	-4.6	221138853
23	26	-3.02	-1.85	530	310	-41411	-30.10	-55.98	-15.00	-4.3	215609467.4
23	36	-2.95	-1.96	530	310	-38294	-27.84	-51.51	-14.03	-3.9	210275986
23	46	-2.85	-2.07	530	310	-34501	-25.08	-46.12	-12.80	-3.5	205079566
23	56	-2.73	-2.17	530	310	-29728	-21.61	-39.44	-11.20	-3.0	200217692.8

Output of the storage area approach (positive values mean flow from sea side to basin side)

Time year	month	day	hour	minute	Level sea m	Level basin m	Width gap 1 m	Width gap 2 m	Q total m3/s	q gap 1	q gap 2	q sluices	u max m/s	A basin m2
2006	April	18	0	6	-2.88	-1.27	397	232	-39508	-35.95	-66.24	-18.28	-5.0	242237388
			0	16	-2.85	-1.37	396	232	-37991	-34.62	-63.66	-17.68	-4.8	237708319.4
			0	26	-2.79	-1.47	395	231	-36244	-33.07	-60.60	-17.01	-4.6	233270134.1
			0	36	-2.72	-1.56	394	230	-34196	-31.23	-56.98	-16.22	-4.3	228955529.4
			0	46	-2.63	-1.65	393	230	-31750	-29.03	-52.64	-15.25	-3.9	224808002.3
			0	56	-2.51	-1.74	392	229	-28762	-26.31	-47.40	-14.01	-3.5	220886101.8
			1	6	-2.38	-1.81	391	229	-24996	-22.88	-40.91	-12.37	-3.0	217270244.4
			1	16	-2.23	-1.88	390	228	-19991	-18.31	-32.46	-10.06	-2.4	214075478.3
			1	26	-2.07	-1.94	389	228	-12361	-11.33	-19.89	-6.33	-1.4	211482233.8
			1	36	-1.89	-1.97	389	227	10308	9.45	16.52	5.33	1.2	209859170.5
			1	46	-1.69	-1.94	388	227	17555	16.13	28.14	9.12	2.0	211223156.1
			1	56	-1.48	-1.89	387	226	22463	20.66	35.96	11.74	2.5	213531157.7
			2	6	-1.27	-1.83	386	226	26533	24.44	42.38	13.97	3.0	216452477.5
			2	16	-1.04	-1.76	385	225	30151	27.80	48.04	16.00	3.4	219856431.6
			2	26	-0.81	-1.68	384	225	33480	30.90	53.18	17.91	3.7	223664684.8
			2	36	-0.57	-1.59	383	224	36601	33.82	57.94	19.75	4.0	227821437.3
			2	46	-0.32	-1.49	382	224	39558	36.59	62.39	21.54	4.3	232282798.7
			2	56	-0.08	-1.39	381	223	42374	39.23	66.56	23.29	4.6	237011970.3
			3	6	0.16	-1.28	380	222	45061	41.76	70.50	25.00	4.8	241976728.1
			3	16	0.41	-1.17	379	222	47623	44.18	74.19	26.67	5.0	247147975
			3	26	0.65	-1.05	378	221	50058	46.48	77.65	28.30	5.2	252498845
			3	36	0.88	-0.93	378	221	52361	48.66	80.87	29.88	5.4	258034621
			3	46	1.11	-0.81	377	220	54524	50.72	83.84	31.40	5.5	263725400.9
			3	56	1.33	-0.69	376	220	56537	52.64	86.56	32.86	5.7	269523423.7
			4	6	1.53	-0.56	375	219	58388	54.41	89.00	34.23	5.8	275406196.9
			4	16	1.73	-0.43	374	219	60064	56.02	91.17	35.53	5.9	281351799.1
			4	26	1.91	-0.31	373	218	61548	57.46	93.03	36.71	5.9	287338735.3
			4	36	2.07	-0.18	372	218	62826	58.71	94.57	37.79	6.0	293345813.6
			4	46	2.22	-0.05	371	217	63880	59.75	95.78	38.73	6.0	299352034.1
			4	56	2.35	0.08	370	217	64692	60.57	96.63	39.54	6.0	305226418.6
			5	6	2.47	0.21	369	216	65243	61.15	97.09	40.18	6.0	310992292.1
			5	16	2.56	0.33	368	215	65513	61.46	97.15	40.64	5.9	316699469.6
			5	26	2.63	0.46	367	215	65479	61.49	96.78	40.91	5.9	322326959.2
			5	36	2.69	0.58	366	214	65121	61.22	95.94	40.96	5.8	327853399
			5	46	2.72	0.70	366	214	64411	60.61	94.61	40.78	5.7	333256907.6
			5	56	2.73	0.81	365	213	63324	59.65	92.76	40.34	5.5	338514899.2
			6	6	2.72	0.93	364	213	61886	58.36	90.42	39.67	5.3	343603845.2
			6	16	2.70	1.03	363	212	60130	56.77	87.65	38.76	5.1	347918613.7
			6	26	2.66	1.14	362	212	58026	54.85	84.40	37.61	4.9	350788603.8
			6	36	2.61	1.24	361	211	55537	52.56	80.62	36.19	4.7	353535512.8
			6	46	2.55	1.33	360	211	52619	49.86	76.26	34.46	4.4	356144131.8
			6	56	2.47	1.42	359	210	49220	46.69	71.23	32.38	4.1	358597625.8
			7	6	2.38	1.50	358	210	45261	42.99	65.42	29.91	3.7	360876911.3
			7	16	2.28	1.58	357	209	40625	38.64	58.67	26.96	3.3	362959628.6
			7	26	2.16	1.64	356	208	35114	33.44	50.68	23.39	2.9	364818300.8
			7	36	2.04	1.70	355	208	28329	27.02	40.87	18.94	2.3	366416630.5
			7	46	1.90	1.75	355	207	19174	18.31	27.67	12.86	1.6	367700503.8
			7	56	1.76	1.78	354	207	-7592	-7.26	-10.97	-5.10	-0.6	368566442.2
			8	6	1.60	1.77	353	206	-19644	-18.84	-28.58	-13.15	-1.6	368224371.2
			8	16	1.44	1.73	352	206	-25800	-24.80	-37.81	-17.21	-2.2	367338465
			8	26	1.27	1.69	351	205	-30292	-29.19	-44.73	-20.13	-2.6	366172145.3
			8	36	1.10	1.64	350	205	-33849	-32.70	-50.39	-22.39	-2.9	364798398.6
			8	46	0.92	1.59	349	204	-36762	-35.61	-55.18	-24.19	-3.3	363257554.4
			8	56	0.73	1.53	348	204	-39180	-38.06	-59.33	-25.65	-3.5	361577025.6
			9	6	0.55	1.46	347	203	-41195	-40.13	-62.94	-26.81	-3.8	359777618.1
			9	16	0.36	1.39	346	203	-42866	-41.87	-66.11	-27.73	-4.0	357876230.8
			9	26	0.18	1.32	345	202	-44237	-43.34	-68.88	-28.44	-4.3	355887206.1
			9	36	0.00	1.25	344	201	-45343	-44.55	-71.29	-28.95	-4.5	353823073.2
			9	46	-0.19	1.17	344	201	-46212	-45.54	-73.39	-29.30	-4.6	351694986.4
			9	56	-0.37	1.09	343	200	-46868	-46.33	-75.18	-29.50	-4.8	349512993.8
			10	6	-0.54	1.01	342	200	-47333	-46.93	-76.70	-29.57	-5.0	347286210.6
			10	16	-0.71	0.93	341	199	-47625	-47.37	-77.96	-29.53	-5.1	343759841.1
			10	26	-0.87	0.85	340	199	-47760	-47.65	-78.97	-29.38	-5.2	339990901.2
			10	36	-1.03	0.76	339	198	-47752	-47.79	-79.74	-29.15	-5.3	336169427.5
			10	46	-1.17	0.68	338	198	-47618	-47.81	-80.30	-28.86	-5.4	332305134
			10	56	-1.31	0.59	337	197	-47371	-47.71	-80.64	-28.50	-5.5	328406900.7
			11	6	-1.43	0.50	336	197	-47023	-47.50	-80.77	-28.09	-5.5	324482856.4
			11	16	-1.55	0.42	335	196	-46587	-47.20	-80.71	-27.65	-5.6	320540470
			11	26	-1.65	0.33	334	196	-46070	-46.82	-80.46	-27.19	-5.6	316586656.9
			11	36	-1.74	0.24	333	195	-45479	-46.35	-80.02	-26.70	-5.6	312627903.3
			11	46	-1.82	0.15	333	194	-44820	-45.80	-79.39	-26.20	-5.6	308670414.9
			11	56	-1.88	0.07	332	194	-44094	-45.18	-78.57	-25.69	-5.6	304720291.5

12	6	-1.93	-0.02	331	193	-43302	-44.47	-77.56	-25.17	-5.5	300756629.5
12	16	-1.97	-0.11	330	193	-42440	-43.69	-76.34	-24.65	-5.4	296718896.9
12	26	-1.99	-0.19	329	192	-41502	-42.82	-74.90	-24.10	-5.3	292707661.5
12	36	-2.00	-0.28	328	192	-40478	-41.85	-73.23	-23.54	-5.2	288731328.8
12	46	-1.99	-0.36	327	191	-39338	-40.74	-71.26	-22.94	-5.1	284799723.1
12	56	-1.96	-0.44	326	191	-38041	-39.46	-68.91	-22.28	-4.9	280926156
13	6	-1.91	-0.52	325	190	-36553	-37.97	-66.14	-21.53	-4.7	277128644.6
13	16	-1.85	-0.60	324	190	-34827	-36.22	-62.87	-20.67	-4.4	273429672.4
13	26	-1.76	-0.68	323	189	-32802	-34.14	-59.01	-19.64	-4.1	269857625.4
13	36	-1.66	-0.75	322	189	-30392	-31.66	-54.44	-18.37	-3.8	266448727.9
13	46	-1.54	-0.82	321	188	-27472	-28.63	-48.95	-16.78	-3.4	263249868.2
13	56	-1.41	-0.88	321	188	-23838	-24.86	-42.22	-14.73	-2.9	260323224.3
14	6	-1.27	-0.94	320	187	-19090	-19.91	-33.60	-11.93	-2.3	257755162.3
14	16	-1.11	-0.98	319	186	-12047	-12.57	-21.05	-7.62	-1.4	255678097.3
14	26	-0.94	-1.01	318	186	9056	9.46	15.77	5.77	1.1	254362198.6
14	36	-0.77	-0.99	317	185	16252	17.00	28.32	10.40	1.9	255355069.1
14	46	-0.58	-0.95	316	185	20896	21.89	36.41	13.42	2.4	257139945.7
14	56	-0.40	-0.90	315	184	24611	25.82	42.85	15.89	2.8	259418864.3
15	6	-0.21	-0.85	314	184	27796	29.20	48.34	18.04	3.2	262079423.1
15	16	-0.01	-0.78	313	183	30613	32.20	53.17	19.97	3.5	265053769
15	26	0.18	-0.71	312	183	33144	34.91	57.46	21.75	3.8	268292849.4
15	36	0.36	-0.64	311	182	35432	37.36	61.31	23.39	4.0	271757377.5
15	46	0.55	-0.56	310	182	37498	39.59	64.75	24.91	4.2	275413762.8
15	56	0.72	-0.48	310	181	39354	41.59	67.80	26.30	4.4	279231991.9
16	6	0.89	-0.40	309	181	41003	43.38	70.48	27.57	4.5	283184412.9
16	16	1.05	-0.31	308	180	42443	44.96	72.79	28.72	4.6	287244983.5
16	26	1.19	-0.22	307	179	43669	46.30	74.71	29.73	4.7	291388777.6
16	36	1.32	-0.13	306	179	44673	47.42	76.25	30.60	4.8	295591641.6
16	46	1.44	-0.04	305	178	45443	48.29	77.38	31.32	4.8	299829939.2
16	56	1.54	0.05	304	178	45967	48.90	78.09	31.87	4.9	304007905.1
17	6	1.63	0.14	303	177	46231	49.24	78.36	32.25	4.9	308121254.3
17	16	1.69	0.23	302	177	46218	49.28	78.17	32.42	4.8	312202984.3
17	26	1.74	0.32	301	176	45910	49.01	77.49	32.39	4.7	316230235.4
17	36	1.77	0.41	300	176	45288	48.40	76.30	32.12	4.6	320179748
17	46	1.78	0.49	299	175	44326	47.43	74.54	31.61	4.5	324027639.1
17	56	1.77	0.58	299	175	43049	46.12	72.28	30.85	4.4	327749112.5
18	6	1.75	0.65	298	174	41480	44.49	69.55	29.88	4.2	331322302.3
18	16	1.72	0.73	297	174	39591	42.52	66.30	28.65	4.0	334728155.9
18	26	1.67	0.80	296	173	37342	40.16	62.47	27.14	3.7	337945801.7
18	36	1.61	0.87	295	172	34682	37.35	57.97	25.32	3.4	340951816.1
18	46	1.54	0.93	294	172	31531	34.00	52.67	23.11	3.1	343719058.1
18	56	1.45	0.98	293	171	27763	29.98	46.36	20.43	2.7	346214663
19	6	1.36	1.03	292	171	23141	25.03	38.64	17.09	2.3	347853063.6
19	16	1.25	1.07	291	170	17093	18.52	28.55	12.66	1.7	348957778.9
19	26	1.13	1.10	290	170	6851	7.43	11.45	5.09	0.7	349771209
19	36	1.00	1.11	289	169	-13468	-14.65	-22.65	-9.99	-1.3	350096471.5
19	46	0.86	1.09	288	169	-18850	-20.57	-31.93	-13.94	-1.9	349457635.2
19	56	0.72	1.06	288	168	-22706	-24.86	-38.77	-16.74	-2.3	348561872.4
20	6	0.57	1.02	287	168	-25774	-28.31	-44.38	-18.93	-2.7	347480146.3
20	16	0.41	0.97	286	167	-28316	-31.20	-49.19	-20.71	-3.0	345767476.5
20	26	0.24	0.92	285	167	-30459	-33.68	-53.41	-22.17	-3.3	343539621.2
20	36	0.07	0.87	284	166	-32273	-35.81	-57.14	-23.37	-3.6	341127665.9
20	46	-0.10	0.81	283	165	-33805	-37.65	-60.47	-24.35	-3.8	338553990.9
20	56	-0.27	0.75	282	165	-35090	-39.23	-63.43	-25.12	-4.0	335837588.3
21	6	-0.45	0.69	281	164	-36153	-40.58	-66.06	-25.72	-4.2	332995140.3
21	16	-0.62	0.63	280	164	-37014	-41.71	-68.39	-26.15	-4.4	330041632.7
21	26	-0.79	0.56	279	163	-37692	-42.65	-70.45	-26.44	-4.6	326990718.6
21	36	-0.96	0.49	278	163	-38203	-43.41	-72.24	-26.60	-4.8	323854938.1
21	46	-1.13	0.42	277	162	-38563	-44.01	-73.78	-26.64	-5.0	320645852.9
21	56	-1.30	0.35	276	162	-38785	-44.45	-75.10	-26.58	-5.1	317374128.4
22	6	-1.46	0.27	276	161	-38885	-44.76	-76.19	-26.43	-5.2	314049585.9
22	16	-1.61	0.20	275	161	-38874	-44.94	-77.08	-26.20	-5.4	310681236.9
22	26	-1.75	0.12	274	160	-38765	-45.02	-77.77	-25.91	-5.5	307277309.7
22	36	-1.89	0.05	273	160	-38571	-44.99	-78.27	-25.57	-5.5	303845276.5
22	46	-2.02	-0.03	272	159	-38302	-44.87	-78.59	-25.19	-5.6	300352680.2
22	56	-2.14	-0.10	271	158	-37967	-44.67	-78.75	-24.78	-5.7	296776423.2
23	6	-2.25	-0.18	270	158	-37576	-44.39	-78.73	-24.36	-5.7	293188692.4
23	16	-2.34	-0.26	269	157	-37136	-44.05	-78.56	-23.92	-5.8	289594469.3
23	26	-2.43	-0.34	268	157	-36653	-43.64	-78.23	-23.47	-5.8	285998245.1
23	36	-2.50	-0.41	267	156	-36132	-43.18	-77.73	-23.03	-5.8	282404131.5
23	46	-2.56	-0.49	266	156	-35576	-42.67	-77.08	-22.59	-5.7	278815994.3
23	56	-2.61	-0.57	265	155	-34986	-42.10	-76.27	-22.16	-5.7	275237614.7

ANNEX VI: GPS floater measurements

This annex provides the original data as provided by KRC of the GPS floater measurements of April 16th 2006.

GAP Ⅱ 조류속 측정 결과표(창조)

새만금 제2공구 2006. 4. 16

방조제 GAP2 유속측정 결과 (1번 GPS)

번호	날짜			이동거리		이동시간	순간속도		환산속도		평균속도		좌표	
131	2006-04-16	오후	2:17:17	0.79	m	0:00:01	2.9	kph	0.794	mps	0.86	mps	153148	256327
231	2006-04-16	오후	2:18:57	1.45	m	0:00:01	5.2	kph	1.45	mps	1.38	mps	153244	256363
331	2006-04-16	오후	2:20:37	5.14	m	0:00:01	18	kph	5.14	mps	4.86	mps	153458	256503
431	2006-04-16	오후	2:22:17	2.01	m	0:00:01	7.3	kph	2.01	mps	3.64	mps	153823	256667
531	2006-04-16	오후	2:23:57	2.69	m	0:00:01	9.7	kph	2.69	mps	2.56	mps	154112	256726
631	2006-04-16	오후	2:25:37	2.82	m	0:00:01	10	kph	2.82	mps	2.75	mps	154353	256767

방조제 GAP2 유속측정 결과 (2번 GPS)

번호	날짜			이동거리		이동시간	순간속도		환산속도		평균속도		좌표	
160	2006-04-16	오후	2:27:48	0.993	m	0:00:01	3.6	kph	0.993	mps	0.99	mps	153160	256338
260	2006-04-16	오후	2:29:28	1.72	m	0:00:01	6.2	kph	1.72	mps	1.78	mps	153274	256401
360	2006-04-16	오후	2:31:08	5.24	m	0:00:01	19	kph	5.24	mps	5.48	mps	153618	256585
460	2006-04-16	오후	2:32:48	3.58	m	0:00:01	13	kph	3.58	mps	3.53	mps	154040	256697
560	2006-04-16	오후	2:34:28	1.3	m	0:00:01	4.7	kph	1.3	mps	1.32	mps	154247	256664

방조제 GAP2 유속측정 결과 (3번 GPS)

번호	날짜			이동거리		이동시간	순간속도		환산속도		평균속도		좌표	
138	2006-04-16	오후	2:37:25	0.96	m	0:00:01	3.5	kph	0.96	mps	1.00	mps	153147	256311
238	2006-04-16	오후	2:39:05	1.46	m	0:00:01	5.3	kph	1.46	mps	1.45	mps	153250	256357
338	2006-04-16	오후	2:40:45	5.26	m	0:00:01	19	kph	5.26	mps	5.36	mps	153496	256515
438	2006-04-16	오후	2:42:25	2.7	m	0:00:01	9.7	kph	2.7	mps	2.91	mps	153890	256615
538	2006-04-16	오후	2:44:05	1.46	m	0:00:01	5.3	kph	1.46	mps	1.51	mps	154088	256562

방조제 GAP2 유속측정 결과 (4번 GPS)

번호	날짜			이동거리		이동시간	순간속도		환산속도		평균속도		좌표	
47	2006-04-16	오후	2:45:53	1.24	m	0:00:01	4.5	kph	1.24	mps	1.14	mps	153104	256307
147	2006-04-16	오후	2:47:33	1.64	m	0:00:01	5.9	kph	1.64	mps	1.59	mps	153220	256364
247	2006-04-16	오후	2:49:13	5.58	m	0:00:01	20	kph	5.58	mps	5.42	mps	153468	256520
347	2006-04-16	오후	2:50:53	1.93	m	0:00:01	7	kph	1.93	mps	1.86	mps	153767	256591
447	2006-04-16	오후	2:52:33	1.91	m	0:00:01	6.9	kph	1.91	mps	1.69	mps	153938	256601

방조제 GAP2 유속측정 결과 (5번 GPS)

번호	날짜			이동거리		이동시간	순간속도		환산속도		평균속도		좌표	
85	2006-04-16	오후	2:56:32	1.2	m	0:00:01	4.3	kph	1.2	mps	1.09	mps	153134	256300
185	2006-04-16	오후	2:58:12	1.47	m	0:00:01	5.3	kph	1.47	mps	1.47	mps	153245	256345
285	2006-04-16	오후	2:59:52	5.68	m	0:00:01	20	kph	5.68	mps	5.35	mps	153481	256515
385	2006-04-16	오후	3:01:32	3.73	m	0:00:01	13	kph	3.73	mps	3.55	mps	153857	256676
485	2006-04-16	오후	3:03:12	3.02	m	0:00:01	11	kph	3.02	mps	2.99	mps	154186	256714
585	2006-04-16	오후	3:04:52	3.33	m	0:00:01	12	kph	3.33	mps	2.94	mps	154457	256748

방조제 GAP2 유속측정 결과 (6번 GPS)

번호	날짜			이동거리		이동시간	순간속도		환산속도		평균속도		좌표	
141	2006-04-16	오후	3:07:28	0.766	m	0:00:01	2.8	kph	0.766	mps	1.04	mps	153156	256293
241	2006-04-16	오후	3:09:08	1.45	m	0:00:01	5.2	kph	1.45	mps	1.34	mps	153266	256328
341	2006-04-16	오후	3:10:48	5.73	m	0:00:01	21	kph	5.73	mps	5.32	mps	153462	256499
441	2006-04-16	오후	3:12:28	4.55	m	0:00:01	16	kph	4.55	mps	4.36	mps	153899	256684
541	2006-04-16	오후	3:14:08	2.23	m	0:00:01	8	kph	2.23	mps	2.16	mps	154177	256711

방조제 GAP2 유속측정 결과 (7번 GPS)

번호	날짜			이동거리		이동시간	순간속도		환산속도		평균속도		좌표	
260	2006-04-16	오후	3:19:26	0.662	m	0:00:01	2.4	kph	0.662	mps	0.80	mps	153190	256290
360	2006-04-16	오후	3:21:06	1.22	m	0:00:01	4.4	kph	1.22	mps	1.15	mps	153281	256319
460	2006-04-16	오후	3:22:46	6.05	m	0:00:01	22	kph	6.05	mps	3.96	mps	153437	256466
560	2006-04-16	오후	3:24:26	0.495	m	0:00:01	1.8	kph	0.495	mps	0.39	mps	153551	256481
660	2006-04-16	오후	3:26:06	0.315	m	0:00:01	1.1	kph	0.315	mps	0.32	mps	153555	256450
760	2006-04-16	오후	3:27:46	0.204	m	0:00:01	0.74	kph	0.204	mps	0.26	mps	153548	256431

방조제 GAP2 유속측정 결과 (8번 GPS)

번호	날짜			이동거리		이동시간	순간속도		환산속도		평균속도		좌표	
473	2006-04-16	오후	3:33:23	0.726	m	0:00:01	2.6	kph	0.726	mps	0.73	mps	153245	256276
573	2006-04-16	오후	3:35:03	1.15	m	0:00:01	4.1	kph	1.15	mps	0.98	mps	153316	256316
673	2006-04-16	오후	3:36:43	4.99	m	0:00:01	18	kph	4.99	mps	4.31	mps	153460	256483
773	2006-04-16	오후	3:38:23	0.687	m	0:00:01	2.5	kph	0.687	mps	0.84	mps	153651	256548

<별첨2> GPS부표유속계에 의한 유속자료 검토

◦ 조사 현황

- 일시 : '05.04.08(창조, 조차:6.51m, 조시:5시간 39분)
- 장소 : GAP1, GAP2
- 측정장비 : GPS부표유속계 8조
- 방법 : 4개의 부표를 개방구간을 같이 통과하게 투하

◦ Gap1 유속 측정 결과

구분	위치	번호	발생시각	순간속도	이동평균	이격거리
Gap1-1차	No.31+42	G111	11:52:46	4.0	3.32	67(해)
	No.27+62	G112	11:53:54	4.6	3.75	40(해)
	No.24+53	G114	11:54:35	4.1	3.72	2(내)
	No.23+33	G113	11:59:00	4.1	3.77	90(내)
Gap1-2차	No.30+05	G123	12:21:06	4.2	3.97	30(내)
	No.27+25	G124	12:19:38	4.6	4.16	8(해)
	No.25+00	G121	12:22:42	4.3	3.59	120(내)
	No.23+02	G122	12:26:48	4.5	3.81	59(내)

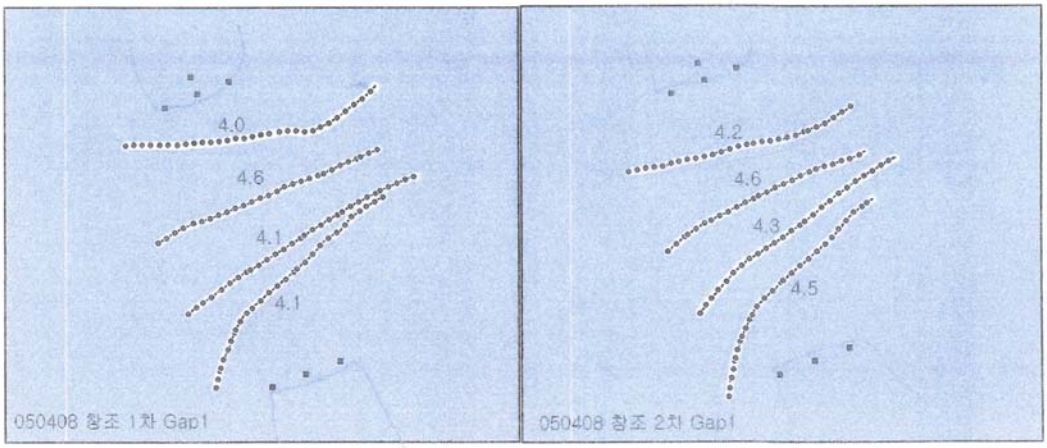

- 4개의 부표를 개방구간에서 최대통과유속 비교
- Gap1 1,2차 측정 결과, 중앙부에서의 4.6m/s로 유속이 크게 발생하고 사석제 남측 선단부를 돌아서 중앙쪽으로 휘는 흐름에 의한 유속이 크게 발생

ANNEX VII: Delft 3D output

The Delft 3D output as provided by RRI of March 25th and March 26th 2006 are given in this annex. These dates were not dates on which maximum flow velocities occurred.

Delft 3D output, RRI

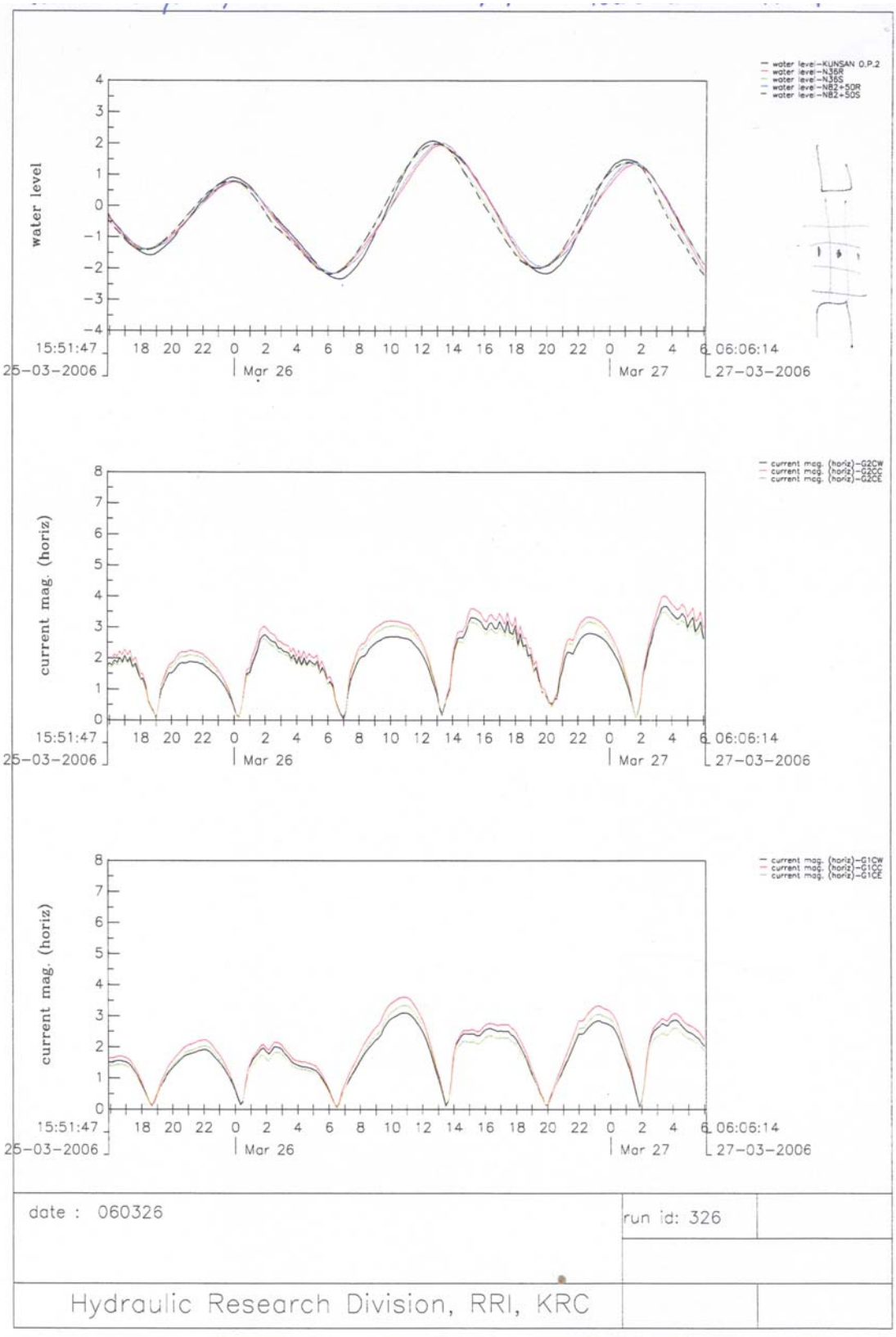

Delft 3D output, RRI

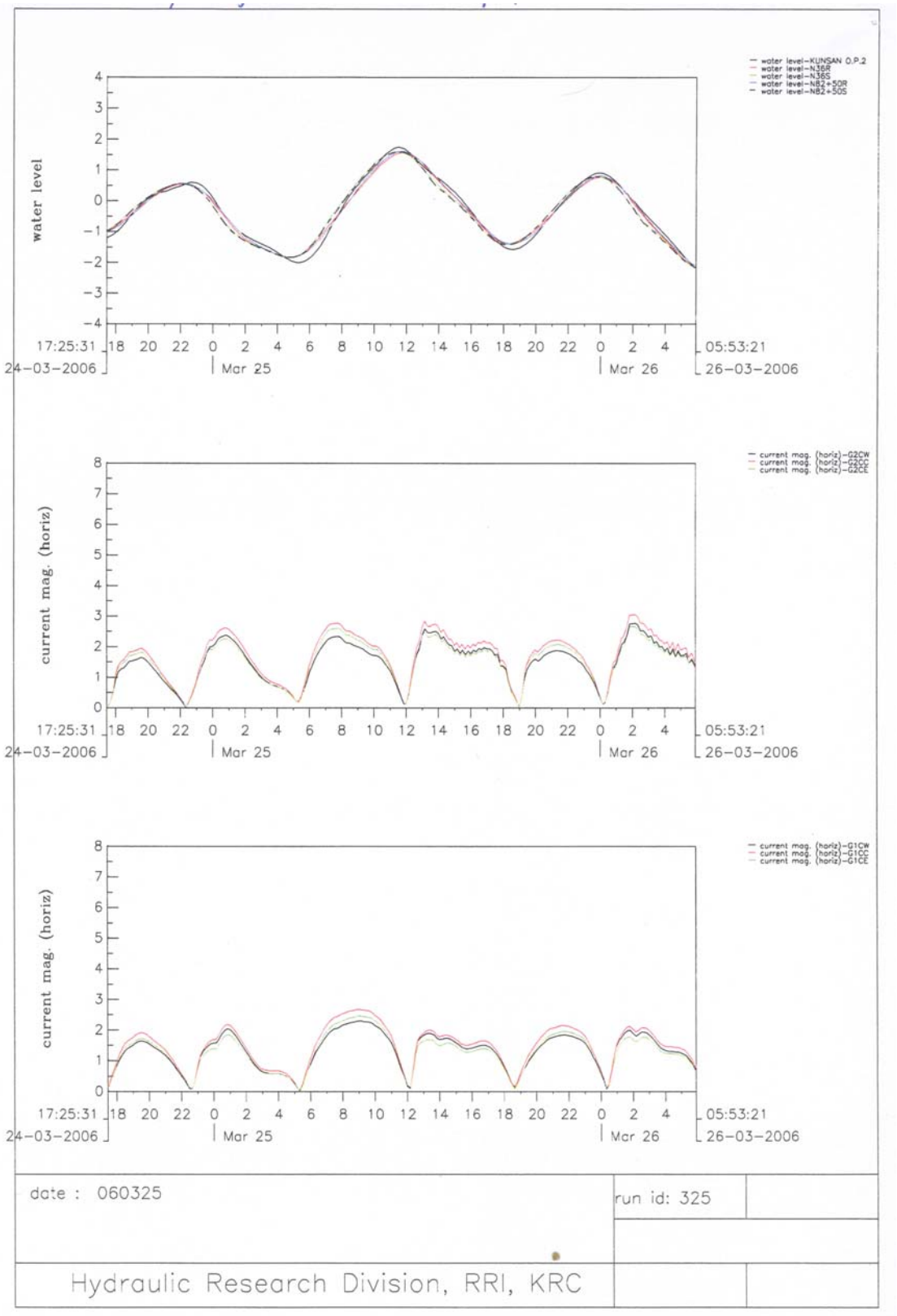

ANNEX VIII: DHL model tests on box gabions

In 1982 DHL (Delft Hydraulics Laboratory) did model tests on the stability of box gabions in order to see if they could be used at the 'Oosterschelde' project. The box gabions proved not to be necessary and have not been applied at the 'Oosterscheldekering'.

This annex provides a summary of the DHL model tests on box gabions and will be used as a comparison for the methods and results of the Delft model tests. It must be kept in mind that the DHL tests are done on rigid box gabions while the Delft tests are done on flexible sack gabions, which obviously leads to different results. Also the calculation methods are different; The DHL tests are based on the volume of a gabion while the Delft tests are based on the mass of a gabion. These methods can be converted to each other (paragraph 2.4).

Tests were performed by DHL on model box gabions (cube shaped) with different sizes and on concrete cubes as a reference. Also reference tests were done on stones with a nominal diameter of 60-300 kg.

The results are given in table VIII.1 and figure VIII.1 which come from DHL (1982 II).

Table VIII.1: Results of DHL model tests on box gabions (volume based)

Elements	D	Δ	u_c	h	C	ψ_c
	(m)	(-)	(m/s)	(m)	($m^{1/2}$/s)	(-)
Gabions	0.100	1.08	4.2	2.2	38.2	0.11
Gabions	0.062	1.08	3.4	1.7	39.9	0.11
Cubes	0.083	1.73	>3.3	1.7	37.6	>0.054
Cubes	0.060	1.50	2.6	2.1	41.8	0.043
Rip Rap	0.400	1.75	4.1	1.2	22.9	0.045

In this case the critical flow velocity is depth averaged.

Knowing that the porosity of the model gabions was 32 %, the results of the volume based approach can be converted to a mass based approach to compare the results of the model tests of DHL and Delft.

To compare these results with the results of the Delft model tests on sack gabions, a mass based approach is used and formula [18] is applied. From the data of the rip rap, a factor β is derived. All other data is taken from (DHL 1982 II).

Table VIII.2: Calculations for comparison with sack gabions (mass based)

Elements	D	M	ρ	D_n	Δ	β	u_c
	(m)	(kg)	(kg/m^3)	(m)	(-)		(m/s)
Gabions	0.100	1.76	2600	0.088	1.6	0.82	2.05
Gabions	0.062	0.42	2600	0.054	1.6	0.82	1.61
Cubes	0.083	1.56	2728	0.083	1.73	0.82	1.85
Cubes	0.060	0.54	2500	0.060	1.50	0.82	1.47
Rip Rap	0.400	176	2750	0.400	1.75	0.82	4.09

In this case the flow velocity is local.

If table VIII.1 is compared to table VIII.2 it shows that the stability of box gabions is over 2 times higher than the stability of sack gabions (not taken into account the difference between a local and a depth averaged flow velocity). Box gabions have a less flexible casing and must be placed in a neat manner to have an optimal effect.

proef nr.	D (m)	Δ	massa kg	laagdikte (m)	$\bar{u}$ (m/s)	h (m)	aantal verplaatste gabions (cummulatief)	schade 40-230 mm	opmerkingen
T1	0,10	1,08	1,76	0,075	1,88	2,21	1	-	
					2,04	2,19	1	-	
					2,18	2,14	2	-	
					2,54	1,98	4	-	
					2,77	1,88	7	-	
					3,04	1,82	7	-	
					3,35	1,68	7	x	begin verplaatsing 40-230 mm
T2 (paal)	0,10	1,08	1,76	0,075	1,9	2,29	-	-	
					2,1	2,23	4	x	rondom paal 0,10 m erosie
					2,3	2,04	6	x	rondom paal 0,20 m erosie
T3 (paal)	0,10	1,08	1,76	0,15	1,8	2,30	-	-	
					2,0	2,22	-	x	begin verplaatsing 40-230 mm
					2,4	2,12	4	-	
					2,5	2,04	13	-	
					2,9	1,81	14	x	rondom paal 0,06 m erosie
					-	-	25	x	rondom paal 0,15 m erosie
T4	0,10	1,08	1,76	0,075	1,84	2,29	-	-	
					2,02	2,25	-	-	
					2,31	2,07	-	-	
					2,48	2,00	-	-	
					2,84	1,84	-	x	1 staalslak verplaatst
					3,04	1,78	-	x	1 staalslak verplaatst
					3,24	1,70	-	x	13 staalslakken verplaatst
					3,24	1,69	-	-	
T5	0,083 beton	1,73	1,56	0,062	1,91	2,31	-	-	
					2,09	2,24	-	-	
					2,35	2,19	-	-	
					2,60	2,10	-	-	
					2,81	2,03	-	-	
					3,03	1,94	-	-	
					3,26	1,85	-	x	begin verplaatsing
					3,40	1,68			transport staalslakken
T6	0,062	1,08	0,42	0,045	1,64	2,20	*	-	verschuiving gabions in het vak
					1,86	2,16	*	-	
					2,07	2,06	1	-	
					2,36	2,04	2	-	
					2,64	1,90	3	-	
					2,81	1,84	4	-	
					2,99	1,74	5	-	
					3,15	1,72	5*	-	2 rijen verschoven
					3,19	1,74	5*	x	geen verdere verplaatsing gabions schade 40-230 mm, waar stenen weg zijn
T7	0,060	1,50	0,54	0,045	1,8	2,31	-	-	
					2,1	2,21	x	-	verschuiving 5 cm in het vak
					2,3	2,16	x	-	verschuiving 10 cm in het vak
					2,6	2,09	6	-	
					2,8	2,02			bezwijken

Tabel 1 Overzicht verrichte proeven en resultaten

Figure VIII.1: Results of DHL model tests on box gabions